Università degli Studi di Cagliari

DOTTORATO DI RICERCA

Sviluppo e sperimentazione dei farmaci antinfettivi

Ciclo XXVII

Characterization of *ftsA* conditional lethal mutants shows that FtsA is required at early and late stages of cell division in *Streptococcus pneumoniae*

Settore scientifico disciplinare di afferenza
BIO/19

Presentata da: **Andrea Mura**

Coordinatore Dottorato: **Prof. Alessandra Pani**

Tutor: **Prof. Orietta Massidda**

Relatore: **Prof. Orietta Massidda**

Esame finale anno accademico 2013 – 2014

Table of Contents

Summary

FtsA is an essential cell division protein fairly conserved among Eubacteria. It is an actin-like protein that structurally differs from actin because it lacks one of the four subdomains that is replaced by an additional one located elsewhere in the structure. FtsA localizes early at the cell division site, together or immediately after FtsZ, where it is needed both to tether FtsZ to the membrane and also to recruit to midcell the other cell division proteins. In agreement with this, FtsA interacts, at least, with itself, FtsZ, ZapA and the septal PBP, FtsI.

Despite the advances in understanding cell division in *Streptococcus pneumoniae*, little is known about the early stages of the process. Here I present the characterization of *S. pneumoniae ftsA* thermosensitive (Ts) mutants, obtained by error-prone random PCR, allelic replacement and subsequent screening for ability to grow at 28°C (permissive temperature) but not at 40°C (non permissive temperature). Out of 8000 transformants screened, three, named $A19_{TS}$, $A20_{TS}$ and $A21_{TS}$, were identified and shown to carry mutated *ftsA* alleles and express the corresponding mutated protein. The mutations mapped in different domains of the FtsA structure, thought to be involved in FtsA polymerization, interactions with FtsZ and/or with other cell division proteins. Temperature shifting experiments, carried out in rich medium, showed that in contrast to the Rx1 wild type, that grew well at both 28°C and 40°C, the FtsA Ts mutants stopped growing and started lysing about 60 to 90 minutes after shifting to the non permissive temperature, in a mutation specific manner. The lysis was greatly reduced when the shift to 40°C was performed in a chemically-defined medium or in a *lytA*- background. Detection of $FtsA_{wt}$ and $FtsA_{TS}$, in crude extracts, derived from cultures after shifting at 28°C and 40°C, revealed that all the FtsA Ts proteins are stable at both temperatures, indicating that protein degradation is not the cause of the Ts phenotype.

Protein-protein interaction assays showed that all three $FtsA_{TS}$ proteins lost their ability to self-interact but retained their ability to interact with the $FtsA_{WT}$ protein and FtsZ. Consistently, GFP-$FtsA_{WT}$, expressed under the control of the P_{Zn} inducible promoter at the ectopic *bga* locus of the

S. pneumoniae chromosome, fully complemented the Ts phenotype of two, $A20_{TS}$ and $A21_{TS}$, mutants. Interestingly, the Ts phenotype of the $A19_{TS}$ mutant was only partially complemented by GFP-$FtsA_{WT}$, which localized as multiple rings in the partially complemented elongated $A19_{TS}$+P_{Zn}-GFP-$FtsA_{WT}$ cells, suggesting the $FtsA19_{TS}$ may be dominant over $FtsA_{WT}$.

Localization studies, using fluorescence microscopy, showed that CFP-FtsZ, DivIVA-GFP, GFP-StkP, GFP-GpsB and GFP-PBP2x exhibited proper localization in the $Rx1_{WT}$ at 28°C and 40°C, while in the FtsA Ts mutants these cell division markers were localized properly at 28°C but retained or lost their localization upon shifting to 40°C depending on the specific mutant. Notably, in all FtsA Ts mutants, FtsZ lost its septal localization after shifting to 40°C. The results are consistent with what was observed in a zinc dependent *ftsA* conditional lethal *S. pneumoniae* mutant, where the only source of FtsA was GFP-FtsA expressed under the control of the P_{Zn} inducible promoter, indicating that *S. pneumoniae* FtsA is required for efficient midcell localization of FtsZ and supporting the notion that in Gram-positives, which lack ZipA, FtsA may be absolutely necessary for anchoring FtsZ to the membrane.

Together these results confirm that FtsA is essential in *S. pneumoniae* and further validate it as a target to develop novel inhibitors active on septation. Moreover, the data suggest that an early block in cell division in *S. pneumoniae* impairs both growth and division, supporting a model in which a single machinery, containing both complexes, one for peripheral elongation and one for septum formation, directed by FtsZ, and likely by FtsA, is present at the midcell of oval-shaped cocci.

Introduction

1. *Streptococcus pneumoniae*: a commensal and a pathogen

Streptococcus pneumoniae (the *pneumococcus*) is an important Gram-positive human pathogen but also a typical commensal specie of the nasopharynx, where it is present as a non-pathogenic biofilm (Bogaert *et al.*, 2004; Kadioglu *et al.*, 2008; Gilley & Orihuela; 2014; Chao *et al.*, 2015).

S. pneumoniae colonizes the nasopharynx of children and adults, and carriage is thought to be required for its spread among its human hosts (Henriques-Normark & Normark, 2010; Kadioglu *et al.*, 2008). *S. pneumoniae* can also cause a variety of diseases that range from middle ear infections to pneumonia, bacteremia, and meningitis (Henriques-Normark & Normark, 2010; van der Poll & Opal SM*,* 2009; Weiser, 2010). Pneumococcal invasive diseases are particularly prevalent among individuals with underdeveloped or compromised immune systems, such as infants, the elderly, and HIV patients (Black, 2010), and following certain respiratory infections, such as influenza (Klugman, 2011) and the childhood deaths caused by pneumococcus are estimated at 1 million per year (O'Brien *et al.*, 2009; Walker *et al.*, 2013).

The polysaccharide envelope, known as the pneumococcal capsule, is responsible for its virulence, because it allows the bacterium to escape the host immune defenses while the unencapsulated strains are not virulent. The available vaccines against *S. pneumoniae* are all based on the capsular polysaccharide epitopes, but given the fact that there are more than 90 serotypes of *S. pneumoniae* strains known, the effectiveness of these vaccines is limited and their use has recently led to a switch in the strains causing disease, where serotypes included in the vaccine were replaced with the serotypes for which there was no available vaccine (Erdmann, 2010; Feldman & Anderson, 2014; Rodrigo & Lim, 2014).

The presence of the capsule gives the *S. pneumoniae* colonies a glossy aspect and this feature was useful to Frederick Griffith in 1928, during one of the most famous experiments in the history of microbiology. He distinguished between smooth ("S", encapsulated virulent strains) and rough

("R", unencapsulated avirulent strains) and found that only the S bacteria, when inoculated in mice, were able to produce a disease and kill the animals, whereas the R variants were not. Likewise, inactivated S variants, heat-killed with high temperature did not cause disease. However, when the heat-killed S variants and the live R variants were inoculated simultaneously in mice, the animals got sick and died and only S variants could be recovered from the dead animals, suggesting that *S. pneumoniae* cells were able to uptake a "transforming factor" from the environment, change their genotype/phenotype and transmit it to the following generations (Griffith, 1928).

At that time, the nature of this "transforming factor" was unknown, and remained a mystery for almost two decades, until another historic experiment, performed by Avery and colleagues, showed that DNA, isolated from virulent pneumococcal strains, was responsible for the transformation, proving clearly that *S. pneumoniae* is able to naturally acquire DNA from the environment and integrate it in its chromosome (Avery *et al.*, 1944). This ability, known as natural competence, represents an advantage because it allows the pneumococcus to change crucial genes as the one involved in antibiotic resistance, and promotes vaccine escape *via* capsule switching. Moreover, natural competence has been exploited by scientists to easily manipulate its genome (Cornick & Bentley, 2012; Johnston *et al.*, 2014; Straume *et al.*, 2014).

Because of the severe toll of *S. pneumoniae* on human health, further exacerbated by the rapid and widespread diffusion of resistance to many of the commonly used antibiotics (CDC report 2013), new antimicrobials and vaccine development against pneumococcal infection continues to be a major area of research activity (Sham *et al.*, 2012).

2. Bacterial cell division as a target to develop new antibacterials active on septation

Bacterial cell division is an essential process, the mechanism of which is still poorly understood. The attention aroused by this process is due also to the possibility of using the cell division proteins as primary targets for developing new broad spectrum antibacterial drugs. Indeed, the

proteins involved in bacterial cell division are in the first position of the list for new potential targets for developing new antibacterial molecules. Given the fact that many of the cell division proteins are essential for bacterial life, historically the use of cell division filamentous thermosensitive (Ts) mutants, in the model organisms, *Escherichia coli* and *Bacillus subtilis*, has allowed the identification of the genes that encode most of the proteins involved in the division process. These mutants are able to divide at the so-called "permissive-temperature" (usually 30°C) but are not able to carry out division at the "non-permissive" temperature (usually 42°C-45°C) producing long unseptated filaments, from which the name "*fts*" (*filamentous thermosensitive*) to the genes and "Fts" the corresponding proteins involved in the process.

In 1933 Frederick Gates, published a first study about the appearance of *E. coli* filamentous cells after UV-rays exposure (Gates, 1933). In this study, Gates understood in advance the difference between the cell division machinery and the cell elongation one in *E. coli*. For several years after Gates researchers studied the ability of bacteria to survive after exposure to radiations or chemical mutagens but only in the 1940s, did it become clear that this resistance was due to genetic mutations and, in several cases, these mutations were affecting the efficiency of the cell division machinery resulting in cell filamentation (Witkin, 1946). In 1964, Van de Putte and colleagues created the *fts* acronym as a marker to designate the strains of *E. coli* that form filamentous cells, also called "snakes", upon shifting to the non-permissive temperature of 42°C, (van de Putte *et al.*, 1964). Since then many other *fts* genes has been discovered.

Most of the *fts* genes are located in a chromosome region, highly conserved among different bacterial species, known as the *d*ivision and *c*ell wall (*dcw*) cluster, that contains also the genes for the cytoplasmic steps of peptidoglycan (PG) synthesis, showing a close relationship between the two processes. Recent advances in cell division have shown that, at least in its essential steps, the process of cell division is conserved in all Eubacteria. Despite this, the exact biochemical function of the cell division proteins has been clarified only for some of them, decreasing the possibilities to test inhibiting molecules, with the aim of developing new drugs able to block the bacterial cell division machinery.

2.1 Bacterial cell division in the model organisms

Far from being a clear and simple process, division septum formation needs the hierarchic localization of specific proteins and their assembly at the cell division site in a multi-protein apparatus, called the *septosome* or *divisome*, whose molecular events have been clarified in more detail for the rod-shaped model organisms *E. coli* and *B. subtilis* (Adams and Errington, 2009; de Boer, 2010; Lutkenhaus *et al.*, 2012; Egan and Vollmer, 2013). Moreover, the cell division site is commonly located at the center of the cell, perpendicular to the long axis, to allow the generation of two identical daughter cells, each corresponding more or less to the half of the mother cell (Trueba, 1982).

In the model organisms, about twelve common proteins (FtsZ, FtsA, ZapA, ZapB, FtsE/X, FtsK, FtsQ, FtsL, FtsB, FtsW, FtsI) have been identified to localize to the division septum, in a hierarchic and interdependent order. In the hierarchical sequence of localizations, every protein (or group of them) once localized to the septum is also responsible for the localization of the protein(s) that arrive subsequently (de Boer, 2010; Lutkenhaus *et al.*, 2012; Egan and Vollmer, 2013; Huang *et al.*, 2013; Massidda *et al.*, 2013). However, the hierarchical recruitment of the divisome components seems to be less stringent in *B. subtilis* (Errington *et al.*, 2003; Adams and Errington, 2009). Moreover, specific proteins such as ZipA, ZapC & D have been found only in *E. coli* and other Gram-negative species, while other proteins, like EzrA, SepF and DivIVA, have been found only in Gram-positives, as *B. subtilis* and *S. pneumoniae*.

FtsZ is the first protein that localizes to the septum at the beginning of cell division (Bi and Lutkenhaus, 1991). In *E. coli*, immediately after FtsZ, FtsA and ZipA are then recruited to midcell, and these proteins have the ability to anchor FtsZ to the cell membrane and stabilize the Z-ring; moreover they are also responsible for the recruitment of the later proteins of the divisome (de Boer, 2010; Lutkenhaus *et al.*, 2012; Egan and Vollmer, 2013; Huang *et al.,* 2013). Both FtsA and ZipA are essential for the correct assembly of the divisome (Hale and de Boer, 2002; Goehring and Beckwith, 2005; Vicente *et al.*, 2006) and the double mutant lacking both proteins fail to assemble

the Z-ring (Pichoff and Lutkenhaus, 2002). However, their conservation in different bacterial species is not the same, with FtsA much more conserved than ZipA, which is present only in γ-proteobacteria (Vicente *et al.*, 2006).

Consistently, in Gram-positive bacteria ZipA is not present. In *B. subtilis* the *ftsA* gene is not essential and its deletion gives rise to long filamentous thermosensitive cells lacking the division septum (Beall & Lutkenhaus, 1992; Jensen *et al.*, 2005). However, other proteins may have a function similar to that of ZipA, like the negative modulator of cell division EzrA (Lutkenhaus *et al.*, 2012) and another protein named SepF that shows common functions with FtsA (Ishikawa *et al.*, 2006), as the simultaneous deletion of both EzrA and SepF is lethal for *B.subtilis* (Hamoen *et al.* 2006).

ZapA, ZapB, ZapC and ZapD are all non-essential components of the divisome that also contribute to the stabilization of the Z-ring; ZapC and ZapD have been found in *E. coli* but not in *B. subtilis* (Gueiros-Filho & Losick, 2002; Ebersbach *et al.*, 2008; Mohammadi *et al.*, 2009; Durand-Heredia *et al.*, 2012).

Once the Z-ring is formed, the process of recruiting the late proteins of the divisome is gradual and requires time to be achieved. After the earliest proteins are localized to the division site, two proteins, FtsE and FtsX, are recruited to the divisome and form a complex. This complex is an ABC transporter recruited to midcell directly by FtsZ through interaction with FtsE (Schmidt *et al.*, 2004; Corbin *et al.*, 2007; Reddy, 2007). In *B. subtilis* the FtsEX complex is not essential for cell division, but is required for the asymmetric cell division during sporulation (Garti-Levi *et al.*, 2008).

An important member of the divisome is FtsK, which is involved in chromosome partitioning before septum closure (Liu *et al.*, 1998; Massey *et al.*, 2006) and the recruitment of other cell division proteins such as FtsQ (DivIC), FtsB (DivIC) and FtsL (Buddelmeijer and Beckwith, 2004). Another essential member of the late division proteins is FtsW, an integral transmembrane protein, responsible for the translocation of the peptidoglycan precursor Lipid II (Mohammadi *et al.*, 2011). FtsW is also responsible for the recruitment of another essential protein of the divisome

FtsI (*E. coli* Pbp3) that together with another interacting PBP, Pbp1B, synthesizes the septal PG during cell division (Bertsche *et al.*, 2006; Egan and Vollmer, 2013).

The last protein to be localized to the *E. coli* divisome is FtsN, which is required for the latest steps of cell division. FtsN is thought to be the signal to the other proteins in the cytoplasmic face of the complex for completion of the divisome, allowing contraction of the division machinery with the contemporary synthesis of septal PG (Gerding *et al.*, 2009; Rico *et al.*, 2010; Busiek *et al*., 2012; Pichoff *et al*., 2015). FtsN is not present in Gram-positive bacteria, as *B. subtilis* and *S. pneumoniae.*

During the cell cycle, cell division is closely related to cell wall synthesis and the two processes are strictly regulated and coordinated with each other to avoid cell damage and aberrant morphology. In rod-shaped bacteria, the machinery involved in the peripheral PG synthesis, the *elongasome*, is also a multi-protein complex, orchestrated by the actin-like MreB protein, which is responsible for cell elongation (den Blaauwen *et al.*, 2008; Typas *et al.*, 2012) and is physically separated from the multi-protein complex involved in septal PG synthesis, the *divisome,* which is orchestrated by the tubulin-like FtsZ protein and is responsible for cell division (Goehring and Beckwith, 2005; Vicente *et al.*, 2006; Lock and Harry, 2008; de Boer, 2010; Lutkenhaus *et al.*, 2012; Egan and Vollmer, 2013). Despite that the elongasome and the divisome are somehow connected (van der Ploeg *et al*., 2013), it is widely accepted that, in the rod-shaped organisms, the two machineries compete with each other and lateral PG synthesis is inhibited during cell division and *vice versa* (Lleo *et al.*, 1990).

In *E. coli*, the elongasome is composed of MreB, MreC, MreD, PBP2, PBP1A, RodA and RodZ. The elongosame of *B. subtilis* has the same proteins, but in addition carries two MreB paralogs, MbI and MreBH (Carballido-López & Formstone, 2007), and another protein, GpsB (Claessen *et al.*, 2008; Tavares *et al.*, 2008) which are absent in *E. coli*. GpsB has been shown to interact with BsPbp1, MreC and EzrA and is proposed to have a complex role, along with EzrA, in shuffling of Pbp1 between the elongation and the division cycles (Claessen *et al.*, 2008). Deletion of *gpsB* does not lead to altered phenotype, but has a synthetic lethal effect when combined with deletion of

ezrA (Claessen *et al.*, 2008) or with *ftsA* (Tavares *et al.*, 2008). The membrane proteins MreC and MreD, together with MreB, can be considered core proteins of the elongasome and they form a membrane complex that is essential in both *E. coli* and *B. subtilis*: MreB forms actin-like cables beneath the cell surface, with MreC interacting with itself and both MreB and MreD (Kruse *et al.*, 2005). This complex is responsible for the localization of the other proteins that synthesize PG along the longitudinal axis, resulting in cell elongation (Jones *et al.*, 2001; Kruse *et al.*, 2005; Leaver and Errington, 2005). The last discovered member of the elongasome is RodZ (Shiomi *et al.*, 2008), that interacts with and tethers MreB to the membrane (van den Ent *et al.*, 2010) and seems required for cell shape maintenance (Bendezú *et al.*, 2009; Gerdes, 2009).

2.2 Cell division in *Streptococcus pneumoniae*

The interest in cell division of *S. pneumoniae* has started mainly to identify and characterize targets to develop novel antimicrobials. Initially, the *dcw* gene cluster of *S. pneumoniae* was identified and shown to differ in its organization from the *dcw* clusters of other bacteria (Massidda *et al.*, 1998; Fig. 1), despite cell division proteins encoded by the dcw gene being significantly conserved. Genomic analysis of the *dcw* cluster of *S. pneumoniae* also led to the identification of an extended syntenic region downstream of the *ftsA* and *ftsZ* genes, present in both low and high GC% Gram-positive bacteria and cyanobacteria, but absent in Gram- negatives, which contained yet uncharacterized genes as well as genes encoding homologs of YlmG, YlmF/SepF and DivIVA that are involved in chromosome segregation, cell morphology and/or cell division in various species (reviewed in Massidda *et al.*, 2013).

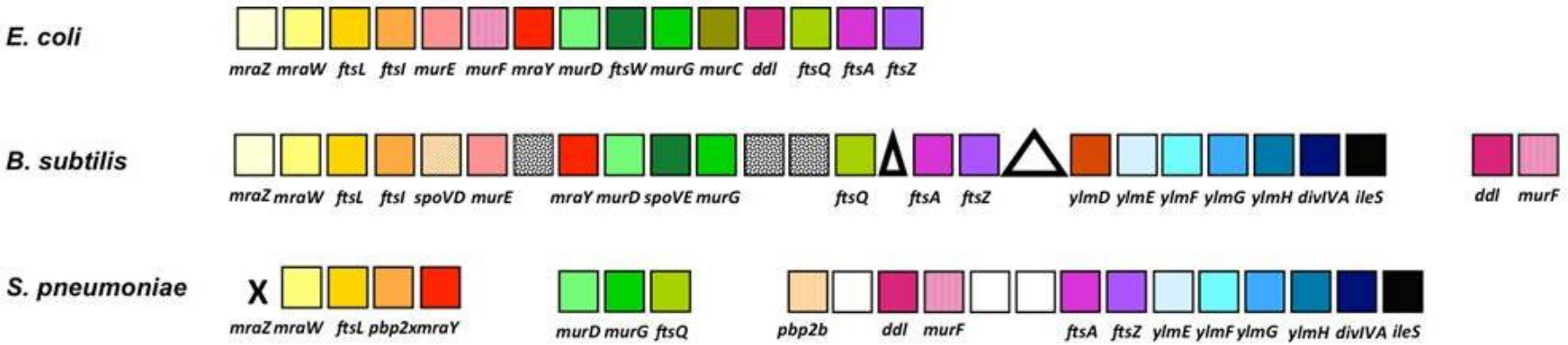

Figure 1. Organization of the dcw cluster of *S. pneumoniae* in comparison with that of *E. coli* and *B. subtilis*. The genes are indicated with boxes and their respective names are designated below. Identical colours or shading patterns in different species indicate orthologs. The stippled boxes indicate that the ortholog is present in the genome but is located in another chromosomal region. The X indicates orthologs that are missing in that genome. The empty boxes indicate unrelated genes and are thus not named. The triangle indicates a small insertion of variable length (adapted from Massidda *et al.*, 1998)

In agreement with the accepted model for streptococcal growth and division (Higgins and Shockman, 1970 and 1976), like the model rods, *S. pneumoniae* maintains its oval cell shape by alternating peripheral PG synthesis, that occurs during cell elongation, with septal PG synthesis, that occurs during cell division (Massidda *et al.*, 2013; Pinho *et al.*, 2013).

As explained above for *E. coli* and *B. subtilis*, these processes are guaranteed by specialized proteins that assemble in two distinct separate machineries, the divisome (de Boer, 2010; Lutkenhaus *et al.*, 2012; Egan & Vollmer, 2013; Rico *et al.,* 2013) and the elongasome (Typas *et al.*, 2012). In agreement with these findings, the *S. pneumoniae* chromosome encodes proteins that are proven or likely to be part, respectively, of the divisome and/or the elongasome machineries.

S. pneumoniae contains the cell division proteins present in *B. subtilis* and other Gram-positives, and lacks some present in *E. coli*, like ZipA, ZapC, ZapD and FtsN. Almost all of these proteins have been shown to localize to the septum in dividing *S. pneumoniae* cells with a few that localize both at midcell and the cell poles (Massidda *et al.*, 2013). While a precise order of recruitment to the septum has not yet been established, the timing of localization based on fluorescence studies suggests that, also in pneumococci, divisome formation occurs in at least two steps.

The essential cell division initiator proteins FtsZ and FtsA localize to midcell at the earliest stages of the process (Morlot *et al.*, 2003; Lara *et al.,* 2005), while the septal markers DivIB (FtsQ), DivIC (FtsB), FtsL, FtsW, PBP2x, PBP1a (Morlot *et al.*, 2003; 2004; Noirclerc-Savoye *et al.*, 2005; Peters *et al.*, 2014; Tsui *et al.*, 2014), and the cell division protein DivIVA (Fadda *et al.*, 2007; Beilharz *et al.*, 2012) localize only after the Z-ring has assembled. In addition, other cell division proteins, like GpsB that, together with PBP2x is required for septum closure, has been also shown to localize to midcell, and its localization overlaps only in part with that of FtsZ (Land *et al.*, 2013). The Z-ring formation requires about half of the cell cycle before septation can occur (Fadda *et al.*, 2007), in agreement with the observation that about 50% of the cell cycle is devoted to cell elongation and the other 50% to division (Wheeler *et al.*, 2011; Fig. 2).

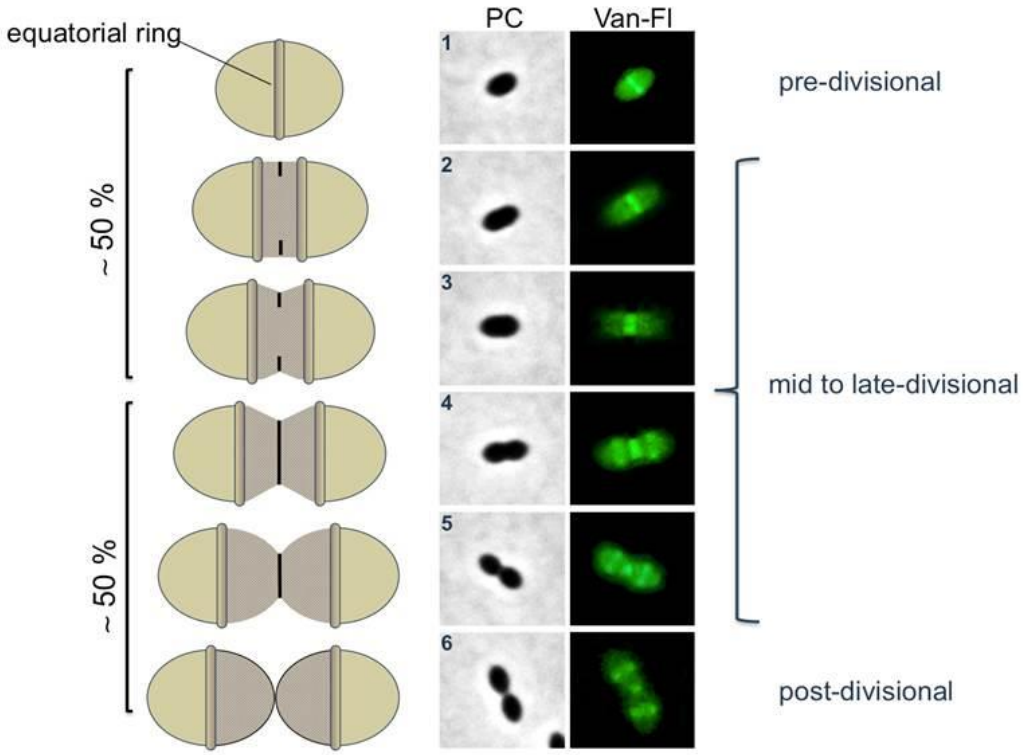

Figure 2. Model for growth and division in *S. pneumoniae*. Schematic view of the six stages of the pneumococcal cell division (left panel) and site of insertion of the new synthetized peptidoglycan (PG) detected with Van-Fl staining (right panel). PC: phase-contrast and and VanFL: Bodipy-Vancomycin.

As all the non rod-shaped bacteria*, S. pneumoniae* lacks the rod-shape determinant MreB, but has all the other components that are known to constitute the elongasome, including MreC, MreD and PBP2b, which are part the pneumococcal elongation machinery (Land and Winkler, 2011; Berg et al, 2014). Together, these results support the previous hypothesis that, similarly to the rod-shaped models, *S. pneumoniae* has two PG biosynthetic complexes (Massidda *et al.*, 1998; Morlot *et al.*, 2003; Zapun *et al.*, 2008). However, unlike the model rods, both the elongation and the cell division components localize to midcell, raising the question if in *S. pneumoniae*, proteins involved in the peripheral and septal PG synthesis are assembled into two distinct and separate complexes or into a single large one.

Recent advances in pneumococcal cell division support a model in which a single large machinery, containing both the peripheral and septal PG synthesis complexes, assembles at midcell and

governs growth and division (Massidda *et al.*, 2013; Fig. 3). To function properly, such a large machinery would require regulatory mechanisms able to monitor the cell cycle progression and to signal when it is time to stop elongating and start dividing. Although in streptococci, regulation of growth *vs* division may be achieved by the action of the eukaryotic-type Ser/Thr protein kinase, StkP, (Beilharz *et al.*, 2012; Fleurie *et al.*, 2012), the molecular mechanisms at the base of the process are still unknown and a matter of intense debate and it seems now to involve some unpredicted players among the cell division proteins (Fleurie *et al.*, 2014a).

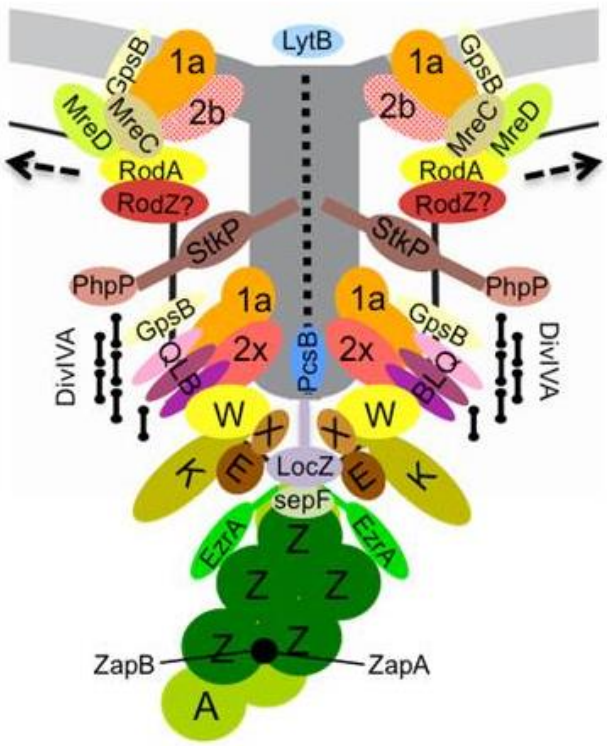

Figure 3. Schematic representation of the S. pneumoniae peptidoglycan (PG) biosynthetic machinery at the midcell, containing the complexes involved in cell elongation and in cell division. The 'old' cell wall is in black, the peripheral wall is in light grey and the septal wall is in dark grey. Z, A, E, X, K, Q, B, L, W, 1a, 2x and 2b stand for FtsZ, FtsA, FtsE, FtsX, FtsQ (DivIB), FtsB (DivIC), FtsL, FtsW, PBP1a, PBP2x and PBP2b, respectively. The black bars represent DivIVA. The midcell localized StkP and PhpP proteins that regulate growth and division by signaling are also shown. The localizations of ZapA, ZapB, EzrA, SepF, GpsB, RodA and RodZ are extrapolated from what is known in the model rods and awaits experimental verification (Massidda *et al.*, 2013)

Very recently a protein called LocZ or MapZ, respectively (Holečková *et al.*, 2014; Fleurie *et al.*, 2014) has been found as the responsible factor for the proper spatial placement of the Z-ring by two independent research groups. LocZ/MapZ localizes to the midcell before FtsZ and FtsA, together with the equatorial rings or wall bands that mark the cell equator and its localization is required for proper localization of FtsZ and FtsZ-associated proteins (Fleurie *et al.*, 2014; Holečková *et al.*, 2014). Consistently, the lack of LocZ/MapZ leads to Z-ring misplacement, resulting in misshaped cells with asymmetric septa and minicells, some of which devoid of nucleoids (Holečková *et al.*, 2014). Interestingly, LocZ/MapZ is also a substrate for StkP, although the role of phosphorylation remains controversial (Fleurie *et al.*, 2014; Holečková *et al.*, 2014). Finally, LocZ/MapZ is a unique protein, conserved only in a closely phylogenetically related group of bacteria, such as streptococci, lactococci, and enterococci, suggesting that they evolved a highly specific solution to select their cell division site, reflecting the specific requirements of the group to maintain cell symmetry and shape.

3. The importance of FtsA in cell division

As mentioned above, the division process in bacteria starts with the localization of FtsZ at midcell and FtsZ is the most widespread cell division protein, conserved in almost all species (reviewed in Busiek & Margolin, 2015).

Despite the poor sequence homology, the FtsZ crystal structure is considerably similar to tubulin, supporting the notion that these two proteins share a common ancestor (Löwe & Amos, 1998).

Consistently, upon GTP binding, FtsZ polymerizes into protofilaments and attachment of FtsZ to the cell membrane is believed to be crucial for its assembly into a ring-like structure, known as the Z-ring. Even if FtsZ does not have a direct affinity for the membrane, all models for the formation of the Z-ring predict FtsZ binding with the membrane in order to keep its structural integrity during septum formation and/or to exert the constriction force to allow septation.

In a recent study, Szwedziak and colleagues demonstrated that FtsZ and FtsA together are able to polymerize *in vitro* and produce membrane shrinkage of liposomes, creating a negative curvature (Szwedziak *et al.*, 2014). In the study, the Z-ring is proposed as a spiral complex of FtsZ and FtsA filaments that, although discontinuous, are able to form a continuous ring which, after initial polymerization, constricts by a sliding mechanism, reducing its diameter and thus resulting in membrane constriction and, at the end of the process, in two separated spirals that allow abscission of the membrane (Szwedziak *et al.*, 2014). The important role of FtsZ and FtsA in bacterial growth and division has been recently reviewed by Busiek and Margolin, 2015.

FtsA is the second protein recruited to the septum. Less conserved than FtsZ, FtsA is also widespread in different bacterial species and is believed to be recruited to midcell together or immediately after FtsZ, at the earliest stages of the division process, and its correct localization depends on the localization of FtsZ.

FtsA is an ATP-binding protein structurally similar to actin (van den Ent & Löwe, 2000). However, differently from actin which contain four structural subdomains (1A, 1B, 2A and 2B), FtsA is characterized by the absence of subdomain 1B and the presence of an additional subdomain, 1C, on the opposite site of the molecule (van den Ent *et al.*, 2001, Fig. 4). Subdomain 1C, composed of three anti-parallel β-chains and one α-helix, is significantly different from the other subdomains of actin and the other actin-like proteins of the Hsp70 superfamily, suggesting a crucial importance of this domain for the function of FtsA (van den Ent & Lowe, 2000).

As the eukaryotic actin, FtsA is an ATP-binding protein (Sanchez *et al.*, 1994; van den Ent & Lowe, 2000; Feucht *et al.*, 2001; Lara *et al.*, 2005) and its ATP binding site is located in the hydrophobic cleft made by subdomains 1A, 2A and 2B (van den Ent & Lowe, 2000). Consistently, FtsA polymerizes *in vitro* in the presence of ATP (Lara *et al.,* 2005), but no polymerization is observed in its absence (Lara *et al.*, 2005; Krupka *et al.*, 2012 and 2014). Despite the ability of FtsA to bind ATP, up to now (Herricks *et al.*, 2014) an FtsA ATPase activity has never been clearly shown and the ability of FtsA to hydrolyze ATP remains controversial.

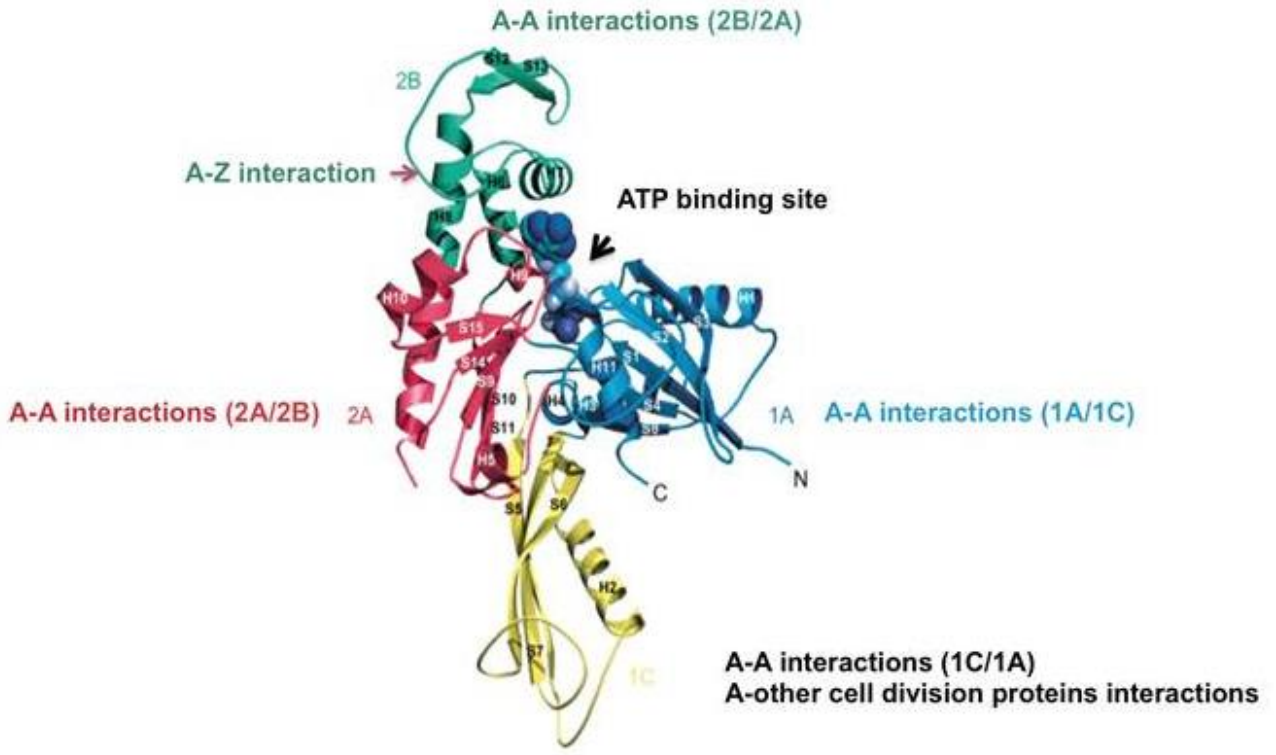

Figure 4. Crystal structure of FtsA from Thermotoga maritima. The four subdomains are shown in different colors and the ATP binding site is indicated by an arrow (van den Ent & Lowe, 2000).

In *E. coli*, FtsA is an essential protein, while its absence is tolerated in *B. subtilis,* where its deletion results in thermosensitive filaments, showing dramatic defects in growth and morphology as well as in Z-ring assembly (Beall and Lutkenhaus, 1992). FtsA has been reported to be essential also in *S. pneumoniae*, where the deletion of *ftsA* gene is lethal (Lara *et al.*, 2005).

In *E. coli*, there is strong evidence that both FtsA and ZipA act to tether FtsZ to the membrane (Fig. 5). Interestingly, several mutations in *ftsA*, able to suppress the lack of ZipA, have been identified (Geissler *et al.*, 2007; Pichoff *et al.*, 2012), suggesting that these proteins have a similar function in stabilizing the Z-ring and explaining why, when both proteins are absent, the Z-ring is not able to form. However, many bacteria, as all the Gram-positives, lack a ZipA homolog and the dynamics of tethering FtsZ to the cell membrane in these species remains to be clarified.

FtsA is able to interact with itself and with both early and late proteins of the divisome, and some of the interactions are conserved between *E. coli* and *S. pneumoniae* FtsA (EcFtsA and SpFtsA,

respectively). Fig. 5 shows the complex network of interactions within the members of the divisome of these two organisms, detected using a bacterial two-hybrid assay, including FtsA (Di Lallo *et al.*, 2003; Karimova *et al.*, 2005; Maggi *et al.*, 2008). As in *E. coli*, SpFtsA shows interactions with itself, FtsZ, ZapA and FtsI (PBP2x and PBP3, respectively). Specific interactions were identified between SpFtsA with FtsL and FtsK (Maggi *et al.*, 2008) and for EcFtsA with FtsN (Busiek *et al.*, 2012). Moreover, in other studies SpFtsA has been shown to interact also with the cell division proteins DivIVA and EzrA (Fadda *et al.*, 2007; unpublished results), which are specific of Gram-positives.

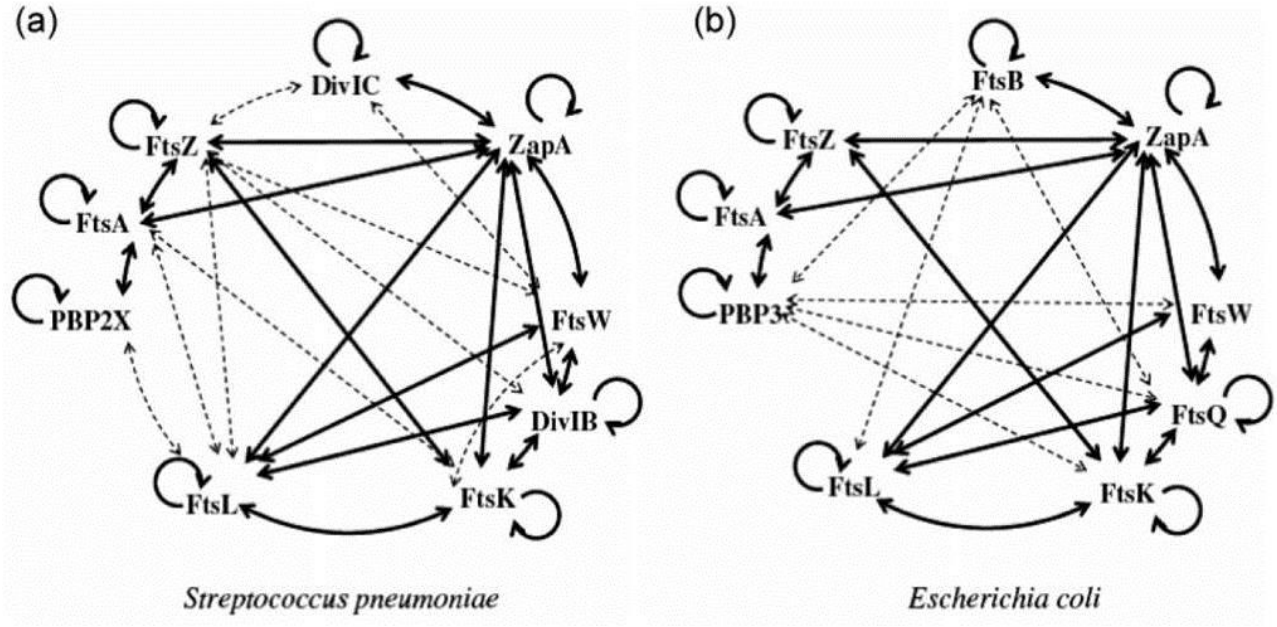

Figure 5. Interaction network between some of the members of *S. pneumoniae* and *E. coli* divisomes. Conserved interactions are shown with unbroken arrows, species-specific interactions are shown with dashed arrows and self-interactions are shown with circular arrows (Maggi *et al.*, 2008).

It is now commonly accepted that binding of FtsA to ATP, and thus polymerization of FtsA, is crucial for its *in vivo* function (Carrettoni *et al.*, 2003; Lara *et al.*, 2005; Pichoff and Lutkenhaus, 2005; Shiomi & Margolin, 2008; Szwedziak *et al.*, 2012 and 2014; Krupka *et al.*, 2012).

The ability of FtsA to polymerize *in vitro* in the presence of ATP has been reported first in *S. pneumoniae* (Lara *et al.,* 2005), but its *in vivo* biological significance awaits confirmation. However, two variants of the *S. pneumoniae* FtsA protein truncated in domain 1C or 2B (β-strand S12 and

S13), previously shown to impair *E. coli* FtsA functionality *in vivo* (Rico *et al.*, 2004), were found to inhibit the ATP-dependent polymerization of the pneumococcal wild-type protein and its ability to polymerize *in vitro*, confirming the importance of these regions for FtsA function (Krupka *et al.*, 2012). In a more recent study, it has been proposed that binding of ATP with *S. pneumoniae* FtsA leads to a conformational change of the C-terminus of the protein, allowing polymerization and its binding to the cytoplasmic membrane (Krupka *et al.*, 2014). The FtsA C-terminus is a non-organized part of the protein, (van den Ent & Löwe, 2000), but computer models predict the presence of an amphiphatic helix, indicated as MTS (Membrane Targeting Sequence), that seems responsible for the attachment and localization of FtsA to the cell membrane and thus crucial for the correct function of the protein to interact with FtsZ.

FtsA polymerization has been found to be important for FtsA *in vivo* function in *E. coli* (Pichoff and Lutkenhaus, 2005; Shiomi & Margolin, 2008, Pichoff *et al*., 2012). The results are supported in a more recent study, based on its crystal structure, which showed for the first time that indeed FtsA can polymerize in the presence of a lipid monolayer surface and forms actin-like protofilaments (Szwedziak *et al.*, 2012; Fig. 6).

In *E. coli*, FtsA is needed to both tether FtsZ to the membrane and to recruit later division proteins to the septum. Interestingly, using genetic screening with cells mutated in *ftsA*, it has been shown that several mutations located in subdomain 2B, impairing the ability of FtsA to interact with FtsZ in the two-hybrid assay but not its ability to localize to the cell membrane, are not able to complement a *ftsA Ts* phenotype, demonstrating that subdomain 2B is indeed responsible for the interaction of FtsA with FtsZ and this function is crucial for the cell (Pichoff and Lutkenhaus, 2007). Moreover, a "gain-of-function" mutation in *ftsA*, R286W (also known as FtsA*), that is able to bypass the essentiality of ZipA, mapped in the S13 β-strand also in subdomain 2B (Geissler *et al.*, 2007). The FtsA* allele was shown to have increased interaction with FtsZ, but, surprisingly, similarly to other mutated FtsA alleles, decreased self-interactions, raising the interesting possibility that FtsA polymerization status competes with its monomeric status, required to recruit

the late division proteins, acting as a negative regulator of the divisome (Pichoff *et al.*, 2012) and thus that the ability of FtsA to recruit the late cell division proteins is inversely proportional to its propensity for self-interactions, which is negatively modulated by ZipA (Pichoff *et al.*, 2012).

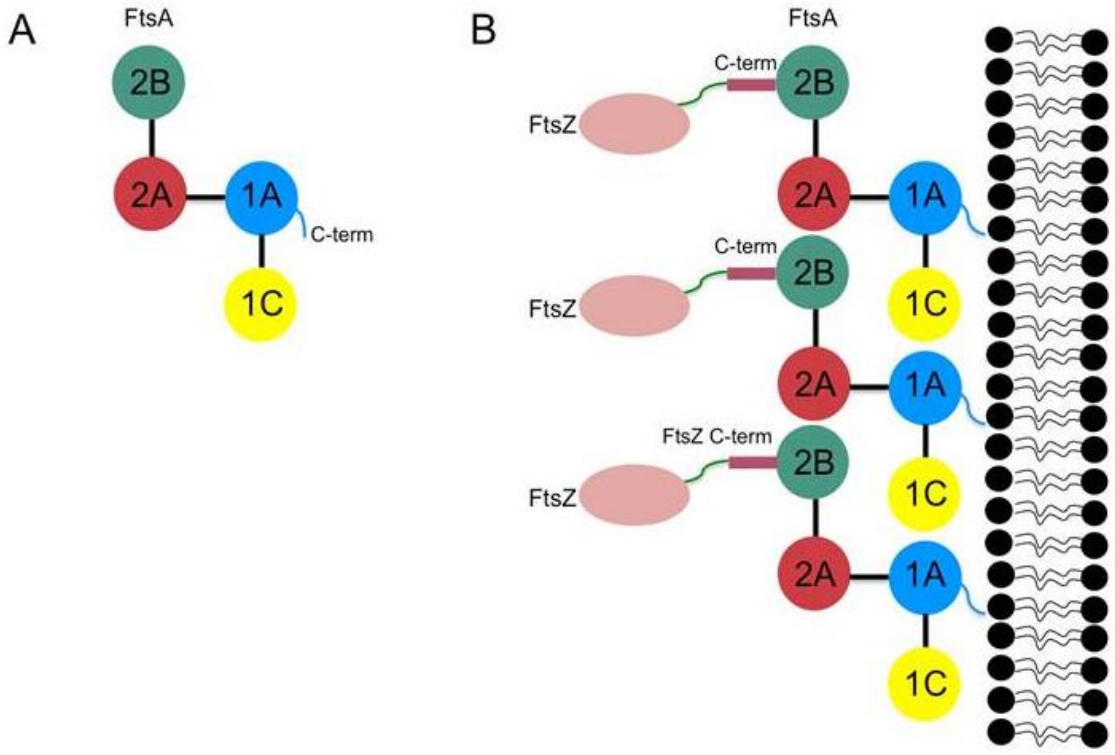

Figure 6. Role of the FtsA actin-like protein for cell division in *E. coli*. FtsA with the 4 subdomains (1A, 1C, 2A, and 2B, shown in different colors) and with the carboxy-terminal amphipathic helix that serves as a membrane anchor. Although not well characterized, ATP binding seems to be required for the formation, from monomeric FtsA **(A),** of FtsA head-to-tail polymers of **(B)**, which then may be able to interact with FtsZ polymers at the membrane.(Busiek & Margolin, 2015).

Aim of the work

Given the importance of FtsA in bacterial cell division, the main scope of my work was to generate and characterize S. pneumoniae ftsA thermosensitive mutants to: a) elucidate the role of FtsA in pneumococcal cell division, b) understand the physiological role of its polymerization and c) validate FtsA as a cell division target in this clinically important Gram-positive pathogenic coccus.

For this purpose, I have constructed, by a random mutagenesis, three conditional lethal ftsA Ts mutants and characterized them by studying the effects on growth and morphology upon shifting to the non permissive-temperature, in temperature-shifting experiment.

I have also performed complementation studies with GFP-FtsA and tested the interactions between the mutated FtsA Ts proteins with themselves and with the other cell division proteins that are known to interact with FtsA, like FtsZ, using a bacterial two-hybrid system.

Finally, I have tested how the FtsA Ts mutations affects the localization of other cell division proteins like FtsZ, DivIVA, GpsB, StkP and PBP2x, using both GFP and IEM fluorescence.

Materials and Methods

1. Bacterial strains, plasmids and growth condition

Bacterial strains and plasmids used in this study are listed in Table 1. *S. pneumoniae* strains were derived from Rx1, a non-encapsulated well characterized laboratory strain (Ravin, 1959). Bacteria were routinely grown in Columbia Agar (CA) or Tryptone Soya Agar (TSA; Oxoid) supplemented with 5% defibrinated sheep blood (CBA or TSBA) or Tryptone Soya Broth (TSB; Oxoid) at 37°C statically or in an atmosphere of 5% CO_2, as previously described (Fadda *et al.*, 2003; Fadda *et al.*, 2007). Alternatively, bacteria were grown in the semi-synthetic C medium (Lacks and Hotchkiss, 1960) supplemented with 0.1% yeast extract (C+Y). In particular, this medium was used in protein expression experiments from the PZn promoter, as allows a more precise control of $ZnCl_2$ induction as well as a better visualization of the GFP fluorescence (Eberhard *et al.*, 2009; Beilharz *et al.*, 2012). Growth of the FtsA temperature-sensitive (ts) mutants was carried out at 32°C or 28°C. In temperature shifting experiments, incubation was carried out at 28°C and shifted to 40°C (see below). When appropriate, chloramphenicol (4.5 μg/ml) and/or tetracycline (1.0 μg/ml or 2.5 μg/ml, respectively) were added to the growth medium. For induction of the PZn promoter, $ZnCl_2$ (Sigma-Aldrich) was added to liquid medium and blood agar plates at different concentrations, depending on the medium used (Beilharz *et al.*, 2012). Competent *S. pneumoniae* cells were prepared and transformed by the addition of competence-inducing peptide CSP-1, as previously described (Fadda *et al.*, 2003).

Escherichia coli DH5a strain (Hanahan, 1983) was used as a host for cloning and growth in Luria–Bertani (LB) broth and agar at 37°C, supplemented with ampicillin (100 μg/ml) and kanamycin (50 μg/ml) when required. *E. coli* BTH101 were used as hosts in bacterial two-hybrid assay (Karimova *et al.*, 1998; Karimova *et al.*, 2005) and cultivated in LB broth or agar at 37°C or 30°C, supplemented when required with ampicillin (100 μg/ml) or kanamycin (50 μg/ml).

2. Construction of *S. pneumoniae ftsA* temperature-sensitive (Ts) mutants

S. pneumoniae ftsA temperature-sensitive (Ts) mutants were generated by error-prone PCR, using the GeneMorph II random mutagenesis kit (zero to four mutations per kbp; Stratagene), as described by Sham *et al.*, 2011. pRSETA(spn*ftsA*) plasmid DNA, containing the *S. pneumoniae* $ftsA_{WT}$ gene (Lara *et al.*, 2005, Table 1) was purified using a Qiagen Plasmid Mini Kit and used as a template in PCR experiments, according to the manufacturer's instructions, using primers spnBF-*ftsA* and spnER-*ftsA* (Table 2). About 100-200 ng of error-prone *ftsA* PCR fragments, obtained were then transformed into Rx1 competent cells. In the absence of a selectable marker, different ten-fold dilutions were plated onto TSBA plates and incubated at 32°C for 16-18 h. Putative transformant colonies were then patched onto two duplicate TSBA plates. One plate was incubated at 32°C and the other plate was incubated at 40 °C. Colonies that grew at 32 °C but not 40 °C were single colony isolated on TSBA plates for three passages at 32 °C and 40 °C, before being confirmed Ts and stored as frozen glycerol stocks. Mutations in *ftsA* were verified by double-strand sequencing the corresponding *ftsA* amplicons obtained by PCR using the proofreading ExTaq DNA polymerase (Takara) and the primers listed in Table 2.

3. Growth curves, viability, and microscopy.

For physiological and morphological analysis, cells were inoculated from frozen glycerol stocks into pre-warmed TSB or C+Y medium and incubated at the appropriated temperature. Growth was monitored turbidimetrically every 30 min with an Ultrospec 3100 (Amersham Pharmacia Biotech) or with a DU 730 spectrophotometer (Beckman Coulter) at 650 nm (TSB) or 600 nm (C+Y). Viable counts were determined every 90 min by tenfold serial dilution of the cultures and spotting 20 µl onto TSBA plates , followed by incubation at the appropriate temperature for 16-18 h.

For temperature shifting experiments cells from frozen stocks were diluted in TSB or C+Y medium, pre-warmed to 28°C, and grown until they reached 0.3 OD (*i.e.*, 4-5 doublings). At this point cultures were diluted in the respective pre-warmed media and incubated at 28°C (permissive

temperature) or shifted to 40°C (non-permissive temperature). Growth after shifting was monitored every 30 min for 3 h. For microscopic analysis, samples (100 µl) were taken every 30 min, transferred to Eppendorf tubes and fixed with 4% para-formaldehyde (Immunofix, Bioptica) for 15 min at room temperature. When required, 2 µl of DAPI (0.5 µg/ml) was added to 10 µl of cells, and samples incubated for 5 to 10 min at room temperature in the dark before microscopic examination. Aliquots 2-10 µl were transferred to poly-L-lysine-coated slides and examined using a Zeiss Axioskop HBO 50 or an Olympus CellR IX 81 microscope equipped with 100× phase-contrast and fluorescence objectives. When required, 2 µl of Vecta Shield mounting media for fluorescence with DAPI (1.5 µg/ml) (Vector Laboratories, Inc.) were added to 10 µl of cells, and samples were incubated for 5 to 10 min at room temperature in the dark before microscopic examination. Photographs were taken with a Zeiss MC100 Spot camera or with an Olympus FV2T Digital B/W Fireware camera.

4. Plasmid Construction and DNA Manipulation

Standard protocols for molecular cloning, transformation, and DNA analysis were performed as described by Sambrook *et al.*, 1989. Oligonucleotides were ordered from Sigma-Aldrich. Restriction enzymes, DNA polymerase and T4 ligase were purchased from Roche Diagnostics or New England Biolabs, unless otherwise specified. Plasmids and primers used in this study are listed in Table 1 and 2, respectively.

Plasmids encoding the $FtsA_{TS}$ mutated proteins for their overproduction and purification were obtained by subcloning their respective *ftsA* genes, obtained by PCR from chromosomal DNA of each $FtsA_{TS}$ mutant using primers MK1/MK18 (Table 2), purified with Quiaquick PCR purification kit (Quiagen), digested with BamHI and EcoRI and subcloned into the corresponding sites of the of pRSETA vector (Invitrogen). The respective recombinant plasmids were then transformed into *E. coli* DH5α and positive clones selected onto LB agar plates supplemented with ampicillin. The correct sequence was confirmed by double-strand DNA sequencing. pRSETA*ftsA* (Lara *et al.*, 2005)

was used as a source of $FtsA_{wt}$. pRSETA plasmid harboring mCherry-*ftsA*$_{wt}$ and mCherry-*ftsA*$_{TS}$ mutated genes were obtained by replacing the His tag with the mCherry gene (Krupka *et al.*, 2014).

For bacterial two-hybrid plasmid constructions, *S. pneumoniae ftsA*$_{TS}$ and *ftsZ* genes were amplified by PCR from chromosomal DNA of each of the $FtsA_{TS}$ mutant or $Rx1_{WT}$, using the primers pairs MK17(+1)/MK18 and MK25(+1)/MK26, respectively (Krupka *et al*., 2012; Table 2). PCR fragments were purified, digested with BamHI and EcoRI and subcloned into the corresponding sites of the BACTH vectors pKT25 and pUT18C (Karimova *et al.*, 2005), to generate the corresponding hybrid proteins fused at the C-terminal end of T25 and T18 fragments. As reported for *E. coli ftsZ* (Karimova *et al*, 2005), also *S. pneumoniae* FtsZ fused to the C-terminal end of the T25 fragment (T25-FtsZ) was not functional. For this reason, a PCR-amplified *ftsZ* gene, obtained with the primer pair Z-T25-PF/Z-T25-BR (Table 2), was digested with PstI and BamHI and subcloned into the corresponding sites of the BACTH vector pKNT25 and pUT18 (Karimova *et al.*, 2005), to generate FtsZ fused, respectively, to the N-terminal end of the T25 fragment (FtsZ-T25) and T18 fragment (FtsZ-T18). The respective recombinant plasmids were then transformed in *E. coli* DH5α and, after double-strand sequenced verification, used in complementation assays, as described below. Plasmids pMKV24 and pMKV19 (Krupka *et al.*, 2012; Table S1), carrying a pKT25-*ftsA*$_{WT}$ and pUT18-*ftsA*$_{WT}$, respectively, were used as a source of T25-$FtsA_{WT}$ and T18-$FtsA_{WT}$.

5. Bacterial hybrid assays

The interactions among FtsA and its mutated variants were analyzed by the bacterial two-hybrid (BATCH) method based on the reconstitution of the adenylate cyclase to lead to the cAMP synthesis (Karimova *et al.*, 1998). Each pair of plasmids were co-tranformed in the *E. coli cya* strain BTH101 and co-transformants were plated onto LB agar plated supplemented with ampicillin (100 μg/ml), kanamycin (50 μg /ml), X-Gal (40 μg/ml) and IPTG (0.5 mM), following incubation at 30°C for 24 to 36 h, as previously described (Karimova *et al.*, 2005). Interactions were further confirmed

in MacConkey base/1% maltose agar plates, supplemented with the appropriate antibiotics, and in M63-0.2-0.4% maltose, agar minimum medium, also supplemented with the appropriate antibiotics, and X-Gal (40 □g/ml) with or without IPTG (0.5 mM). Both these media are indicated to detect weak interactions, as they allowed incubation time up to 96 h (Battesti & Bouveret, 2012).

In the case of the FtsA-FtsA pairs, the efficiency of the interactions between the two tested hybrid proteins were also quantified by measuring the β-galactosidase (β-Gal) activity in liquid cultures, accordingly to the Euromedex manual. The enzymatic activity, A (in units per milliliter), was calculated as follows: A = 200 X (OD_{420} of the culture-OD_{420} in the control tube)/minutes of incubation) X dilution factor. One unit of β-galactosidase activity corresponds to the hydrolysis of 1 nmol of ONPG per min at 28°C. The specific activity of β-galactosidase was defined in units per milligram (dry weight) of bacteria. A level of β-galactosidase activity at least four- to fivefold higher than that measured for BHT101(pKT25/pUT18C) (Karimova *et al.*, 2005) cells was considered to indicate an interaction. Each set of experiment was performed at least five times and results expressed as average with standard error indicated.

6.1 Construction of strains expressing PZn-GFP-FtsA and complementation assays

To test complementation, PvuI-digested pJWV25-*gfp-ftsA* plasmid, which carries a copy of the $ftsA_{WT}$ gene under the control of the PZn inducible promoter (Beilharz *et al.*, 2012) was used to transform the $A19_{TS}$, $A20_{TS}$ and $A21_{TS}$ mutants as well as the Rx1 parent strain, as a control. Transformants were selected on TSBA plates, containing 2.5 µg/ml tetracycline, at 28°C. Complementation for growth at 40°C was checked by replica-plating: 50 independent colonies from each transformation were patched onto TSBA plates, containing 2.5 µg /m tetracycline, with or without 0.25 mM $ZnCl_2$, and incubated for 16-18 h at 28°C and 40°C, respectively. Four transformants for each strains were further checked by PCR, and sequenced, using primers listed in Table 2, to verify the correct sequence and integration of the constructs by double cross-over at the *bga* locus.

Complementation at 40°C was also tested in C+Y medium in temperature shifting experiment. Strains were inoculated from frozen glycerol stocks into 10-40 ml of C+Y medium with or without the appropriate $ZnCl_2$ concentrations (0.05-0.15 mM) and serially diluted into the same medium. Overnight cultures with OD_{600} ~ 0.3-0.4 were diluited in the same fresh pre-warmed medium and grown to 28°C until they reached again 0.3 OD. At this point the culture was split in two subcultures and incubated at 28°C and 40°C, respectively. Growth was measured every 30 min and samples for fluorescence microscopy and Western blotting were also taken. For GFP fluorescence microscopy, 2 µl of culture were spotted onto microscope slide, covered with 1% PBS agarose slab and observed using an Olympus CellR IX 81 microscope equipped with Olympus FV2T Digital B/W Fireware.

6.2. Construction of strains expressing other tagged cell division proteins

To obtain *S. pneumoniae* strains expressing the desired protein under the control of the PZn promoter and tagged with GFP at their N-terminal or C-terminal domain (GFP-tagged or tagged-GFP), competent $Rx1_{WT}$ and its isogenic $FtsA_{TS}$ mutants were transformed respectively with plasmids pJWV25-*divIVA-gfp*, pJWV25-*gfp-stkP*, pJWV25-*gfp-gpsB,* pJWV25-*gfp-pbpP2x* (Beilharz *et al*., 2012; Peters *et al.*, 2014, Table 1). As described above, plasmids linearized with PvuI or linear constructs were inserted *via* transformation at the *bga* locus in the respective *S. pneumoniae* strains. Transformants were selected on TSBA or CBA plates, containing 2.5 µg/ml tetracycline, at 28°C. Correct integration by double cross-over of the constructs at the *bga* locus was confirmed by PCR amplification with the oligonucleotides listed in Table 2. Expression of GFP-tagged proteins and GFP fluorescence microscopy at 28°C and 40°C was performed as described above for strains expressing P_{Zn}GFP-FtsA.

To obtain *S. pneumoniae* strains expressing FtsZ-mCherry or CFP-FtsZ, Rx1 and $FtsA_{TS}$ mutants competent cells were transformed with an *ftsZ::mCherry-erm* construct (Sham *et al.*, 2011) or with plasmid pBCSMH036 (Henriques *et al*., 2013). Transformants were selected on TSBA or CBA plates,

containing 0.25 μg/ml erythromycin or 1 μg/ml tetracycline, respectively. Fluorescence microscopy of cell expressing FtsZ-mCherry or CFP-FtsZ proteins at 28°C and 40°C was performed as described above.

7. Western Blot analysis and immunodetection

Western blot analysis was performed to test cellular production of native and/or fusion proteins. Cells were grown in TSB or in C+Y medium at the required temperature, with or without the addition of the appropriate concentration of antibiotics and/or $ZnCl_2$, and monitored turbidimetrically until they reached an OD of 0.4. Cultures (2 ml) were rapidly chilled in an ice bath and microcentrifuged (15,800 x *g*, 3 min, 4°C). When necessary, different culture volumes were taken to contain approximately the same cellular dry weight, as calculated from the ODs (Massidda *et al.*, 1996). Pellets were resuspended in 40 μl of SEDS lysis buffer (SDS 0.02 %; EDTA 15 mM; deoxycholate 0.01%; NaCl 150 mM) and incubated for 5 min at 37°C (Beilharz *et al.*, 2012). Lysates were then mixed with 40 μl of 2X Laemmli buffer (Bio-Rad) and boiled at 100°C for 5 min. After separation by SDS/PAGE, proteins were transferred to a nitrocellulose (Protran BA83, Schleicher and Schuell) or a PVDF (Immobilon-P) membrane. After blocking, membranes were incubated with anti-FtsA and anti-FtsZ (Lara *et al.*, 2005), anti-DivIVA (Fadda *et al.*, 2007), anti-StkP (Beilharz et *al.*, 2012), anti-PBP2x and anti-PBP1a (Peters *et al.*, 2014) polyclonal antibodies, at the appropriate dilution, for 1 h at room temperature and, after washing, with HRP-conjugated antibodies (Bio-Rad) or A8275 (Sigma). Finally, chemiluminescent bands were detected using the Immune-Star HRP Chemiluminescent Kit (Bio-Rad) and Kodak Biomax light films or SuperSignal West Pico Chemiluminescent Substrate (Thermo Scientific) and Agfa Medical X-Ray film blue.

Table 2. Bacterial strains and plasmids used in this study.

Strain	Relevant genotype[a]	Reference
S. pneumoniae		
Rx1	unencapsulated wild type	Ravin, 1959
$A19_{TS}$	Rx1*, ftsA-M209K/D316Y*	this study
$A20_{TS}$	Rx1*, ftsA-V135E/R356S*	this study
$A21_{TS}$	Rx1*, ftsA-P264R/F272S/E281V*	this study
Rx1 FtsZ-mCherry	Rx1, *erm, ftsZ::ftsZ-mCherry*	this study
$A19_{TS}$ FtsZ-mCherry	$A19_{TS}$*, erm, ftsZ::ftsZ-mCherry*	this study
$A20_{TS}$ FtsZ-mCherry	$A20_{TS}$*, erm, ftsZ::ftsZ-mCherry*	this study
$A21_{TS}$ FtsZ-mCherry	$A20_{TS}$ *erm, ftsZ::ftsZ-mCherry*	this study
Rx1+CFP-FtsZ	Rx1, *tet,* pBCSMH036	this study
$A19_{TS}$ +CFP-FtsZ	$A19_{TS,}$ *tet,* pBCSMH036	this study
$A20_{TS}$+CFP-FtsZ	$A20_{TS}$ *tet,* pBCSMH036	this study
$A21_{TS}$ +CFP-FtsZ	$A21_{TS}$ *tet,* pBCSMH036	this study
Rx1+PZn-*gfp-ftsA*	Rx1, *tet, bgaA::*P_{czcD}*-gfp-ftsA*	this study
$A19_{TS}$ +PZn-*gfp-ftsA*	$A19_{TS}$ *tet, bgaA::*P_{czcD}*-gfp-ftsA*	this study
$A20_{TS}$ +PZ*n-gfp-ftsA*	$A20_{TS}$, *tet, bgaA::*P_{czcD}*-gfp-ftsA*	this study
$A21_{TS}$ +*PZn-gfp-ftsA*	$A21_{TS}$, *tet, bgaA::*P_{czcD}*-gfp-ftsA*	this study
Rx1+PZn-*divIVA-gfp*	Rx1, *tet, bgaA::*P_{czcD}*-divIVA-gfp*	this study
$A19_{TS+}$ PZn-*divIVA-gfp*	$A19_{TS}$, *tet, bgaA::*P_{czcD}*-divIVA-gfp*	this study
$A20_{TS+}$PZn-*divIVA-gfp*	$A20_{TS}$, *tet, bgaA::*P_{czcD}*-divIVA-gfp*	this study
$A21_{TS+}$PZn-*divIVA-gfp*	$A21_{TS}$, *tet, bgaA::*P_{czcD}*-divIVA-gfp*	this study
Rx1+PZn-*gfp-stkP*	Rx1, *tet, bgaA::*P_{czcD}*-gfp-stkP*	this study
$A19_{TS}$+*PZn-gfp-stkP*	$A19_{TS}$, *tet, bgaA::*P_{czcD}*-gfp-stkP*	this study
$A20_{TS}$+PZn-*gfp-stkP*	$A20_{TS}$, *tet, bgaA::*P_{czcD}*-gfp-stkP*	this study
$A21_{TS}$+*PZn-gfp-stkP*	$A21_{TS}$, *tet, bgaA::*P_{czcD}*-gfp-stkP*	this study
Rx1+PZn-*gfp-gpsB*	Rx1, *tet, bgaA::*P_{czcD}*-gfp-gpsB*	this study
$A19_{TS}$ +PZn-*gfp-gpsB*	$A19_{TS}$, *tet, bgaA::*P_{czcD}*-gfp-gpsB*	this study
$A20_{TS}$ +PZn-*gfp-gpsB*	$A20_{TS}$, *tet, bgaA::*P_{czcD}*-gfp-gpsB*	this study

$A21_{TS}$ +PZn-*gfp-gpsB*	$A21_{TS}$, *tet, bgaA*::P_{czcD}-*gfp-gpsB*	this study
Rx1+PZn-*gfp-pbp2x*	Rx1, *tet, bgaA*::P_{czcD}-*gfp-pbp2x*	this study
$A19_{TS}$ +PZn-*gfp-pbp2x*	$A19_{TS}$, *tet, bgaA*::P_{czcD}-*gfp-pbp2x*	this study
$A20_{TS}$+PZn-*gfp-pbp2x*	$A20_{TS}$, *tet, bgaA*::P_{czcD}-*gfp-pbp2x*	this study
$A21_{TS}$ +PZn-*gfp-pbp2x*	$A21_{TS}$, *tet, bgaA*::P_{czcD}-*gfp-pbp2x*	this study
Escherichia coli		
DH5α	F^-, 80*dlacZ* M15 *(lacZYA-argF)* U169 *recA1 endA1hsdR17(rk-, mk+) phoAsupE44 -thi-1 gyrA96 relA1*	Hannah, 1983
BTH101	F^-, *cya-99, araD139, galE15, galK16, rpsL1 (*Str^r*), hsdR2, mcrA1, mcrB1*.	Karimova *et al.*, 2005
Plasmid		
pR326	*cm*	Fadda *et al.*, 2003
p*ply::cat*	*cm*	Fadda *et al.*, 2003
pBCSMH036	*tet*	Henriques *et al.*, 2013
pJWV25	*amp*, *tet*, *bgaA*, P_{Zn}-*gfp+*	Eberhardt *et al.*, 2009
pJWV25-*divIVA-gfp*	*amp*, *tet*, *bgaA*, P_{Zn}-*divIVA-gfp*	Beilharz *et al.*, 2012
pJWV25-*gfp-ftsA*	*amp*, *tet*, *bgaA*, P_{Zn}-*gfp-ftsA*	Beilharz *et al.*, 2012
pJWV25-*gfp-stkP*	*amp, tet, bgaA, PZn-gfp-stkP*	Beilharz *et al.*, 2012
pJWV25-*gfp-gpsB*	*amp, tet, bgaA, PZn-gfp-gpsB*	this study
pJWV25-*gfp-pbp2x*	*amp, tet, bgaA, PZn-gfp- pbp2x*	Peters *et al.*, 2014
pKT25	*kan,* pSU40 derivative, encoding T25 fragment of *B. pertussis* CyaA for N-terT25 fusions	Karimova *et al.*, 2005
pUT18c	*amp*, pUC19 derivative, encoding T18 fragment of *B. pertussis* CyaA for N-terminal T18 fusions	Karimova *et al.*, 2005
pKNT25	*kan,* pSU40 derivative, encoding T25 fragment of *B. pertussis* CyaA for C-terminal T25 fusions	Karimova *et al.*, 2005
pUT18	*amp*, pUC19 derivative, encoding T18 fragment of *B. pertussis* CyaA for C-terminal T18 fusions	Karimova *et al.*, 2005
pMKV24	*kan,* T25-$ftsA_{wt}$ in pKT25	Krupka *et al.,* 2012
pMKV19	*amp*, T18-$ftsA_{wt}$ in pUT18C	Krupka *et al*., 2012
pKT25-$ftsA_{19}$	*kan,* T25-$ftsA_{19}$ in pKT25	this study
pUT18c -$ftsA_{19}$	*amp*, T18-$ftsA_{19}$ in pUT18C	this study
pKT25-$ftsA_{20}$	*kan,* T25-$ftsA_{20}$ in pKT25	this study
pUT18c-$ftsA_{20}$	*amp*, T18-$ftsA_{20}$ in pUT18C	this study
pKT25-$ftsA_{21}$	*kan,* T25-$ftsA_{21}$ in pKT25	this study
pUT18c-$ftsA_{21}$	*amp*, T18-$ftsA_{21}$ in pUT18C	this study

pKT25-*ftsZ*$_{wt}$	*kan,* T25-*ftsA*$_{wt}$ in pKT25	this study
pKNT25-*ftsZ*$_{wt}$	*kan, ftsA*$_{wt}$-T25 in pKNT25	this study
pRSETA	*amp*, cloning and expression vector for His tag fusion proteins	Invitrogen
pRSETA-*ftsA*	*amp, ftsA*$_{wt}$ cloned into pRSETA	Lara *et al*., 2005
pRSETA-*ftsA*$_{19}$	*amp, ftsA*$_{19}$ cloned into pRSETA	this study
pRSETA-*ftsA*$_{20}$	*amp, ftsA*$_{19}$ cloned into pRSETA	this study
pRSETA-*ftsA*$_{21}$	*amp, ftsA*$_{19}$ cloned into pRSETA	this study
pRSETA-*mCherry-ftsA*	*amp, mCherry* cloned into pRSETA-*ftsA*	Krupka *et al*., 2014
pRSETA- *mCherry ftsA*$_{19}$	*amp, mCherry* cloned into pRSETA-*ftsA*$_{19}$	this study
pRSETA-*mCherry ftsA*$_{20}$	*amp, mCherry* cloned into pRSETA *ftsA*$_{20}$	this study
pRSETA- *mCherry ftsA*$_{21}$	*amp, mCherry* cloned into pRSETA *ftsA*$_{21}$	this study

[a]*cm*, chloramphenicol resistance marker; *tet*, tetracycline resistance marker, *erm*, erytromicin resistance marker; *amp*, ampicillin resistance marker; *km*, kanamycin resistance marker.

Table 2. Primers used in this study

Purpose	Strain or plasmid	Name	Sequence 5'-3', gene, position	
1. Construction and verification of *S. pneumoniae* Ts mutants	Rx1	spnBF_*ftsA* (+)	CGCGGATCCATGGCTAGAGAAGGCTTTTTTACAGG	*ftsA*, (BamHI) *start codon*
		spnER_*ftsA* (-)	CCGGAATTCCTTGAGCAGCAGCTGTATCAAATG	*ftsA*, (EcoRI) downstream *ftsA*, + 50 bp
		spn*ftsA*_6970 *fow*	ATACGAAGTGCGAAACTTGGA	*ftsA, upstream of ftsA*, - 42 bp
		spn*ftsA*_8450 *rev*	CTTTAATCACTGCCCCTTGAG	*ftsA, downstream ftsA*, + 65 bp
		spn*ftsA*_366 *fow*	GACACCTGACCGTGAAGTCAT	*ftsA*,
		spn*ftsA*_797 *fow*	TAGGCTTCCCCGTAATTCAGT	*ftsA*,
2. Verification of integration of *gfp*- fusions at the ectopic *bga* region	Rx1 derivatives	*bga*_PF_ext_661	GCTCATCATGTTGATTGTCA	*bga region,* (*forward external*)
		PR1_4392	TGTCAATTTGATAGCGGGAAC	*pJW25,* (*reverse internal*)
		PF1_4372	GTTGGGAAGTGGAATGCAGTA	*pJW25,* (*forward internal*)
		*bga*_PR_ext_7834	AGGACAAGAGTTTTTCTTTGG	*bga region,* (*reverse external*)
3. Construction of an *ftsA* conditional knocked-out mutant	Rx1	AKOF1_6297	TGCCACTGTCAGAAAGCCTA	*upstream of ftsA,* -716 bp
		AKOR2_P_{less}	AGTTCATTTGATATGCCTCCTAATCCAAGTTTCGCACTTCGTAT	*cat, ftsA*
	pR326	AKOF3_P_{less}	ATACGAAGTGCGAAACTTGGATTAGGAGGCATATCAAATGAACT	*cat, ftsA*
		AKOR4_P_{less}	CAATACCACCAGGGAGGTCCAATATTATAAAAGCCAGTCATTAG	*cat, ftsA*
	Rx1	AKOF5_P_{less}	CTAATGACTGGCTTTTATAATATTGGACCTCCCTGGTGGTATTG	*cat, ftsA*
		AKOR6_8470	ACCTCCACCGACACCAATTAC	*downstream of ftsA,* +86 bp
4. Construction and verification of plasmids for bacterial two-hybrid assay	pKT25-$ftsA_{TS}$/ pUT18C-$ftsA_{TS}$	MK17 (+1)	CGGGATCCTATGGCTAGAGAAGGCTT	$ftsA_{19,20,21,}$ +1 (BamHI)
		MK18	CGGAATTCTTATTCGTCAAACATGC	$ftsA_{19,20,21,}$ (EcoRI)
	pKT25-*ftsZ*/ pUT18C-*ftsZ*	MK25 (+1)	CGGGATCCTATGACATTTTCATTTGATACAGC	$ftsZ_{wt,}$ +1 (BamHI)
		MK26	CGGAATTCTTAACGATTTTTGAAAAATGGA	$ftsZ_{wt,}$ (EcoRI)
	pKNT25-*ftsZ*/ pUT18-*ftsZ*	*ftsZ*-NT25/18_PF	AACTGCAGGATGACATTTTCATTTGATACAGCTG	$ftsZ_{wt,}$ +1 (PstI)
		ftsZ-NT25/18_BR	CGGGATCCCGATTTTTGAAAAATGGAGGTGTA	$ftsZ_{wt,}$ -1 (BamHI)
	pKNT25-*divIVA*/ pUT18-*divIVA*	*divIVA*-NT25/18_PF	AACTGCAGGATGCCAATTACATCATTAGAAATA	$divIVA_{wt,}$ +1 (PstI)
		divIVA-NT25/18_BR	CGGGATCCTTCTGGTTCTTCATACATTGGG	$divIVA_{wt,}$ -1 (BamHI)
	pKT25	KT25_579 F	GTTCGCCATTATGCCGCATC	*pKT25*, upstream of BamHI site,
		KT25_786 R	GGATGTGCTGCAAGGCGATT	*pKT25*, downstream of EcoRI site,
	pUT18C	UT18c_527F	CGTCGCTGGGCGCAGTGGAACGCC	*pUT18c*, upstream of BamHI site,
		UT18c_639R	CTTAACTATGCGGCATCAGAGC	*pUT18c*, downstream of EcoRI site,

	pKTN25	KTN25_49F	CGCAATTAATGTGAGTTAGC	*pKNT25*, upstream of PstI site,
		KTN25_328R	TTGATGCCATCGAGTACG	*pKNT25*, downstream of BamHI site,
	pUT18	KTN25_49F	CGCAATTAATGTGAGTTAGC	*pUT18*, upstream of PstI site,
6. Construction of plasmids for protein overexpression in *E. coli*	A_{TS}	MK1	CGGGATCCATGGCTAGAGAAGGCTT	*ftsA*, (BamHI) *start codon*
		MK18	CGGAATTCTTATTCGTCAAACATGC	*ftsA*, (EcoRI) *stop codon*
	pRSETA-*ftsA*$_{TS}$	pRSETA_*fow*	ATATACATATGCGGGGTTCT	*pRSETA*, upstream of BamHI site, -110 bp
		pRSETA_*rev*	TAGTTATTGCTCAGCGGTGG	*pRSETA*, downstream of EcoRI site, + 78 bp

[a] Forward and reverse primers are represented by plus (+) or minus (-), respectively.

[b] The sequence underlined in the primer .

[c] - and + indicate respectively upstream and downstream positions relative to the ATG codon of the corresponding gene.

Results and Discussion

1. Generation of FtsA thermosensitive (Ts) mutants and identification of the FtsA Ts mutations.

As *ftsA* in *S. pneumoniae* is essential (Lara *et al.*, 2005), I have generated temperature sensitive (Ts) conditional lethal mutants to further investigate its function. For this purpose, a *ftsA* PCR fragment was obtained with the GeneMorph II Random Mutagenesis kit (Stratagene), using as a template an $ftsA_{wt}$ gene inserted in the pRSETA vector (Lara *et al.*, 2005), setting the error-prone PCR reaction to achieve 0 to 4 mutations/1000 base pairs. The amplicon was transformed into $Rx1_{WT}$ competent cells and the putative transformants were plated, in the absence of a selectable marker, on TSBA plates at 32°C, as described in the Materials and Methods. Isolated colonies were then patched in duplicate and incubated at 32°C and 40°C. Only transformants able to grow at 32°C but not at 40°C were selected and plated serially three times to confirm their Ts phenotype and thus stored as glycerol stocks at -80°C.

Of ~8,000 transformants screened, 24 grew at 32°C but not at 40°C. The Ts transformants were single colony isolated and their *ftsA* gene sequenced. Six of them contained two to three non-synonymous nucleotide changes in the *ftsA* reading frame but none had single change. Three mutants, named $A19_{TS}$, $A20_{TS}$ and $A21_{TS}$, (Fig. 7a) and confirmed to have amino acid substitutions in different domains of the FtsA structure thought to be involved in FtsA polymerization, interactions with FtsZ and/or with other cell division proteins (Fig. 7b), were selected for further characterization.

As shown in Fig 7b, the $A19_{TS}$ mutant has two amino acid substitutions, M209K and D316Y, located respectively in close proximity of the ATP-binding site and in subdomain 2A of FtsA, which may affect both the ability of the $FtsA19_{TS}$ protein to bind ATP, to self-interact with itself and/or to interact with FtsZ; the $A20_{TS}$ mutant has also two mutations, V135I and R356S, mapping respectively in the 1C (H6)

a)

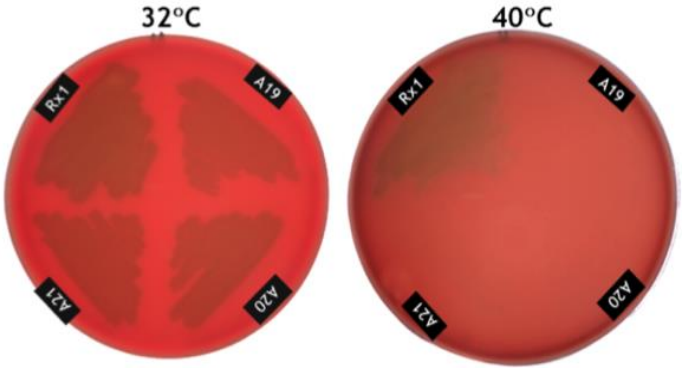

b)

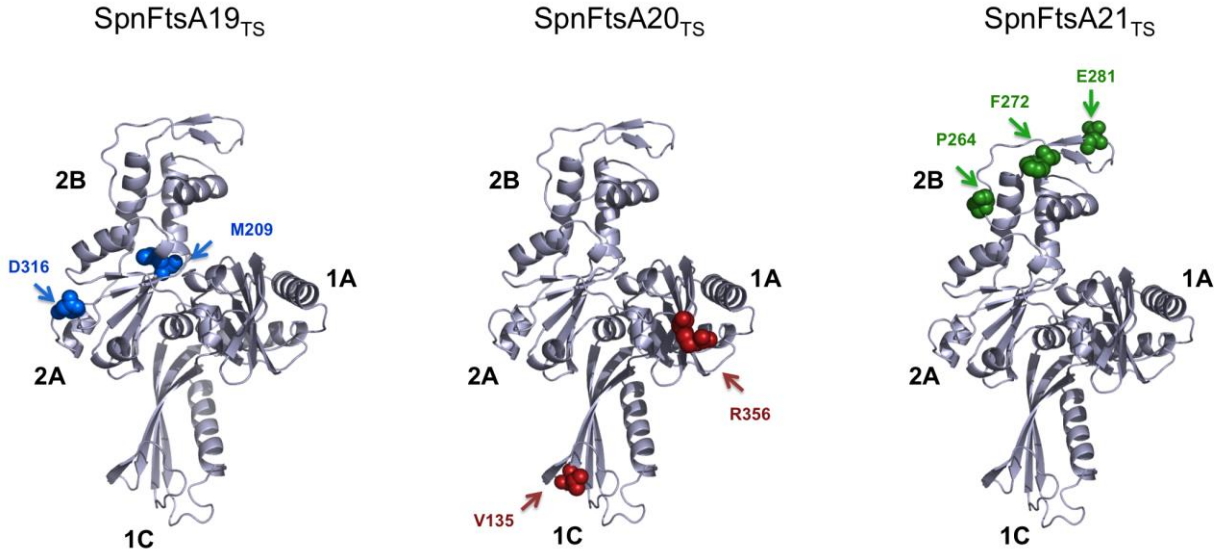

Figure 7. Characteristic of the FtsA Ts mutants. Growth of $Rx1_{WT}$ and of the $FtsA_{TS}$ mutants in TSBA plates at 32°C and 40°C **(a)** and mutations mapped into the 3D structure obtained for *S. pneumoniae* FtsA **(b)**.

and 1A (H11) subdomains, of FtsA which may affect both the ability of the FtsA20$_{TS}$ protein to self-interact and to interact with the later cell division proteins, while the A21$_{TS}$ mutant has three substitutions. All A21 mutations are located in the subdomain 2B of the FtsA protein, with two of them in the ß S12-S13 strand that is involved in FtsA self-interaction and the third one located in a region (H7 -S12) that may be involved in interactions with FtsZ.

2. Growth characteristics and morphology of the FtsA Ts mutants

Initial characterization of the FtsA Ts (A$_{TS}$) mutants with respect to the Rx1 wild type (Rx1$_{WT}$) was carried out at 32°C. However, we noticed that at this temperature the A19$_{TS}$ mutant, albeit able to grow, showed an altered cell morphology (not shown) and for this reason I progressively decreased the growth temperature until 28°C, that was then used as the permissive temperature for subsequent experiments. As shown in Fig. 8a, both the Rx1$_{WT}$ and the three A$_{TS}$ mutants grew well in TSB at 28°C. These differences were confirmed when cell viability was estimated in the same curve by measuring viable counts (Fig. 8b). In these conditions, the Rx1$_{WT}$ showed a doubling time of 55 min (about 1.8 times slower than at 37°C) while the isogenic A$_{TS}$ mutants showed doubling times of 61 min (A19$_{TS}$), 59 min (A20$_{TS}$) and 56 min (A21$_{TS}$), respectively (Fig. 8c). Efficiency of plating (EOP, Fig. 8d), determined as the ratio between the colony forming units (CFUs) recovered at 28°C and 40°C of each mutant with respect to Rx1$_{WT}$, confirmed the growth and viability results at the permissive temperature and gave us an estimate of the survival rate of the three A$_{TS}$ mutants at the non-permissive temperature (40°C), indicating a spectrum of mutational differences, ranging from mild (A21$_{TS}$) to moderate (A20$_{TS}$) to severe (A19$_{TS}$).

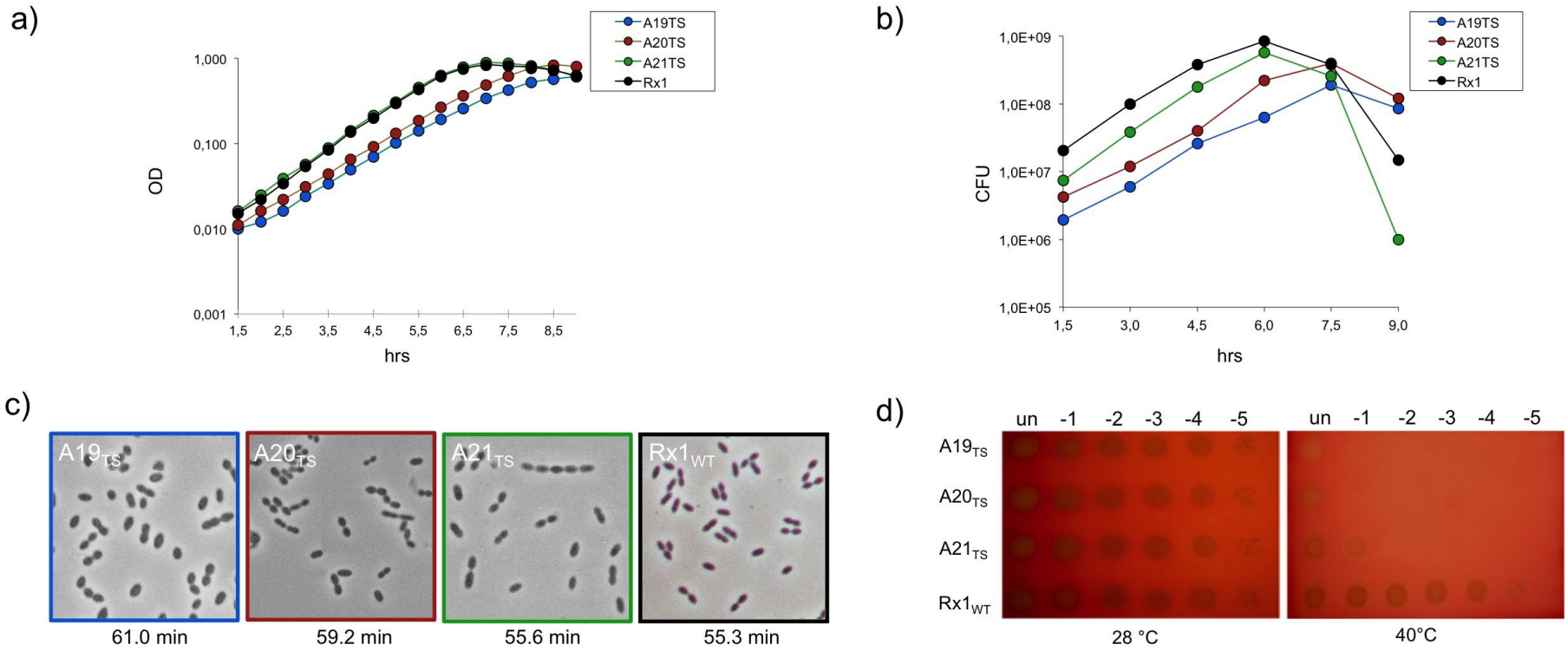

Figure 8. Characterization of the FtsA Ts mutants with respect to $Rx1_{WT}$. Growth **(a)** viability, **(b)**, doubling times (Td) and morphology **(c)** of $Rx1_{WT}$ and FtsA Ts mutants in TSB medium at 28 °C (permissive temperature) and efficiency of plating (EOP) at 28 °C and 40 °C **(d)**

3. Mutations in *ftsA* conferring Ts phenotypes result in a block of cell division and, eventually, cell lysis

The next step was to study the effect of the FtsA Ts mutations on growth and division in temperature shifting experiments. For this purpose, cells growing exponentially at 28°C were shifted to the non-permissive temperature (40°C) and monitored for growth and morphology every 30 min. Parallel cultures were incubated at 28°C.

When temperature shifting experiments were performed in TSB rich medium, both the $Rx1_{WT}$ and the three A_{TS} mutants grew at 28°C (Fig. 9a). In contrast, only the $Rx1_{WT}$ grew after shifting to 40°C, while all the A_{TS} mutants stopped growing and started lysing 30 to 90 min from shifting, in a mutation dependent manner. Lysis was greatly reduced or prevented when the shift to 40°C was performed in C+Y semi-synthetic medium (Fig. 9b), or in a *lytA*- background (not shown). Nevertheless, the overall morphology of the $FtsA_{TS}$ mutants grown in C+Y was similar to that in TSB and characteristic of each mutant, suggesting that the mutations could dissect FtsA-specific functions. In particular, a different degree of thermosensitivity was observed for the different mutants, which ranged from the most severe, $A19_{TS}$, which stopped growing and started lysing shortly after shifting to the non-permissive temperature, to the less affected $A21_{TS}$, and the intermediate behavior of $A20_{TS}$, giving us some clues about the importance of the mutated residues of the protein for the different functions of FtsA. Consequently, also the cellular morphology in samples taken upon shifting to non-permissive temperature was different for the different strains. In particular, upon shifting to 40°C, $A19_{TS}$ mutants enlarged, resulting in bigger and rounder cells with a “lemon-shaped” morphology; the $A20_{TS}$ mutant, instead, showed a mixed phenotype, first with elongated cells and later with bigger and lemon-shaped cells, while the $A21_{TS}$ resulted in quite chainy, elongated cells. Overall, the data suggest that an early block in cell division in *S. pneumoniae* results in an arrest of growth followed by cell lysis, rather than cell filamentation as in rod-shape bacteria.

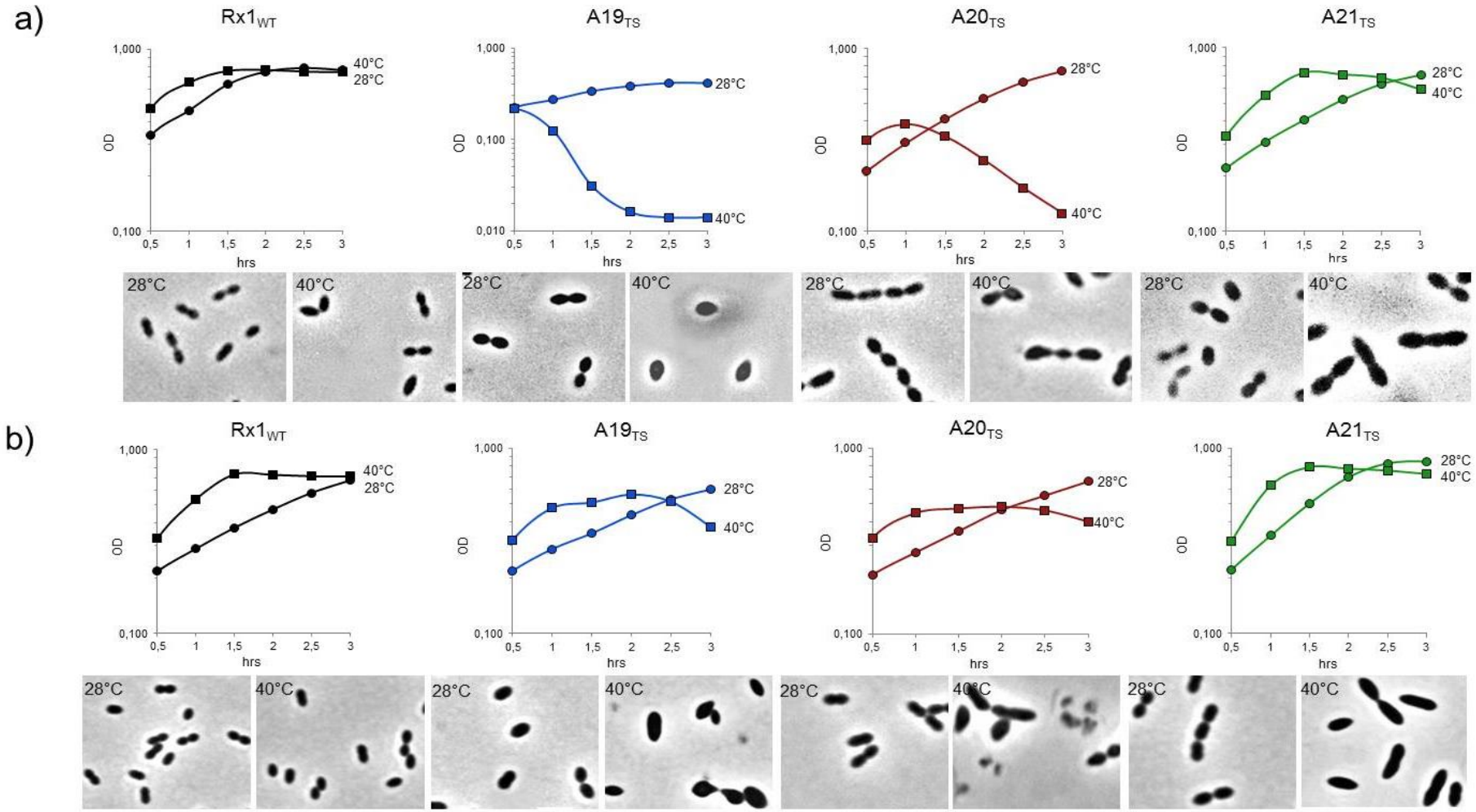

Figure 9. Growth and morphology of $Rx1_{WT}$ and the FtsA Ts mutants in temperature-shifting experiment. TSB **(a)** and C+Y **(b)** medium, respectively. Samples were taken from 1:1 dilution at 90 min from shifting. Despite the difference in lysis, morphology is similar in the two media and characteristic of each mutant.

To exclude that the FtsA Ts phenotype was determined by degradation of the mutated proteins at the non-permissive temperature, the stability of the $FtsA_{TS}$ proteins at 28°C and 40°C, in comparison with $FtsA_{WT,}$ was evaluated by Western blotting using anti-FtsA polyclonal antibodies against crude extracts derived from cultures taken after 90 min upon shifting to 40°C and in parallel cultures at 28°C. As shown in Fig. 10, all the $FtsA_{TS}$ proteins were stable at 40°C in both media, indicating that the Ts phenotype is not due to protein degradation at non-permissive temperature.

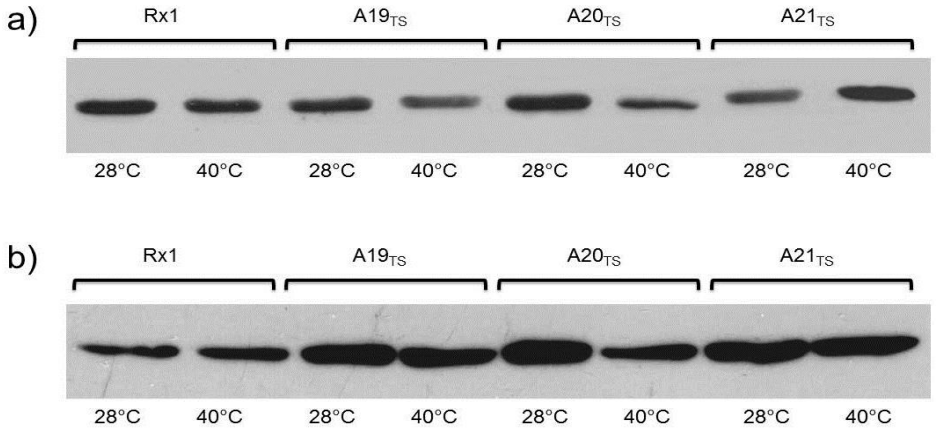

Figure 10. Stability of $FtsA_{WT}$ and $FtsA_{TS}$ at 28°C and 40°C in TSB (a) and C+Y (b) at 28°C and 40°C. Samples were taken 90 min from shifting to 40°C or from parallel cultures at 28°C. Crude extracts were separated by SDS-PAGE and, after transfer to membranes, probed with anti-FtsA polyclonal antibodies.

4. Loss of FtsA biological function is accompanied by the loss of FtsA self-interaction

A characteristic feature of FtsA is its ability to self-interact and interact also with early and late cell division proteins. Indeed, interactions of FtsA with itself, with FtsZ, ZapA, FtsI (the septal PBP transpeptidase) have been reported in *E. coli* and other microorganisms, including *S. pneumoniae* (Ma *et al.*, 1997; Ma and Margolin, 1999; Yim *et al.*, 2000; Di Lallo *et al.*, 2003; Corbin *et al.*, 2004; Rico *et al*., 2004, Karimova *et al.*, 2005; Lara *et al.*, 2005; Maggi *et al.*, 2008; Busiek *et al.*, 2012; Szwedziak *et al.*, 2012) and linked to FtsA functions in early and late stages of cell division.

The ability of FtsA to form large polymers in the presence of ATP *in vitro* was first described for *S. pneumoniae* (Lara *et al.*, 2005). However, given the lack of conditional lethal mutants it still awaits *in vivo* validation. Nevertheless, two variants of the *S. pneumoniae* FtsA protein truncated in domain 1C or 2B (β-strands S12 and S13), previously shown to impair *E. coli* FtsA functionality *in vivo* (Rico *et al.*, 2004), were recently found to inhibit the ATP-dependent polymerization of the pneumococcal wild-type protein and their ability to polymerize *in vitro*, confirming the importance of these regions for FtsA function (Krupka *et al.*, 2012; Krupka *et al.*, 2014). Moreover, FtsA polymerization in *E. coli* was found important for its *in vivo* function (Pichoff and Lutkenhaus, 2005; Pichoff *et al.*, 2012) and these results were further supported in a recent study, based on crystal structure, showing that FtsA can polymerize in the presence of a lipid monolayer surface and forms actin-like protofilaments (Szwedziak *et al.*, 2012). Interestingly, the analysis of several *E. coli ftsA* mutants suggested that the ability of FtsA to recruit the late cell division proteins is inversely proportional to its propensity for self-interaction, which is negatively modulated by ZipA (Pichoff *et al.*, 2012, Pichoff et *al.*, 2014). The strength of FtsA self-interaction seems crucial for its polymerization/depolymerization cycle, which is required first for FtsA interaction with the cytoplasmic membrane and with FtsZ (allowing proper Z ring formation) and then to recruit the later cell division proteins to midcell (allowing completion of cell division).

In this view, it was important to test if the mutated *S. pneumoniae* FtsA Ts proteins have retained or lost their ability to self-interact, to interact with $FtsA_{WT}$ and with FtsZ. For this purpose, we set up the Bacterial Adenylate Cyclase Two-Hybrid (BACTH) System, described by Karimova *et al*., 2005, in collaboration with Daniela Musu and Miguel Vicente's group,. This system is a reliable approach to detect protein-protein interactions *in vivo*. In contrast to the classic yeast two-hybrid system (Y2H), it offers the advantages of working in *E. coli*. The system is based on the interaction-mediated reconstitution of the *Bordetella pertussis* adenylate cyclase (CyaA). It exploits the fact that the catalytic domain of CyaA protein consists of two complementary fragments, T25 and T18, cloned and

expressed in two different plasmids, are not active when physically separated. Instead, when these two fragments are fused to interacting polypeptides, X and Y, heterodimerization of the hybrid proteins results in functional complementation between T25 and T18 fragments and thus in cyclic AMP (cAMP) synthesis and consequent binding of cAMP, produced by the reconstituted chimeric enzyme, to the catabolite activator protein, CAP. The cAMP/CAP complex is a pleiotropic regulator of gene transcription in *E. coli*: it turns on the expression of several resident genes, including genes of the *lac* and *mal* operons involved in lactose and maltose catabolism. Therefore, *cya*- recipent strains become able to utilize lactose or maltose as unique carbon sources and can be easily distinguished on indicator or selective media (Karimova *et al.*, 2005).

In practice, the *ftsA*19$_{TS}$, *ftsA*20$_{TS}$, *ftsA*21$_{TS}$ alleles were cloned, in frame with the genes encoding the T25 and T18 fragments, in the respective pKT25 and pUT18C BACTH vectors, to obtain pKT25-*ftsA*19$_{TS}$/pUT18c-*ftsA*19$_{TS}$, pKT25-*ftsA*20$_{TS}$/pUT18c-*ftsA*20$_{TS}$, pKT25-*ftsA*21$_{TS}$/pUT18c-*ftsA*21$_{TS}$ hybrid plasmids. Correct sequence was verified by double-strand sequence analysis. The hybrid plasmid pairs pKT25*ftsA*$_{WT}$(pMKV24)/pUT18C*ftsA*$_{wt}$ (pMKV19), expressing respectively T25-FtsA$_{WT}$ and T18-FtsA$_{WT}$, were kindly provided by M. Vicente (Krupka *et al.*, 2012). The hybrid plasmid pairs were transformed in the *E. coli* (*cya*$^{-}$) BTH101 recipient strain and tested for protein-protein interactions in four different media: LB+X-gal, LB+X-gal+IPTG, McConkey+1% maltose and M63+1% maltose+Xgal. The use of this last medium is particularly important because, being a minimal medium that contains maltose as the only carbon source, it does not allow growth unless the tested proteins interact. Negative and positive controls were respectively the pKT25/pUT18C and the pKT25-*ftsA*$_{wt}$)/pUT18C-*ftsA*$_{wt}$ plasmid pairs.

Fig. 11 shows the qualitative and quantitative BACTH results regarding the interaction of FtsA$_{TS}$ proteins with FtsA$_{WT}$ and with themselves. All three FtsA$_{TS}$ mutated proteins have retained, although A19$_{TS}$ to a lesser extent, the ability to interact with FtsA$_{WT}$, but have lost their ability to self-interact (Fig. 11a). The results were confirmed by a quantitative assay, mesuring β-galactosidase activity (Fig.

11b), suggesting that the FtsA/FtsA interactions are indeed important for FtsA *in vivo* function. Moreover, these results agree with the initial prediction based on the FtsA 3D structure that at least one of the mutations detected in each of the three different A_{TS} mutants mapped in regions thought to be involved in the polymerization of protein (Swediak *et al.*, 2012).

To test FtsA/FtsZ interaction, we attempted to clone the *ftsZ* gene in the BACTH plasmids. However, the *S. pneumoniae* pKT25-*ftsZ* fusion (T25-FtsZ) was not functional, as no interactions could be detected for pKT25-*ftsZ* and pUT18c-*ftsA*$_{WT}$ or pUT18c-*ftsA*19$_{TS}$, pUT18c-*ftsA*20$_{TS}$, pUT18c-*ftsA*21$_{TS}$ plasmids respectively (not shown). Although this result was surprising, since *S. pneumoniae* FtsA/FtsZ interactions have been reported using the Y2H (Lara *et al.*, 2005) and the B2H based on λ-phage repressor (Maggi *et al.*, 2008), it is possible that, as reported for *E. coli* FtsZ (Karimova *et al.*, 2005), also the T25-FtsZ fusion, which tags T25 at the FtsZ's N-terminal domain, results in non-functional *S. pneumoniae* FtsZ. Moreover, again as reported for *E. coli ftsZ* (Karimova *et al.*, 2005), we were not able to clone *S. pneumoniae ftsZ* wild type gene in the high copy number pUT18C plasmid. For this reason, we cloned *S. pneumoniae* FtsZ in the BACTH vector pKNT25, resulting in the C-terminal tagged protein, FtsZ-T25.

Co-transformation of pKNT25-*ftsZ* with pUT18c-*ftsA*$_{WT}$, pUT18c-*ftsA*19$_{TS}$, pUT18c-*ftsA*20$_{TS}$, pUT18c-*ftsA*21$_{TS}$ plasmids respectively, showed that FtsA$_{WT,}$ as well as all the FtsA$_{TS}$ proteins, have retained the ability to interact with FtsZ (Fig. 12), although the interaction could be visualized only in M63+0.2% glucose+X-gal, possibly due to a toxicity of overexpressed FtsZ for *E. coli* cells in the other media.

a)

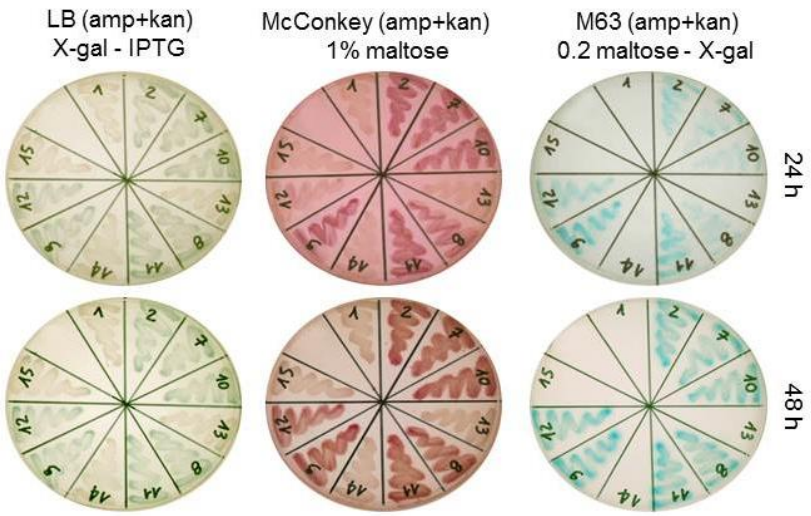

	pKT*ftsA*$_{WT}$*	pKT*ftsA*$_{19}$	pKT*ftsA*$_{20}$	pKT*ftsA*$_{21}$	pKT25
pUT*ftsA*$_{WT}$*	(2) A_{WT}/A_{WT}	(10) A_{19}/A_{WT}	(11) A_{20}/A_{WT}	(12) A_{21}/A_{WT}	
pUT*ftsA*$_{19}$	(7) A_{WT}/A_{19}	(13) A_{19}/A_{19}			
pKT*ftsA*$_{20}$	(8) A_{WT}/A_{20}		(14) A_{20}/A_{20}		
pKT*ftsA*$_{19}$	(9)A_{WT}/A_{21}			(15) A_{21}/A_{21}	
pUT18C					(1) T25-T18

* pMKV24 and pMKV19 respectively (Krupka *et al*., 2012)

b)

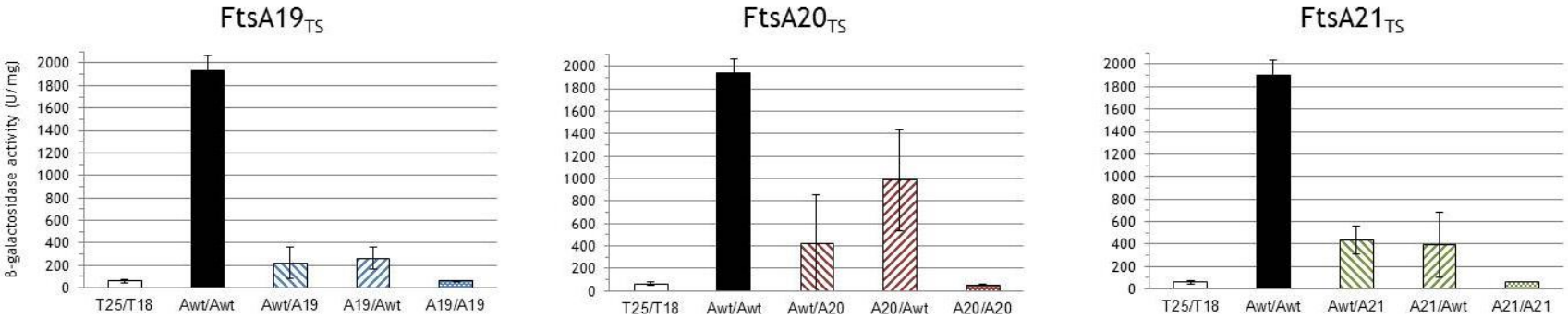

Figure 11. Interactions of the SpFtsA$_{TS}$ proteins with SpFtsA$_{wt}$ and with themselves detected using the BACTH system. Qualitative **(a)** and quantitative **(b)** determinations of the interactions among the FtsA$_{WT}$ and FtsA$_{TS}$ proteins. In contrast to FtsA$_{WT,}$ all the FtsA$_{TS}$ proteins, albeit retaining the ability to interact with the FtsA$_{WT}$, lost the ability to self-interact.

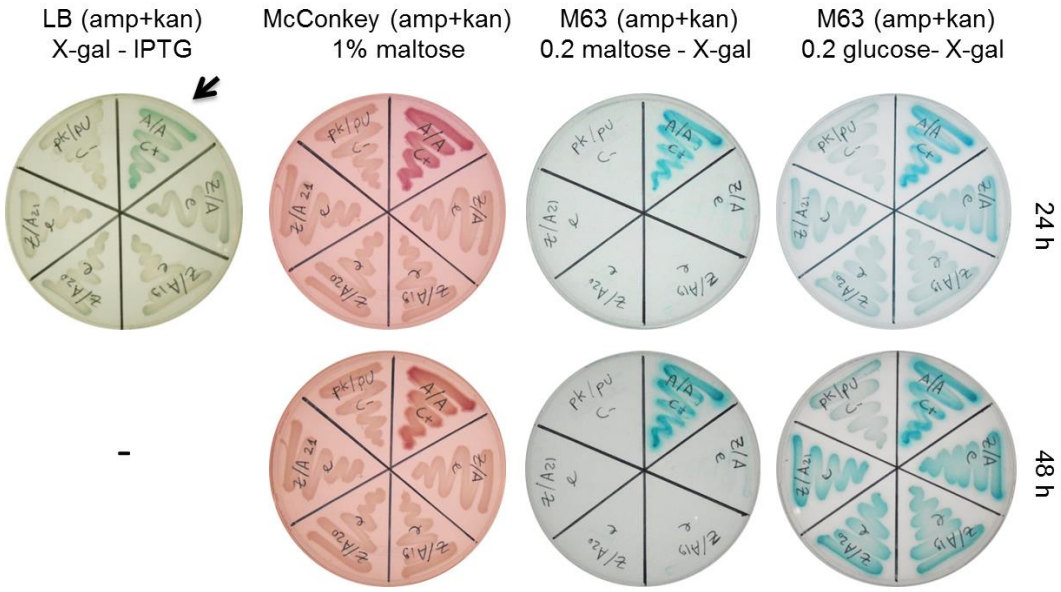

Figure 12. **Interactions of FtsAwt and the $FtsA_{TS}$ proteins with FtsZ detected using the BACTH system**. Clockwise from the arrow: 1) T25-$FtsA_{WT}$/T18$FtsA_{WT}$; 2) FtsZ-T25/T18-$FtsA_{WT}$, 3) FtsZ-T25/T18-$FtsA_{19}$ 4) FtsZ-T25/T18-$FtsA_{20}$, 5) FtsZ-T25/T18-$FtsA_{21}$, 6) pKT25/pUT18c.

5. $FtsA_{WT}$ can fully complement $FtsA_{20}$ and $FtsA_{21}$ Ts, but only partially $FtsA_{19}$ Ts mutations

To check if the $FtsA_{WT}$ protein could complement the phenotype of the three A_{TS} mutants, we took advantage of the Zn^{2+} inducible system that has been efficiently used in *S. pneumoniae* for the fine control of *gfp*-fusion gene expression (Eberhardt *et al.*, 2009; Beilharz *et al*., 2012). Plasmid pJWV25-*gfp-ftsA*, carrying a copy of the $ftsA_{WT}$ gene under the control of the zinc inducible P_{cdcZ} (P_{Zn}) promoter and expressing GFP-$FtsA_{WT}$ upon induction with $ZnCl_2$ (Beilharz *et al.*, 2012), was inserted at the ectopic chromosomal *bga* locus of the $A19_{TS}$, $A20_{TS}$ and $A21_{TS}$ mutants and $Rx1_{WT}$ strain, as a control. The resulting transformants, $A19_{TS}$, $A20_{TS,}$ $A21_{TS}$ and Rx1+P_{Zn}*gfp-ftsA*, were selected at 28°C on TSBA plates containing tetracycline (2.5 μg/ml). Complementation for growth was checked by patching independent colonies onto TSBA plates, with or without 0.15-0.45 mM $ZnCl_2$, following incubation at 28°C and 40°C. As expected, all transformants grew well at 28°C in TSBA plates with or without $ZnCl_2$. On the other hand, with the exception of the Rx1+P_{Zn}*gfp-ftsA* that grew at both temperatures independently of the presence of $ZnCl_2$, the $A19_{TS}$, $A20_{TS,}$ and $A21_{TS}$+PZn-*gfp-ftsA* strains could grow at

40°C only on plates containing $ZnCl_2$, indicating that the GFP-$FtsA_{WT}$ must be functional and able to complement the Ts growth defects of all the $FtsA_{TS}$ mutants (data not shown). A slight growth on TSBA plates without $ZnCl_2$ at 40°C was observed for the $A20_{TS}$+PZn-*gfp-ftsA* and $A21_{TS}$+PZn-*gfp-ftsA* transformants, suggesting that perhaps even a leaky basal expression of the $FtsA_{wt}$ protein from the P_{Zn} promoter, in the conditions tested, could account for the observed growth in two of our FtsA Ts mutants.

Complementation was confirmed in liquid cultures, by monitoring growth, morphology and localization of GFP-$FtsA_{WT}$ by phase-contrast, GFP-fluorescence microscopy and Western blotting. For this purpose, one of each of the transformants, verified for the correct insertion of P_{Zn}*gfp-ftsA* by PCR, was selected for temperature shifting experiments. To obtain better results, we used the chemically defined C+Y medium (Eberhardt *et al.,* 2009), as it allows a more precise control of induction and a better visualization of the fluorescence. Cells were cultured in C+Y medium at 28°C with or without 0.05 mM $ZnCl_2$, until they reached 0.3 OD and then were shifted to 40°C. Parallel cultures were incubated at 28°C. Cells were monitored for growth every 30 min and samples for microscopy were taken at the same times; samples for Western blotting at 90 min from shifting. As shown in Fig. 13, expression of GFP-FtsA only partially complemented the $A19_{TS}$ phenotype and complementation was not achieved even when GFP-FtsA was expressed at higher levels (Fig. 14). Interestingly, $A19_{TS}$+GFP-FtsA cells grown in the presence of 0.05 and 0.10 mM $ZnCl_2$ showed multilple fluorescent FtsA rings inside the elongated cells, suggesting that $FtA19_{TS}$ could be dominant over $FtsA_{WT}$. In contrast, $A20_{TS}$ and $A21_{TS}$ mutants grown in the presence of 0.05 mM $ZnCl_2$ showed a wild-type morphology and proper localization of FtsA at 28°C and after shifting to 40°C (Fig. 15 and 16), similar to that of the $Rx1_{WT}$ (Fig. 17). Western blotting confirmed expression of GFP-FtsA (Fig. 18). These results confirm that GFP-FtsA is functional, despite only partially complementing the $A19_{TS}$ phenotype, as $A19_{TS}$ cells expressing GFP-FtsA could grow and divide at 40°C, but displayed an abnormal elongated phenotype with multiple FtsA rings.

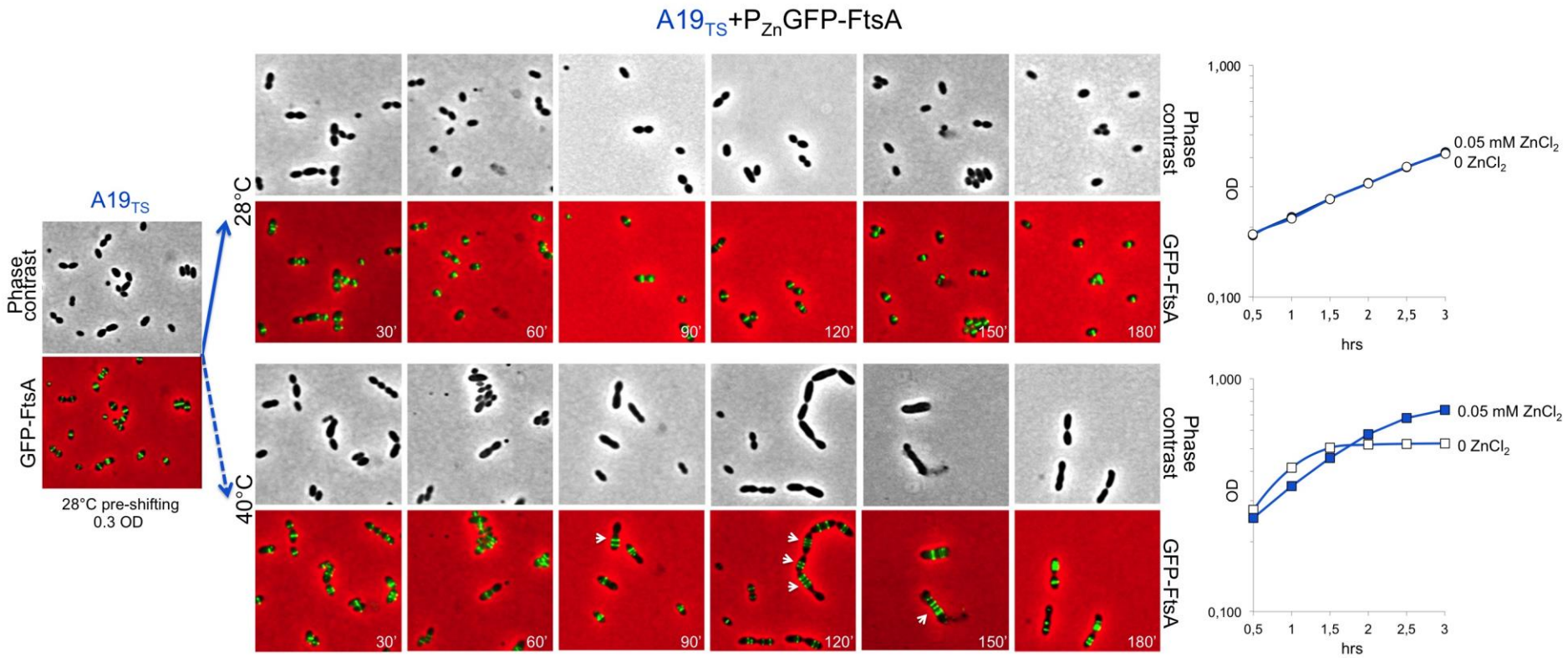

Figura 13. Expression and localization of GFP-FtsA in $A19_{TS}$+PZnGFP-FtsA in temperature-shifting experiment in C+Y with or without 0.05 mM $ZnCl_2$. Complementation of growth defects but only partial complementation of morphological defects could be observed after shifting to 40°C. Elongated $A19_{TS}$ cells with multiple FtsA rings are shown by arrows.

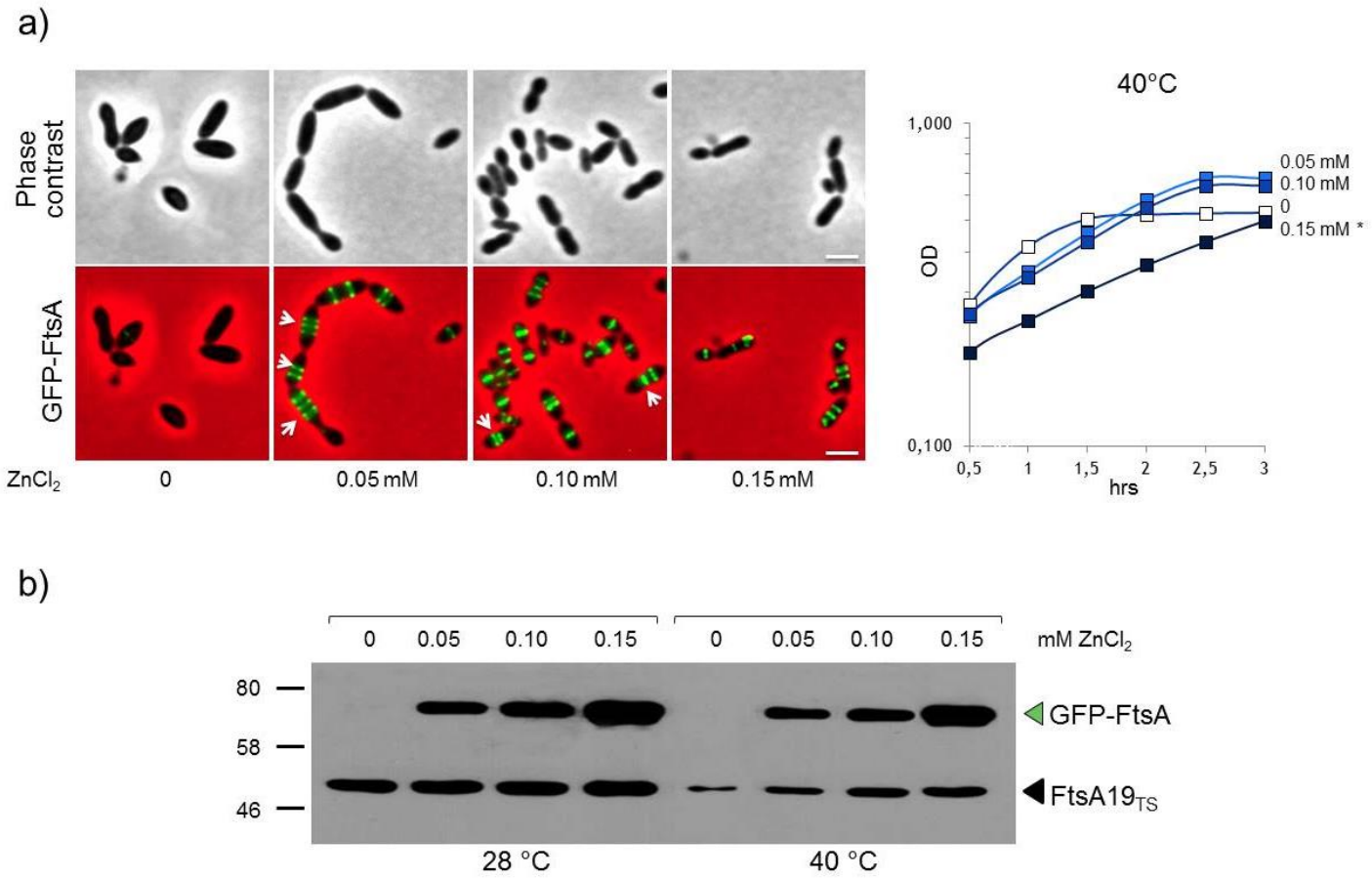

Figure 14. Expression and localization of GFP-FtsA, in $A19_{TS}$+PZnGFP-FtsA after temperature-shifting experiment in C+Y with 0, 0.05, 0.10 and 0.15 mM $ZnCl_2$. Complementation of morphological defects at 40°C were not observed also when cells were induced with 0.1 and 0.15 mM $ZnCl_2$ **(a)** Partial complementation does not seem to be due to the amount of PZnGFP-FtsA, which is well expressed at both 28°C and 40°C in a $ZnCl_2$ concentration dependent manner, as detected with WB using anti-FtsA polyclonal antibodies **(b).**

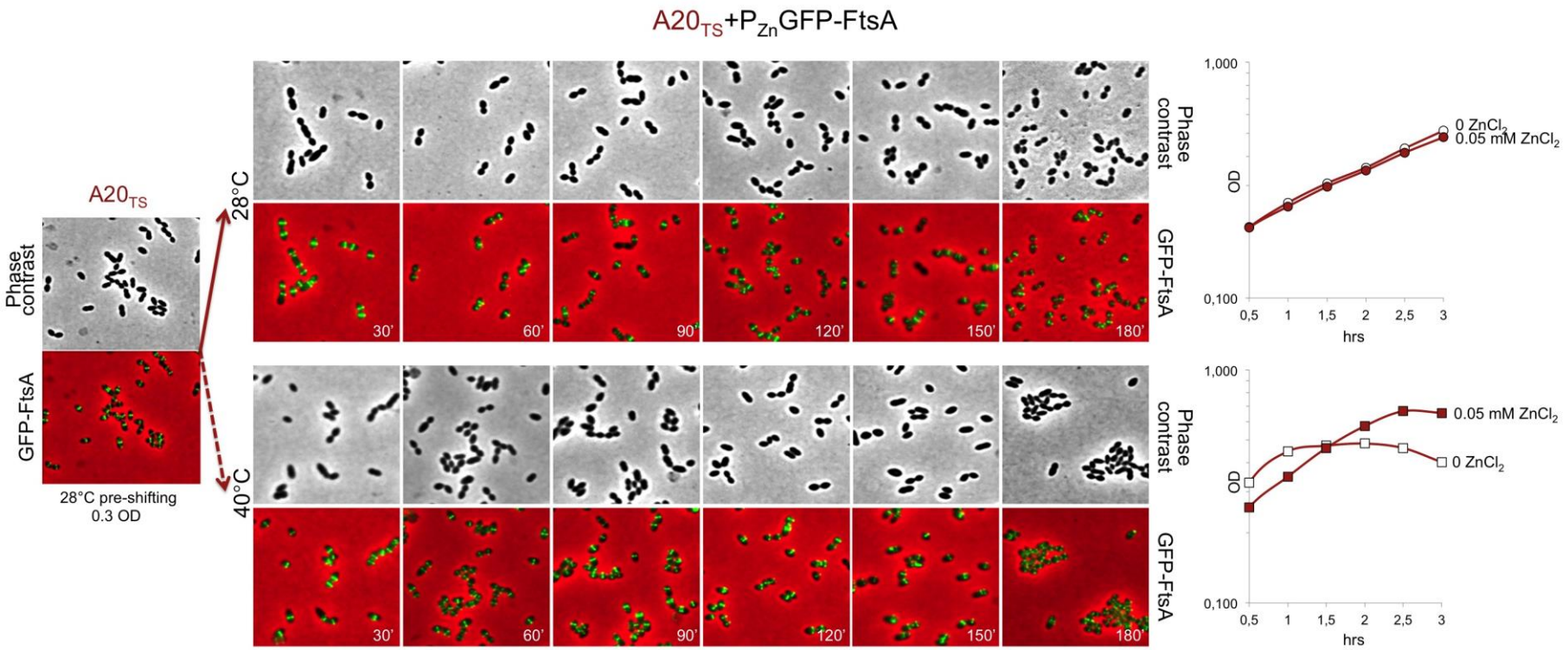

Figure 15. Expression and localization of GFP-FtsA, in $A20_{TS}$+PZnGFP-FtsA after temperature-shifting experiment in C+Y with or without 0.05 mM $ZnCl_2$. Full complementation of growth and morphology can be observed at 40°C upon expression of GFP-FtsA, which is properly localized at midcell in cells showing a wild-type morphology.

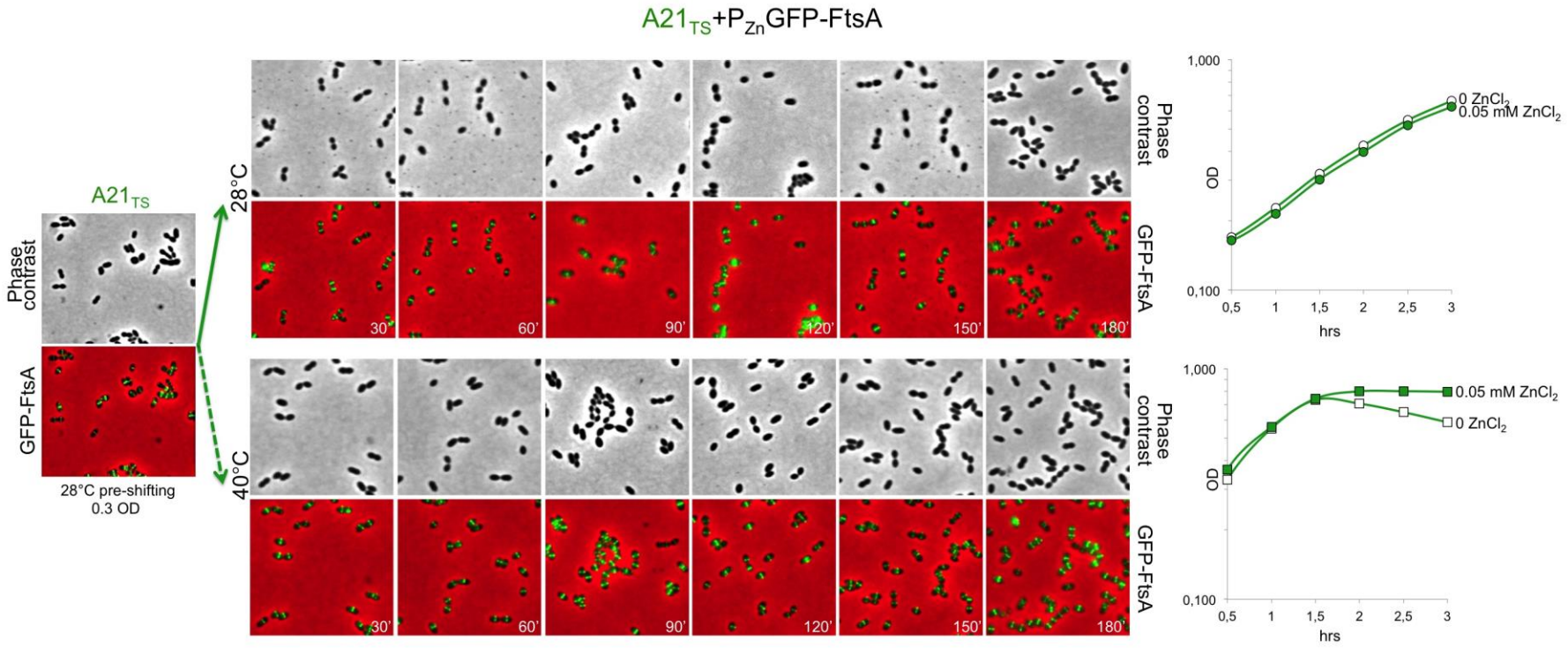

Figure 16. Expression and localization of GFP-FtsA in $A21_{TS}$+PZnGFP-FtsA after temperature-shifting experiment in C+Y with or without 0.05 mM $ZnCl_2$. Full complementation of growth and morphology can be observed at 40°C upon expression of GFP-FtsA, which is properly localized at midcell in cells showing a wild-type morphology.

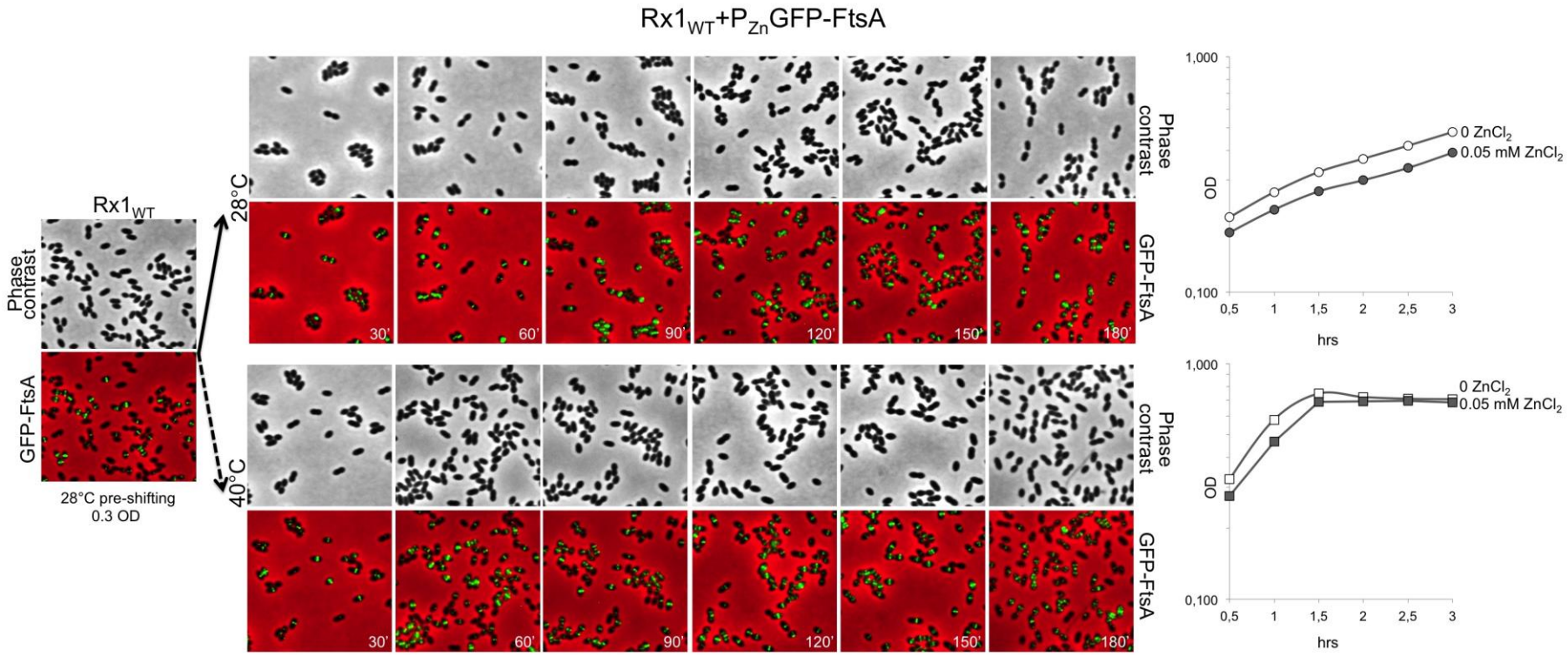

Figure 17. Expression and localization of GFP-FtsA in $Rx1_{WT}$+PZnGFP-FtsA after temperature-shifting experiment in C+Y with or without 0.05 mM $ZnCl_2$. No overexpression phenotype is observed upon expression of GFP-FtsA, which is properly localized at midcell as previously reported for the $R6_{WT}$ strain (Beilhartz *et al.*, 2012).

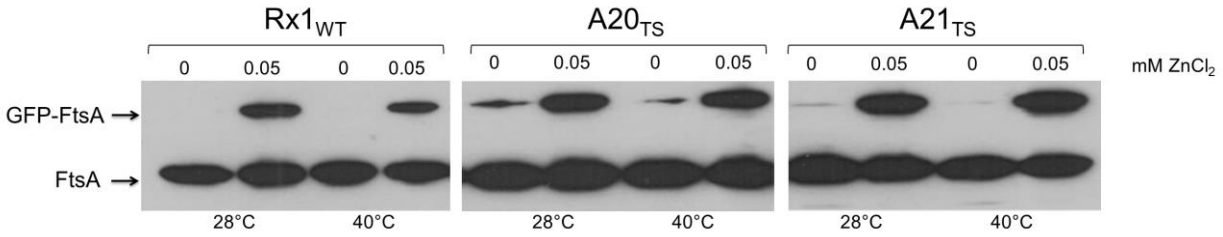

Figure 18. Expression of GFP-FtsA in the $Rx1_{WT}$ and in the $A20_{TS}$ and $A21_{TS}$ mutants. Native and GFP-FtsA were detected by Western blotting from samples grown in C+Y, with or without 0.05 mM $ZnCl_2$, after 90 min from shifting to 40°C and in parallel cultures at 28°C using anti-FtsA antibodies. In the $A20_{TS}$ and $A21_{TS}$ mutants, a slight expression of GFP-FtsA was observed also in uninduced samples, possibly due to a leaky expression of the P_{Zn} promoter.

6. Localization of FtsZ in the absence of functional FtsA

As reported for *E. coli* (Haeusser & Margolin, 2011; Lutkenhaus *et al.*, 2012; Rico *et al.*, 2013; Busiek & Margolin, 2015), also in *S. pneumoniae* FtsA localizes to midcell at the earliest stages of the division process together or shortly after FtsZ (Massidda *et al.*, 2013; Pinho *et al.,* 2013), and its localization is believed to be required for proper Z ring formation and completion of cell division. Consequently, a number of cell division proteins that hierchically follow and/or depend on FtsA for their midcell localization are not localized in *E. coli* FtsA conditional lethal mutants (Addinal *et al.*, 1996; Lutkenhaus *et al.*, 2012).

Therefore, another crucial step in the characterization of our A_{TS} mutants was to determine which other *S. pneumoniae* cell division proteins would be localized in the absence of functional FtsA. For this purpose we chose early and late division markers as FtsZ, DivIVA, GpsB, StkP and Ppp2x, for which the localization profile, timing of arrival to midcell and function in cell division are fairly well established (Morlot *et al.*, 2003; Lara *et al.*, 2005; Fadda *et al.*, 2007; Beilharz *et al.*, 2012; Land *et al.*, 2013; Peters *et al.*, 2014).

To check localization of FtsZ in the $Rx1_{WT}$ and the $FtsA_{TS}$ mutants, the first attempt was to construct a pJW25-PZn-*gfp-ftsZ* fusion to be inserted at the *bga* locus of the *S. pneumoniae* chromosome, as

described above for *gfp-ftsA.* However, all the efforts to express a GFP-FtsZ fusion from the PZn were unsucessful (not shown).

At this point, I took advantage of an *ftsZ-mCherry-erm* construct (kindly provided by Prof. Malcolm Winkler, Indiana University), which was previously shown to be properly expressed and localized in *S. pneumoniae* $R6_{WT}$ strain (Sham *et al.*, 2011). Once introduced *via* transformation, the construct would integrate at the *ftsZ* native locus, resulting in the expression of FtsZ-mCherry from its own promoter, as the only source of FtsZ in the cell. Consistently, erythromycin-resistant transformants, showing a correct insertion of the *ftsZ-mCherry* construct, were promptly obtained for both the $Rx1_{WT}$ and all three A_{TS} mutants in TSBA plates containing erythromycin 0.25 μg/ml at 28°C. However, when the strains were cultivated in liquid cultures to make frozen glycerol stocks, we observed that only $Rx1_{WT}$FtsZ-mCherry grew well, while the A_{TS} mutants were impaired, despite being at the permissive temperature. Inspection of cell morphology and localization of the FtsZ-mCherry from cultures grown at 28°C in solid or liquid media revealed that, in contrast with the $Rx1_{WT}$ which in agreement with what reported previously, by Sham *et al.*, showed a normal morphology and FtsZ localization, expression of FtsZ-mCherry in the A_{TS} mutants resulted in altered cell morphology and FtsZ localization (Fig. 19), which differed depending on the specific mutant. The effect was more pronounced in $A19_{TS}$, which was so severely affected that the cells were unable to grow and lysed soon after inoculation in liquid culture. Given that the respective parental strains, carrying native untagged FtsZ, grew well and FtsZ was properly localized in the same conditions, as detected by IEM using anti-FtsZ polyclonal antibodies (not shown), we concluded that FtsZ-mCherry is either not completely or differently functional with respect to $FtsZ_{wt}$ and, in either case, the A_{TS}-FtsZ-mCherry derivatives could be not used to check FtsZ localization in temperature shifting experiments.

The last attempt to obtain a tagged-FtsZ protein was to use the pBCSMH036 plasmid (Henriquez *et al*., 2013), which carries a *cfp-ftsZ* gene and expresses a CFP-FtsZ fusion under the control of the

constitutive *sigA* promoter, in addition to native FtsZ. To obtain $Rx1_{WT}$ and the A_{TS} mutants expressing CFP-FtsZ, I transformed them with pBCSMH036. All the attempts to obtain transformants at 28°C were unsuccessful, possibly due to the lacking of expression of the *tetL* plasmid resistance marker at this temperature. For this reason, all transformations were carryed out at 37°C, which promptly allowed selection of transformants that, in the case of the Ts mutants, were verified for the Ts phenotype before being used in temperature-shifting experiments. As shown in Fig. 20, expression of CFP-FtsZ in the $Rx1_{WT}$ and in the A_{TS} mutants did not affect growth and all CFP-FtsZ derivatives behaved as their respective parent strains at 28°C and after shifting to 40°C. Consistently, CFP-FtsZ was properly localized at midcell at 28°C and 40°C only in the $Rx1_{WT}$ (Fig. 21), whereas its localization was lost from septa in all three A_{TS} mutant after 60-90 min after shifting to 40°C temperature, while remained properly localized at 28°C (Fig. 22-24), suggesting in the absence of a functional FtsA also localization of FtsZ is compromised. These results were confirmed by electronimmunomicroscopy on $Rx1_{WT}$ and A_{TS} samples taken after 90 min from shifting to the non-permissive temperature using anti-FtsA and anti-FtsZ polyclonal antibodies (not shown), in collaboration with M. Vicente's group (CSIC, Madrid).

The results are consistent with what was observed in a zinc dependent *S. pneumoniae ftsA* conditional lethal mutant, also generated in our lab, where the only source of FtsA was a GFP-FtsA expressed from the P_{Zn} promoter, indicating that FtsA is required for efficient midcell localization of FtsZ and confirm what already observed in *B. subtilis*, where FtsA was found required for efficient FtsZ and FtsZ-ring assembly (Jensen *et al.*, 2005). Taken together the results support the notion that in Gram-positives, that lacks a ZipA homolog, FtsA is required to tether to membrane and to stabilize FtsZ, at least at high temperatures.

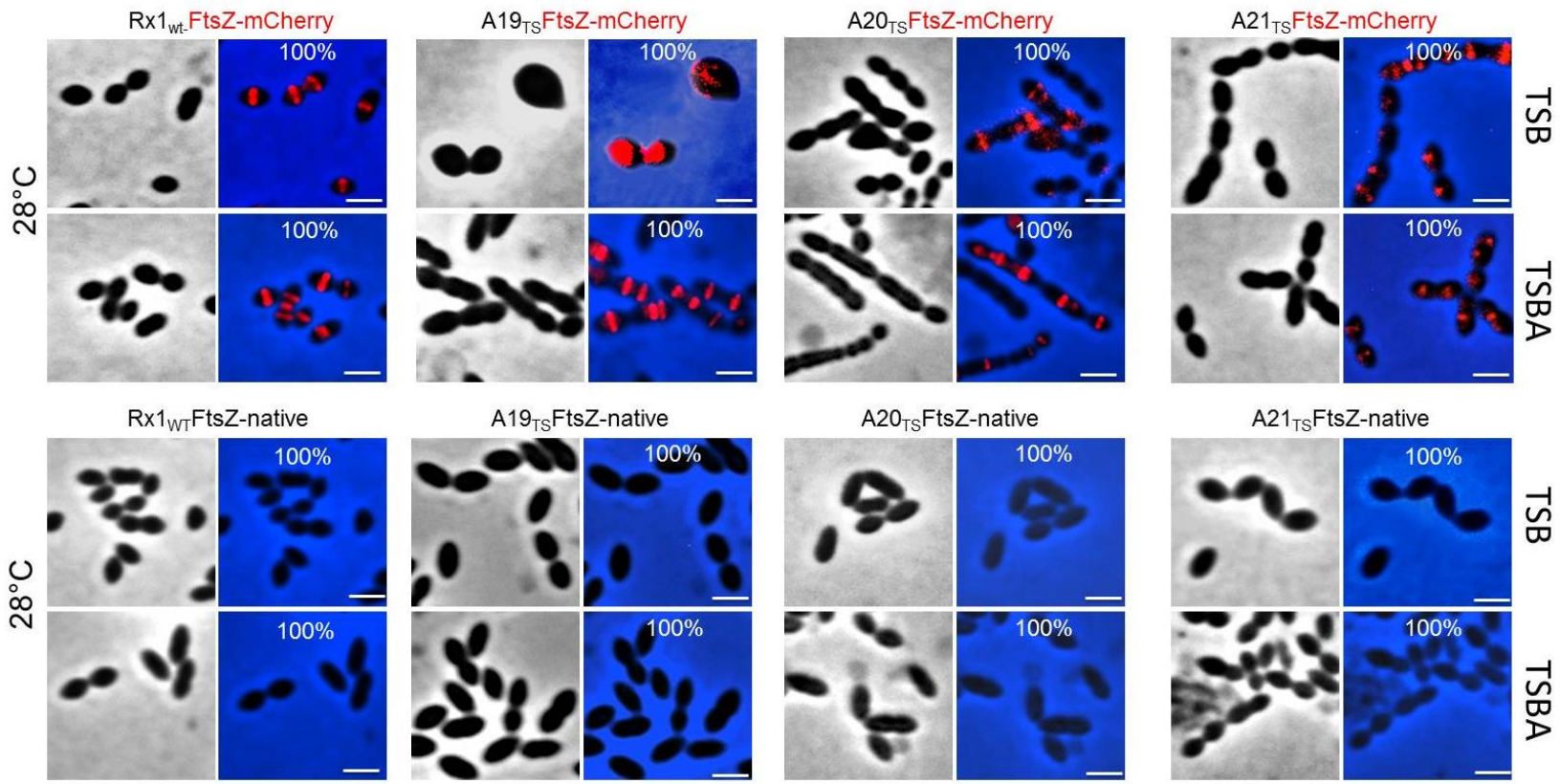

Figure 19. Expression and localization of FtsZ-mCherry in $Rx1_{WT}$ and in the A_{TS} mutants in comparison the with expression of native FtsZ. FtsZ-mCherry, expressed as the only source of FtsZ from its own promoter, behaves differently in all A_{TS} mutant already at 28°C in solid and liquid media.

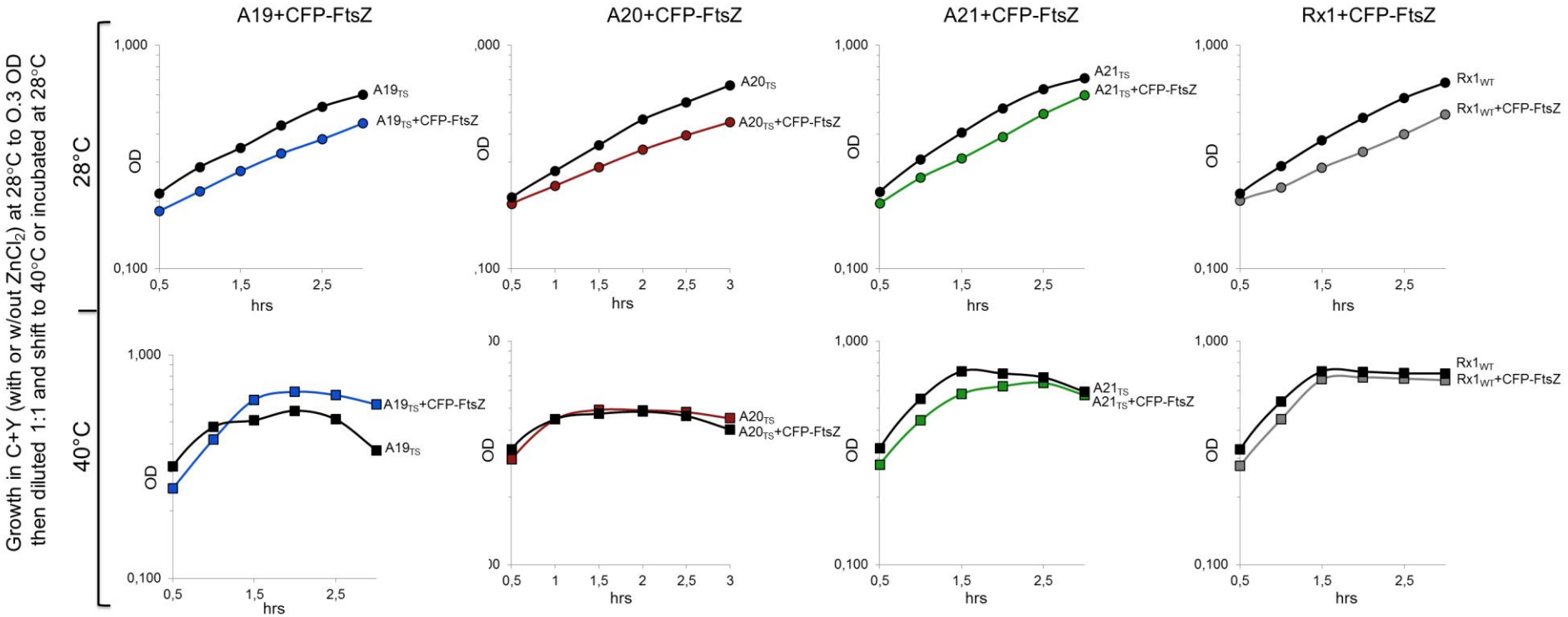

Figure 20. Growth of the $Rx1_{WT}$ and $FtsA_{TS}$+CFP-FtsZ derivatives in comparison with their respective parent strains in temperature-shifting experiments at 28°C (upper panel) **and 40°C** (lower panels).

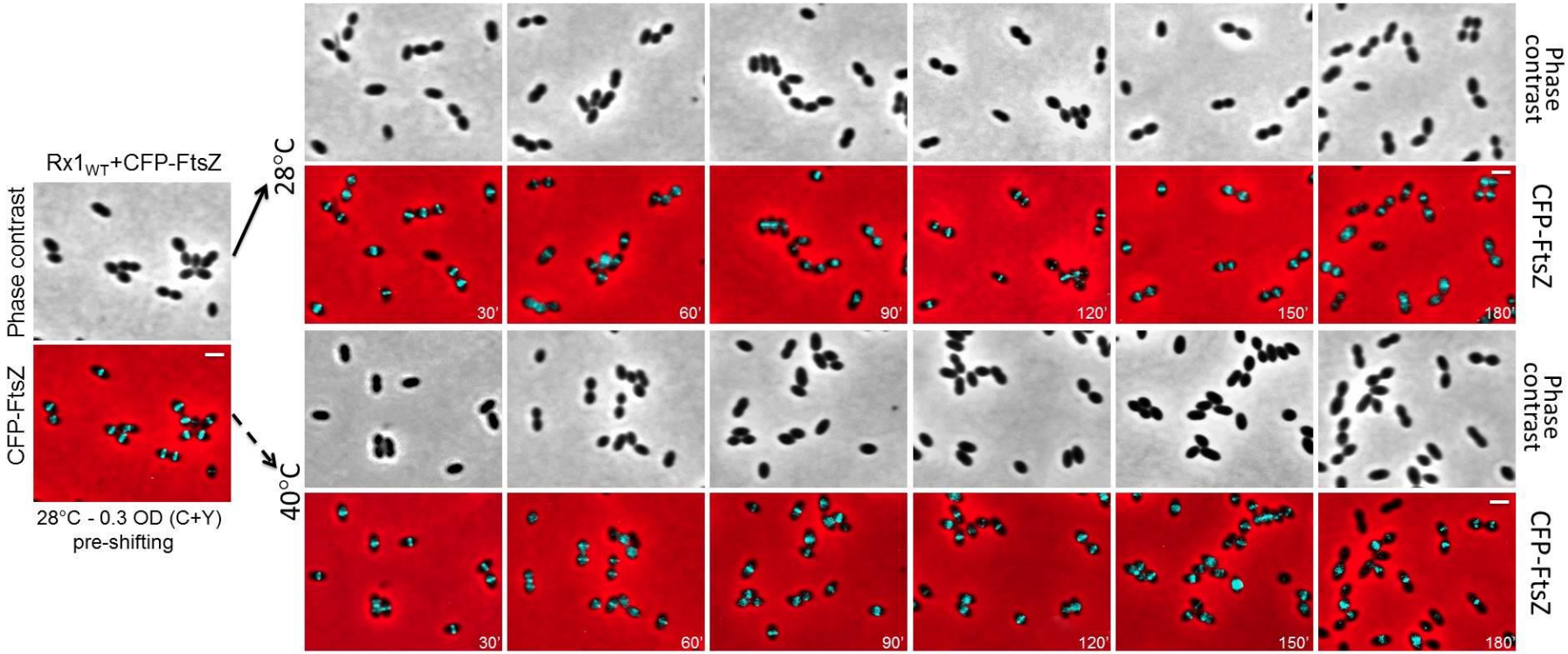

Figure 21. Expression and localization of CFP-FtsZ in the $Rx1_{WT}$ strain in temperature-shifting experiments. CFP-FtsZ is well localized at 28°C (upper panels) and also after shifting to 40°C (lower panels), at least until the cell start entering stationary phase.

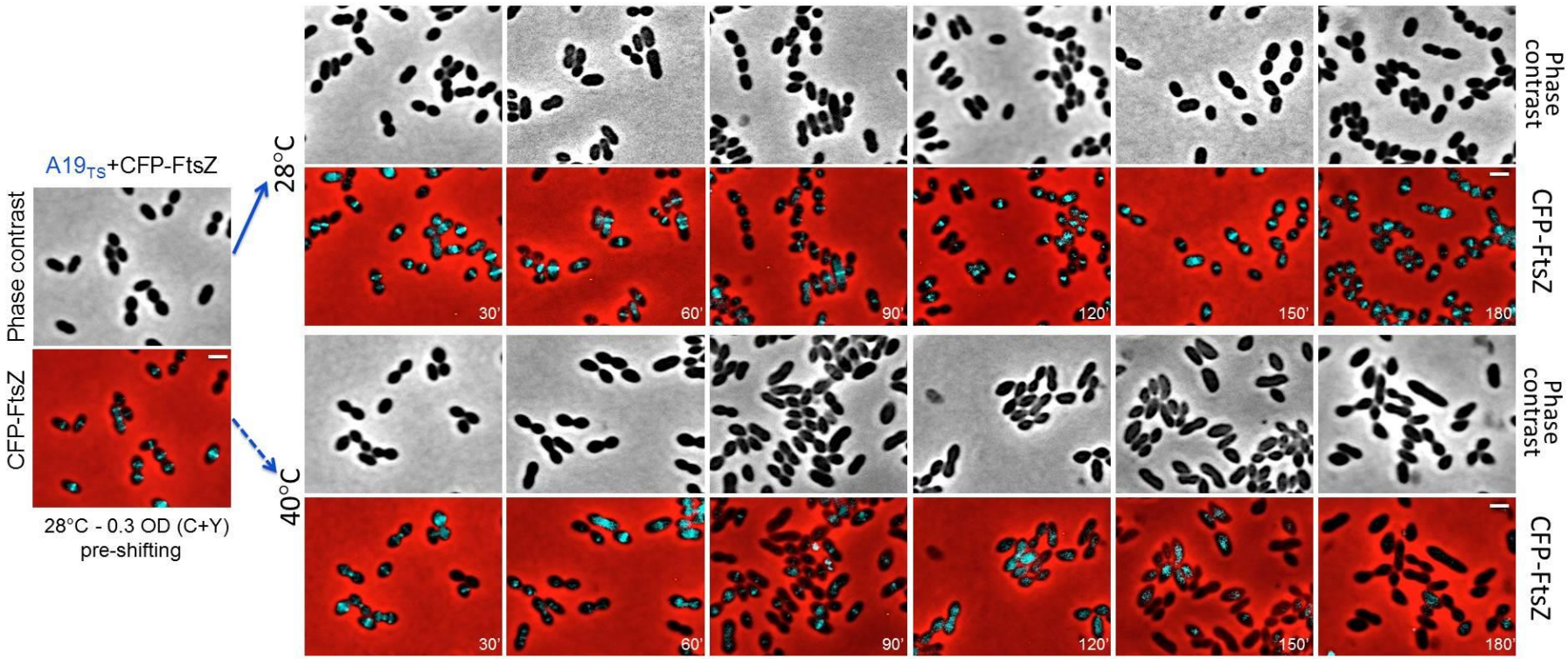

Figure 22. Expression and localization of CFP-FtsZ in the $A19_{TS}$ mutant in temperature-shifting experiments. CFP-FtsZ is well localized at 28°C (upper panels) but rapidly loses its localization upon shifting to 40°C (lower panels).

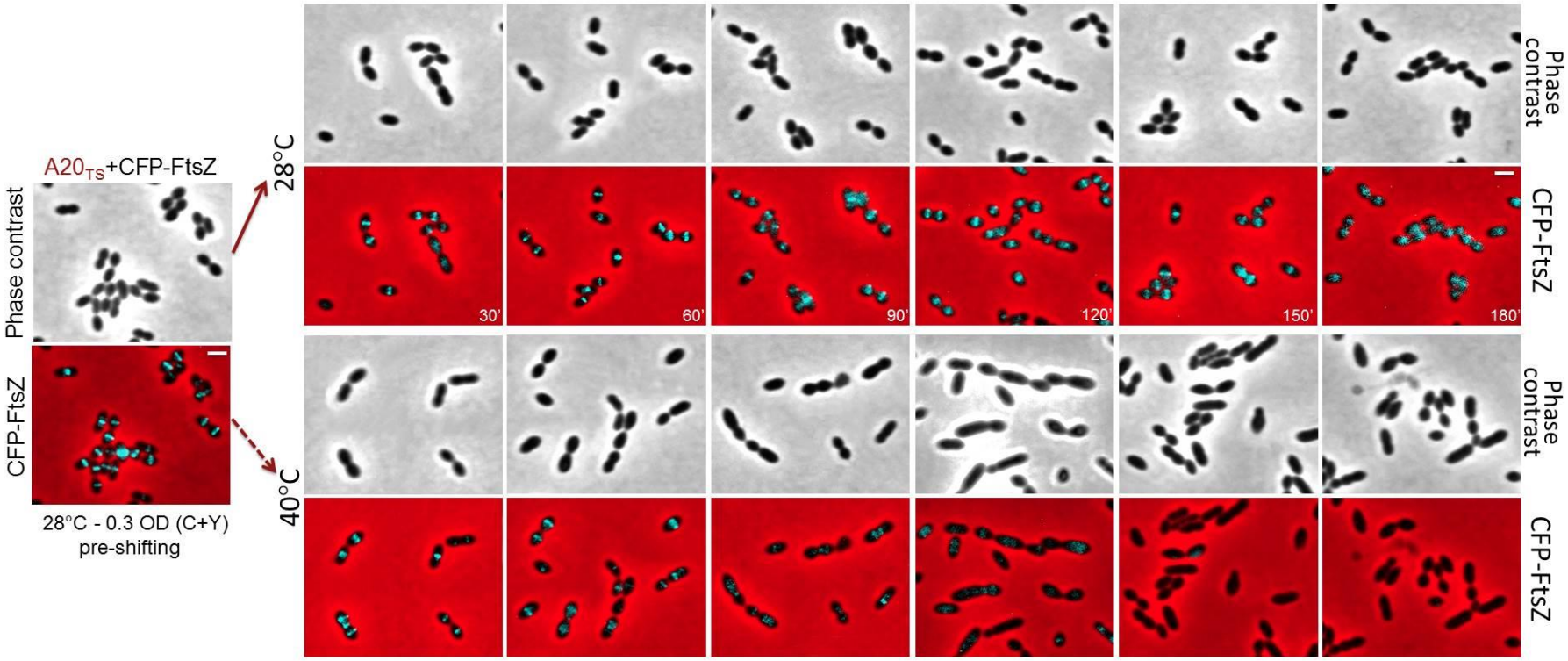

Figure 23. Expression and localization of CFP-FtsZ in the $A20_{TS}$ mutant in temperature-shifting experiments. CFP-FtsZ is well localized at 28°C (upper panels) but get dispersed 90 min after shifting to 40°C (lower panels). Notably, no FtsZ is detectable in the cells after this time.

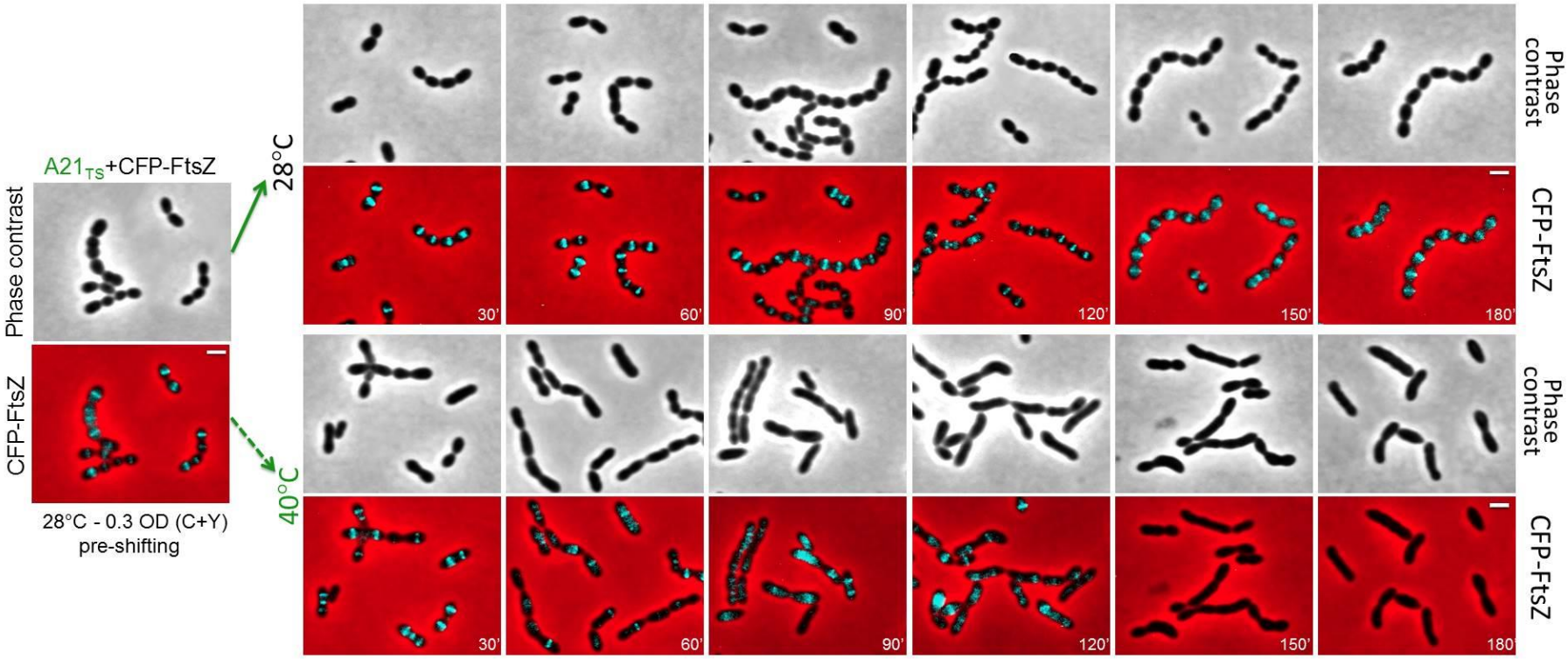

Figure 24. Expression and localization of CFP-FtsZ in the $A21_{TS}$ mutant in temperature-shifting experiments. CFP-FtsZ is well localized at 28°C (upper panels) get dispersed 60-90 min after shifting to 40°C (lower panels). Notably, no FtsZ is detectable in the cells after this time.

7. Localization of other cell division proteins in the absence of functional FtsA.

To check the subcellular localization of the other cell division proteins, as DivIVA, GpsB, StkP and Pbp2x which should localize after FtsA, we transformed $Rx1_{WT}$ and the A_{TS} strains with PvuI digested pJWV25*divIVA-gfp*, pJWV25*gfp-stkP*, pJWV25*gfp-gpsB,* pJWV25*gfp-pbpP2x* plasmids (Beilharz *et al*., 2012; Peters *et al.*, 2014, unpublished), respectively. As for *gfp-ftsA, t*he constructs would insert at the *bga* locus of the respective *S. pneumoniae* strains and express the desired protein tagged with GFP at their N-terminal or C-terminal domain (GFP-tagged or tagged-GFP) under the control of the P_{Zn} promoter (Beilharz *et al.*, 2012; Peters *et al.*, 2014; Fleurie *et al.*, 2014). In this case, all the expressed tagged-proteins were functional, as they have been proven to complement their respective nulls, and their expression does not affect the wild-type phenotype (Beilharz *et al*., 2012; Peters *et al.*, 2014, Rued *et al*., manuscript in preparation). Moreover, they show a localization profile identical to that reported with other methods for the corresponding native proteins (Morlot *et al.*, 2003; Fadda *et al.*, 2007; Beilharz *et al*., 2012). Consistently, the $Rx1_{WT}$ and A_{TS} Ts+P_{Zn}*divIVA-gfp*, +P_{Zn}*gfp-gpsB,* +P_{Zn}*gfp-stkP* and +P_{Zn}*gfp-pbp2x* transformants*,* showing a correct insertion at the *bga* locus in the respective *S. pneumoniae* strains, were promptly obtained and used in temperature-shifting experiments.

As described above, cells were cultured at 28°C until they reach 0.3 OD in C+Y medium without or with 0.05 mM (DivIVA-GFP, GFP-StkP, GFP-GpsB) or 0.15 (GFP-PBP2x) mM $ZnCl_2$ and then diluted in the respective pre-warmed medium and shifted to 40°C. Parallel cultures were incubated at 28°C. Cells were measured every 30 min and at the same times samples for microscopy were taken.

Figs. 25-29 show the growth curves and the localization of DivIVA-GFP in the $Rx1_{WT}$ and in the A_{TS} mutants after shifting to 40°C and in parallel cultures at 28°C. As shown in Fig. 25, expression of DivIVA-GFP in the $Rx1_{WT}$ and in the A_{TS} mutants did not affect growth and all DivIVA-GFP derivatives behaved as their respective parent strains at 28°C and after shifting to 40°C.

Both the $Rx1_{WT}$ and the A_{TS}+DivIVA-GFP derivatives grew similarly in uninduced and induced samples, no suppression of the A_{TS} phenotype was observed after shifting to 40°C.

Consistently, expression of DivIVA-GFP did not affect morphology of the $Rx1_{WT}$ and the A_{TS} mutants and DivIVA-GFP was properly localized at the midcell and the cell poles in all the strain at 28°C whereas upon shifting to 40°C it was properly localized only in the $Rx1_{WT}$ (Figs. 26-29). In particular, in the $A19_{TS}$ mutant DivIVA lost its septal localization soon after shifting to the non-permissive temperature, although it remained localized at the cell pole, at least until the cell started lysing (Fig. 26). In the $A20_{TS}$ and $A21_{TS}$ mutants instead, although DivIVA seemed localized both at midcell and cell poles for some time after shifting to 40°C, it progressively lost septal localization accumulating at the cell poles (Figs. 27-28). As expected, DivIVA-GFP was properly localized at midcell and poles at 28°C and 40°C in the $Rx1_{WT}$ (Fig. 29).

These results suggest that FtsA may be, directly or indirectly, required for the localization of DivIVA to the septum. However, as FtsZ also delocalizes from all the three A_{TS} mutants upon shifting to 40°C, this raise the possibility that proper Z-ring formation may indeed be needed to target DivIVA at midcell, in agreement with the fact that, in *S. pneumoniae*, DivIVA arrives to micell at a later stage of cell division, after the localization of FtsZ and FtsA (Fadda *et al.*, 2007; Beilharz *et al.*, 2012).

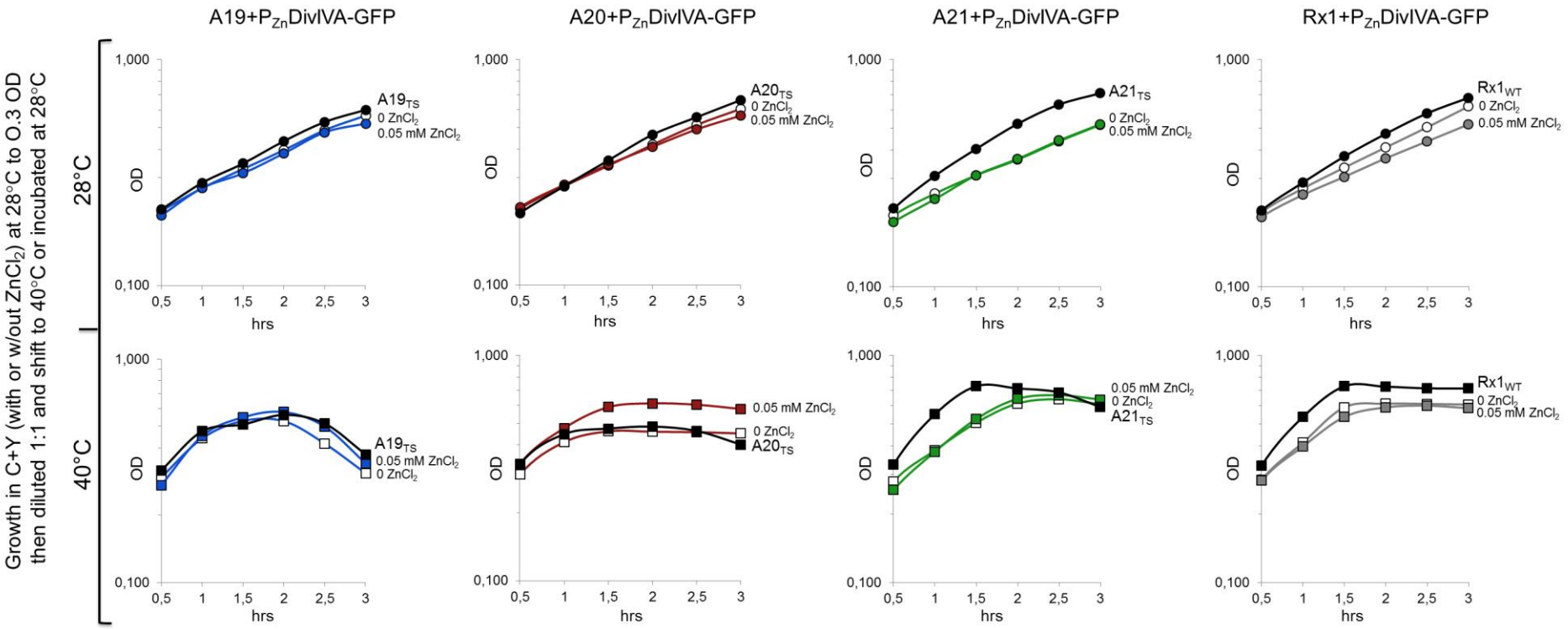

Figure 25. Growth of the Rx1$_{WT}$ and FtsA$_{TS}$+DivIVA-GFP derivatives in comparison with their respective parents in temperature-shifting experiments. Expression of DivIVA-GFP did not affect growth of the Rx1$_{WT}$ strain and the FtsA$_{TS}$ mutants at either 28°C (upper panels) or 40°C (lower panels).

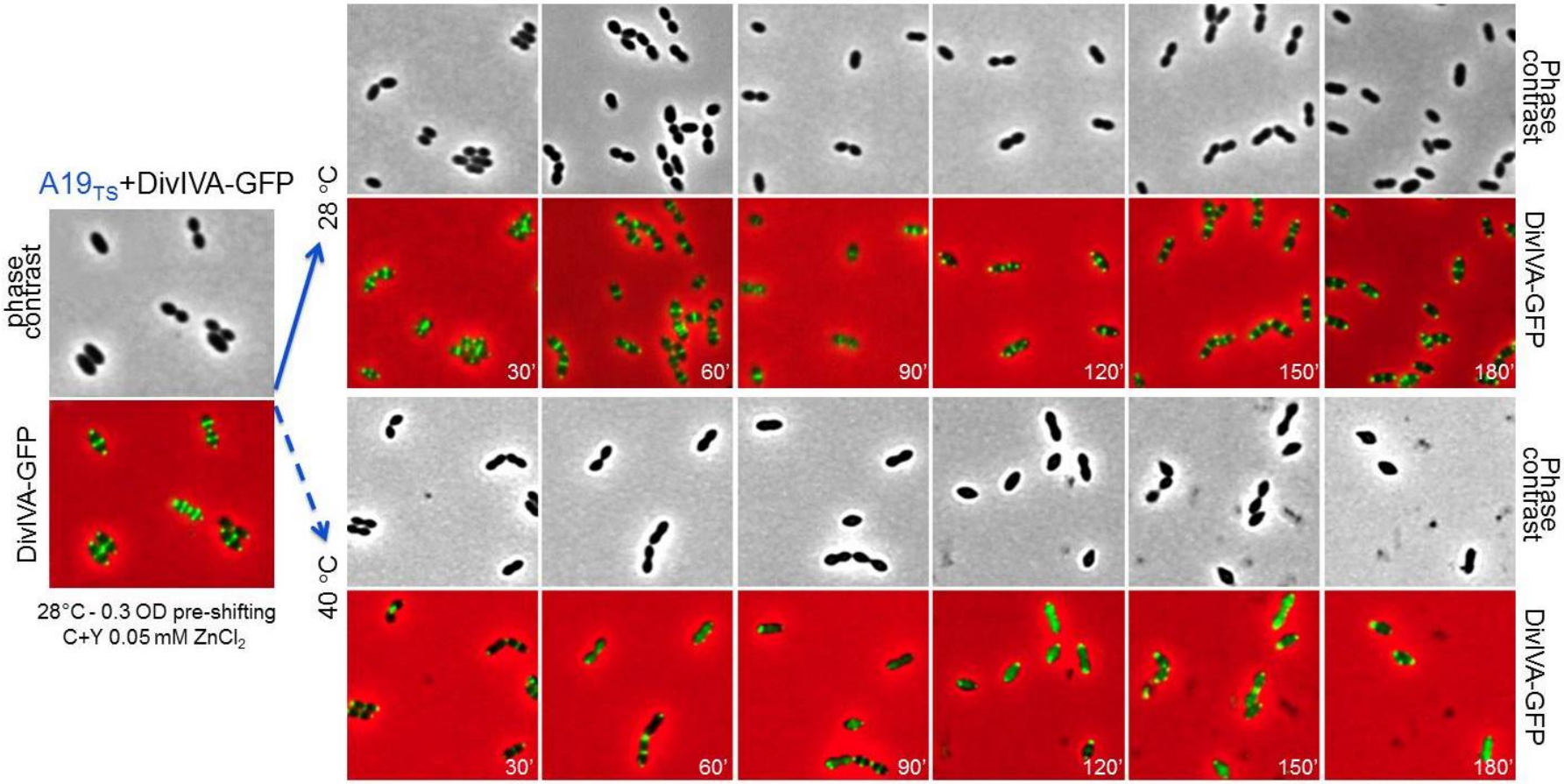

Figure 26. Expression and localization of DivIVA-GFP in the $A19_{TS}$ mutant in temperature-shifting experiments. DivIVA-GFP is correctly localized (midcells and poles) at 28°C but rapidly loses its septal localization upon shifting to 40°C

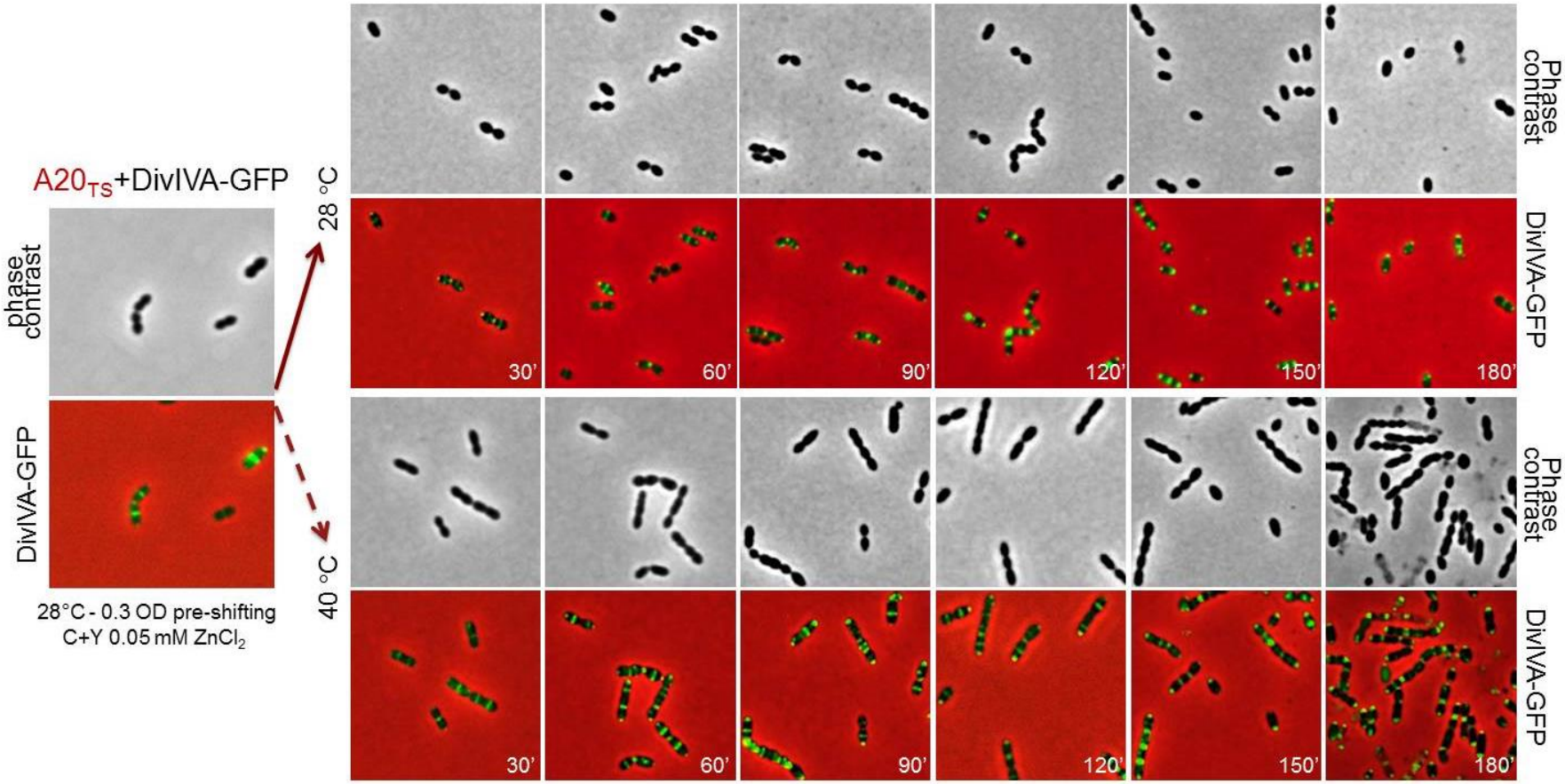

Figure 27. Expression and localization of DivIVA-GFP in the $A20_{TS}$ mutant in temperature-shifting experiments. DivIVA-GFP is correctly localized (midcells and poles) at 28°C and also upon shifting to 40°C, despite the cell division block, suggesting that the $FtsA20_{TS}$ mutations do not compromise localization of DivIVA. Nevetheless polar accumulation of DivIVA can be seen and increases over time after shifting.

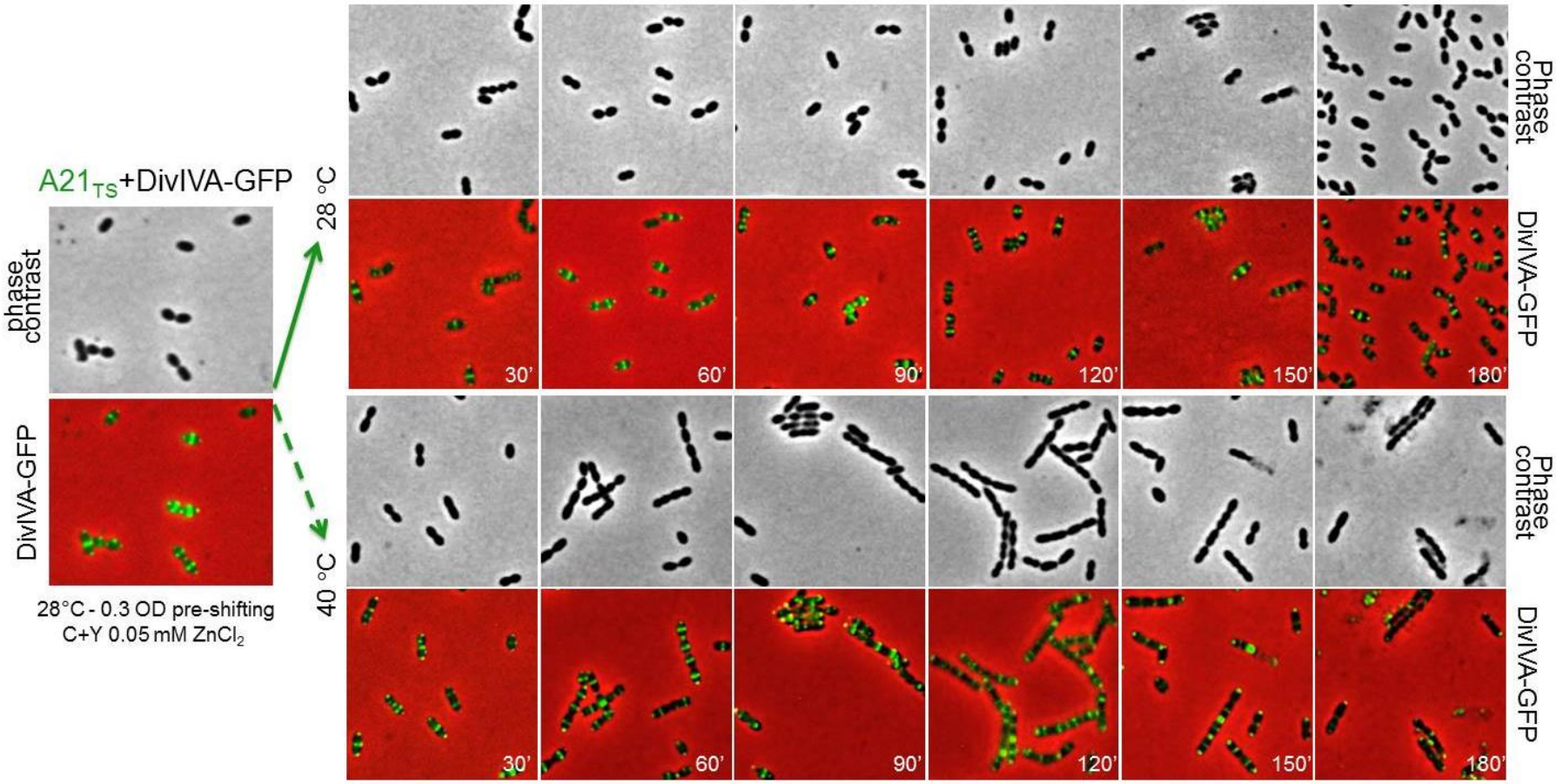

Figure 28. Expression and localization of DivIVA-GFP in the $A21_{TS}$ mutant in temperature-shifting experiments. DivIVA-GFP is correctly localized (midcells and poles) at 28°C but also upon shifting to 40°C, despite the cell division block, suggesting that also the $FtsA21_{TS}$ mutations do not compromise localization of DivIVA

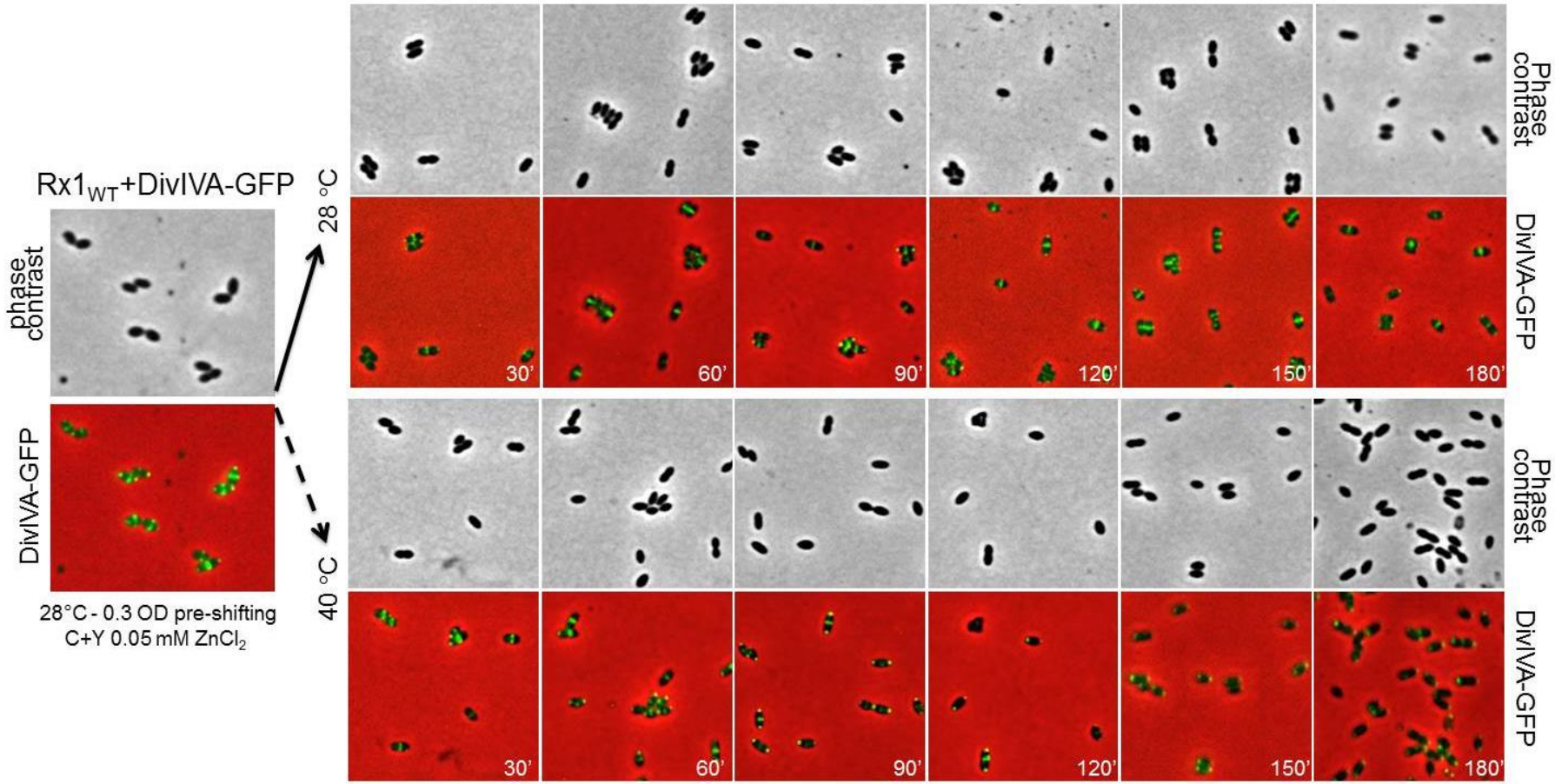

Figure 29. Expression and localization of DivIVA-GFP in the $Rx1_{WT}$ mutant in temperature-shifting experiments. DivIVA-GFP is correctly localized (midcells and poles) at 28°C but also upon shifting to 40°C, despite the cell division block, suggesting that also the $FtsA21_{TS}$ mutations do not compromise localization of DivIVA.

Fig. 30-34 show the growth curves and the localization of GFP-GpsB in the $Rx1_{WT}$ and in the A_{TS} mutants after shifting to 40°C and in parallel cultures at 28°C. As shown in Fig. 30, expression of GFP-GpsB affected the growth of the $A19_{TS}$ and the $A20_{TS}$ mutants that differently from their respective parents strains did not lyse after shifting to 40°C, but not that of $A21_{TS}$ mutant, for which the behaviour was similar to that of the parent strain. No significant differences were observed in the $Rx1_{WT}$+GFP-GpsB derivative, although it grew slightly slower than his $Rx1_{WT}$ parent.

As it could be anticipated by the growth curves, differently from their parent, both $A19_{TS}$+GFP-GpsB and $A19_{TS}$+GFP-GpsB derivative did not lyse upon shifting to 40°C. Consistently, GFP-GpsB was properly localized at the septa in growing and dividing but morphologically altered $A19_{TS}$ and $A20_{TS}$ cells shifted to 40°C (Fig. 31 and Fig. 32), suggesting that overexpression of GpsB (native+GFP-GpsB) could compensate for some but not all the Ts defects of the two A_{TS} mutants, thus resulting in partial suppression of their Ts phenotype. Instead, no effect of overxpression of GpsB could be detected for the $A21_{TS}$+GFP-GpsB mutant, that behaved similarly to its parent strain. Nevertheless, GFP-GpsB was localized in the elongated $A21_{TS}$+GFP-GpsB cells upon shifting to 40°C, suggesting that localization of GpsB is does not depend on previous localization of FtsA (Fig. 33). Finally, GFP-GpsB was well localized in the $Rx1_{WT}$ at 28°C and 40°C and no overxpression phenotype was observed in the conditions tested.

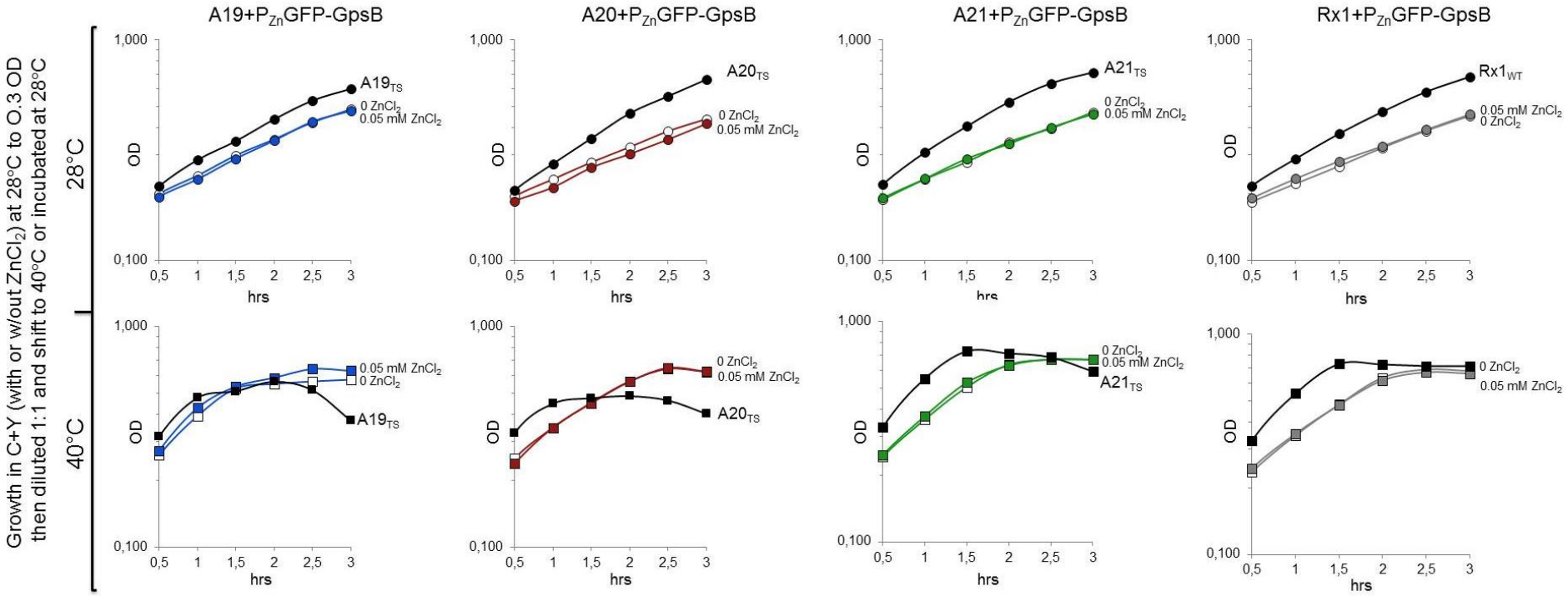

Figure 30. Growth of the Rx1$_{WT}$ and FtsA$_{TS}$+GFP-GpsB derivatives in comparison with their respective parents in temperature-shifting experiments
Expression of GFP-GpsB seems to suppress the growth defects of the A19$_{TS}$ and the A20$_{TS}$ mutants at 40°C, even without induction but not of the A21$_{TS}$ mutant, for which the behaviour was similar of the parent strain. No significant differences were observed in the Rx1$_{WT}$+GFP-GpsB derivative , although it grew slightly slower at 28°C and 40°C with respect to his Rx1$_{WT}$ parent.

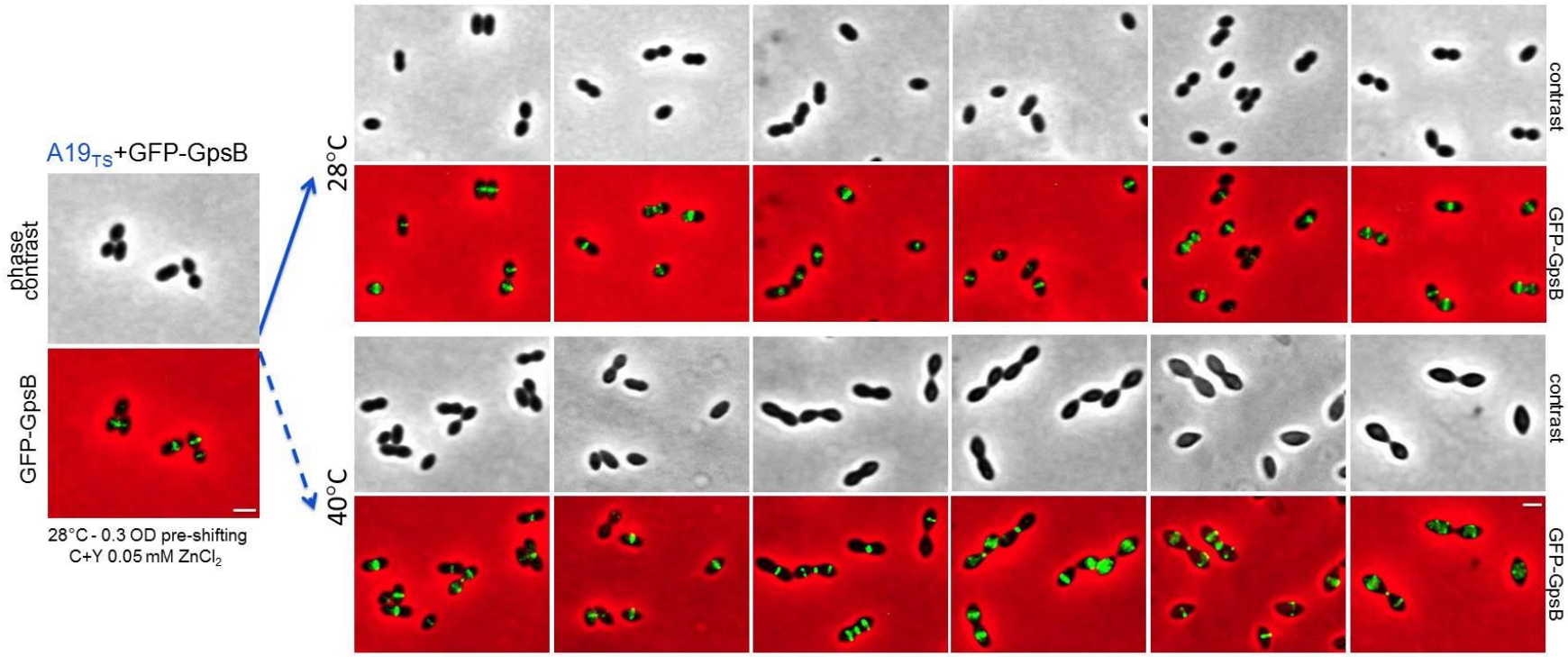

Figure 31. Expression and localization of GFP-GpsB in the $A19_{TS}$ mutant in temperature-shifting experiments. As could be anticipated by the growth curves, differently from its parent, the $A19_{TS}$+GFP-GpsB derivative did not lyse upon shifting to 40°C. Consistently, GFP-GpsB was properly localized at the septa in growing and dividing but morphologically altered $A19_{TS}$ cells shifted to 40°C, suggesting that overexpression of GpsB (native + GFP-GpsB) could compensate for the growth defects but for not the morhologically defects of the $A19_{TS}$ mutant and thus results in partial suppression of the $A19_{TS}$ phenotype.

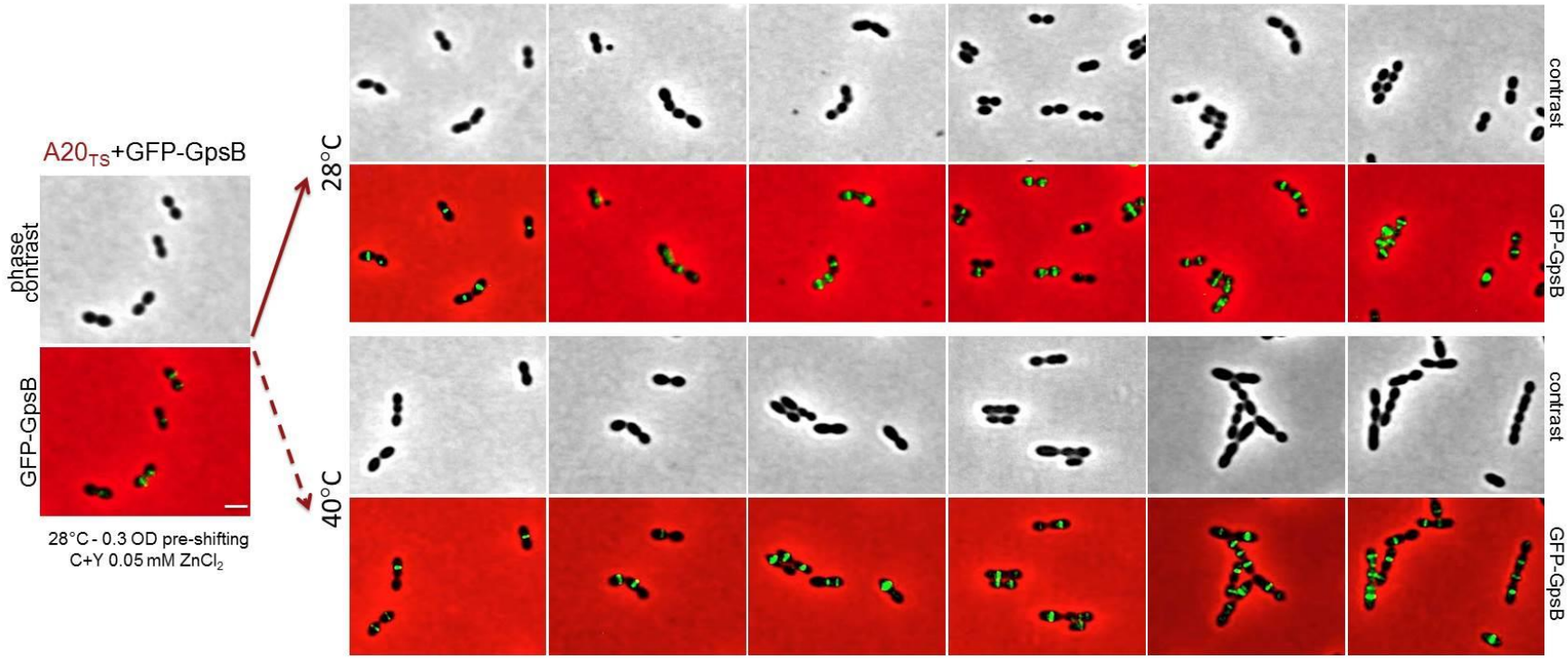

Figure 32. Expression and localization of GFP-GpsB in the $A19_{TS}$ mutant in temperature-shifting experiments. Localization of GpsB in $A20_{TS}$. Differently from its parent, the $A20_{TS}$+GFP-GpsB derivative did not lyse upon shifting at 40°C although, similarly to the $A19_{TS}$+GFP-GpsB, the defects of cell morphology are not completely suppressed in the presence of overexpressed GpsB. This time, uninduced and induced samples are more similar in morphology (not shown)

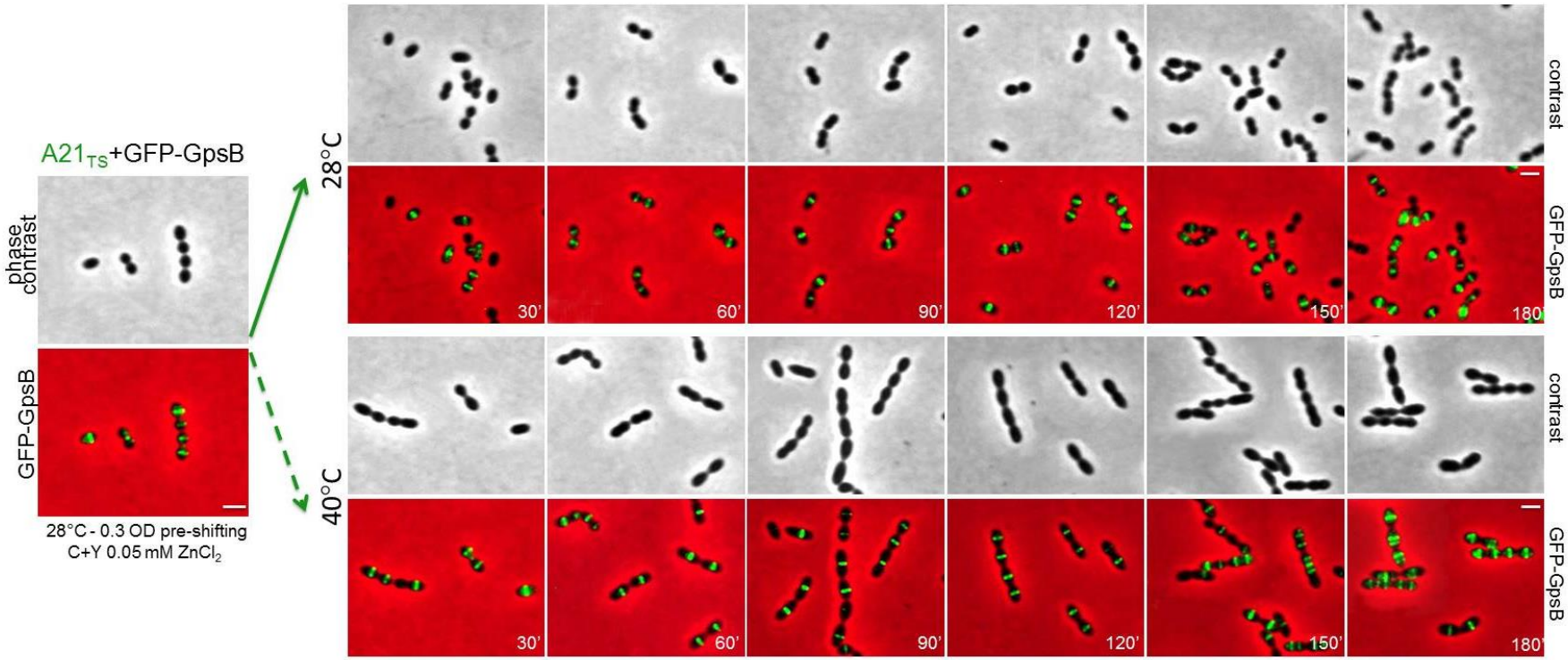

Figure 33. Expression and localization of GFP-GpsB in the A19$_{TS}$ mutant in temperature-shifting experiments. Localization of GpsB in A21$_{TS}$. Expression of GFP-GpsB did not seem to affect or to affect only slightly growth and morphology in both uninduced and induced conditions with respect to the A21$_{TS}$ parent upon shifting to 40°C and GFP-GpsB was localized in the elongated A21$_{TS}$+GFP-GpsB cells.

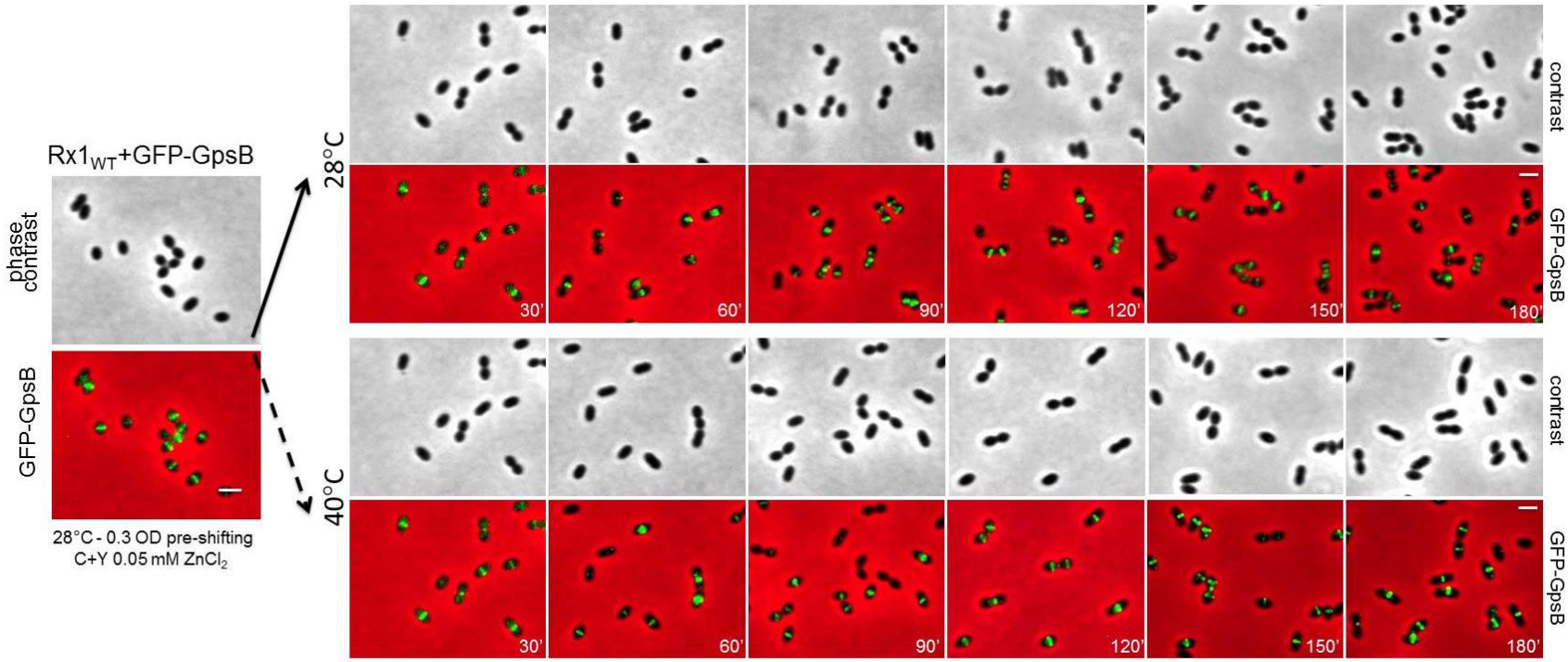

Figure 34. Expression and localization of GFP-GpsB in the $Rx1_{TS}$ strain in temperature-shifting experiments. GFP-GpsB showed a normal localization profile at 28°C and upon shifting to 40°C. Morphology is also normal indicating that there is not an overexpression phenotype at the conditions tested

Figs. 35-39 show the growth curves and the localization of GFP-StkP in the $Rx1_{WT}$ and in the A_{TS} mutants after shifting to 40°C and in parallel cultures at 28°C. As shown in Fig. 35, expression of GFP-StkP affected the growth of the $A19_{TS}$ and the $A20_{TS}$ mutants that, similarly to expression of GFP-GpsB and differently from their respective parents strains, did not lyse after shifting to 40°C. Expression of GFP-StkP did not affect the $A21_{TS}$ mutant, for which, again similar to expression of GFP-GpsB, the behaviour was similar to the parent strain. No differences were observed in the $Rx1_{WT}$+GFP-StkP derivative, confirming what already reported (Beihartz *et al.*, 2012).

As shown in Figs. 36-39, StkP is always localized at the division septum at both the permissive and non-permissive temperatures in the $Rx1_{WT}$ and all three A_{TS} mutants, and in the case of $A19_{TS}$ and $A20_{TS}$, overxpression of GFP-StkP seems to suppress their Ts phenotype (Figs 36-37). These results suggests that FtsA is not required for StkP localization, that indeed has been reported to localize at the division sites through its PASTA domains (Beilharz *et al*., 2012). Together these results suggest a connection between FtsA/GpSB and StkP (see below).

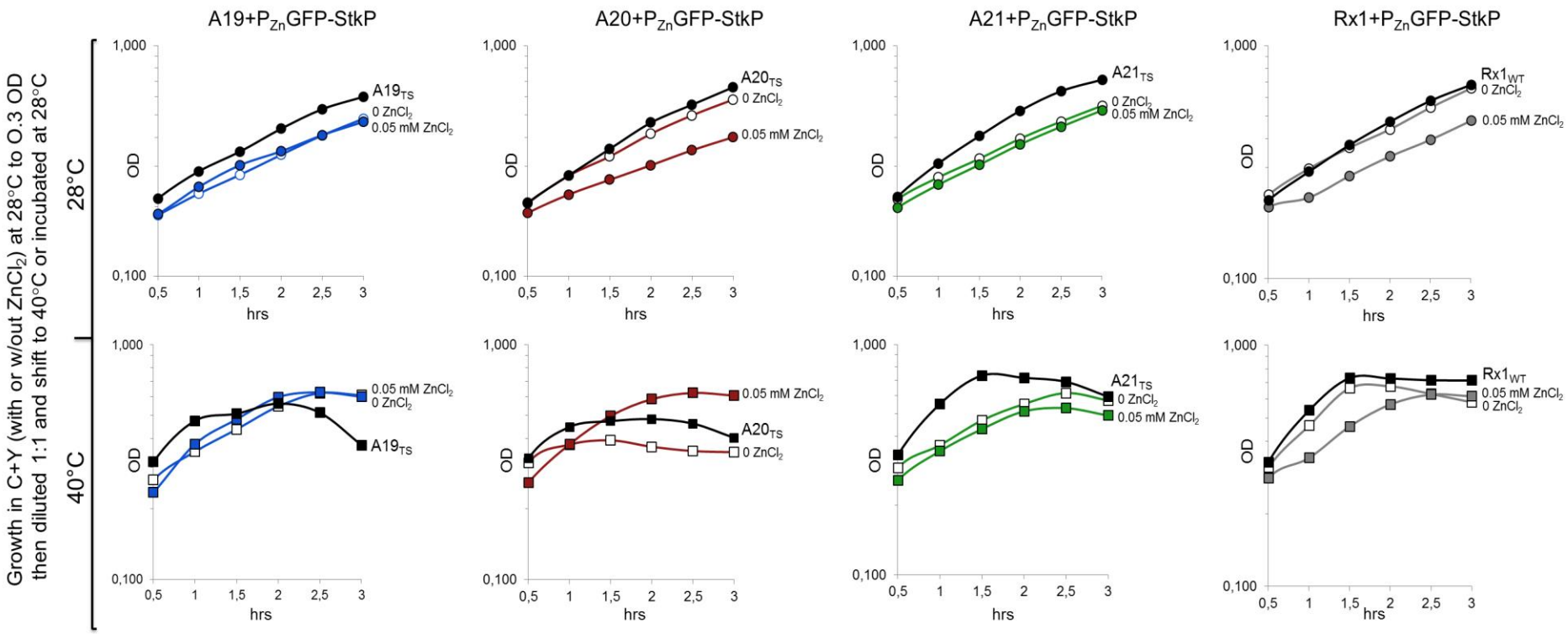

Figure 35. Growth of the Rx1$_{WT}$ and FtsA$_{TS}$+ GFP-StkP -GFP derivatives in comparison with their respective parents in temperature-shifting experiments. Similarly to what observed expressing GFP-GpsB, curves of the A19$_{TS}$+GFP-StkP (also without $ZnCl_2$ induction) and the A20$_{Ts}$+GFP-StkP (only upon induction ZnCl2) derivatives also show suppression of the growth defects at 40°C, whereas the behavior of A21$_{TS}$+GFP-StkP is instead similar in uninduced or induced cultures, and to that of its parent A21$_{TS}$ strain. As expected, no differences were observed in the Rx1$_{WT}$+GFP-StkP strain.

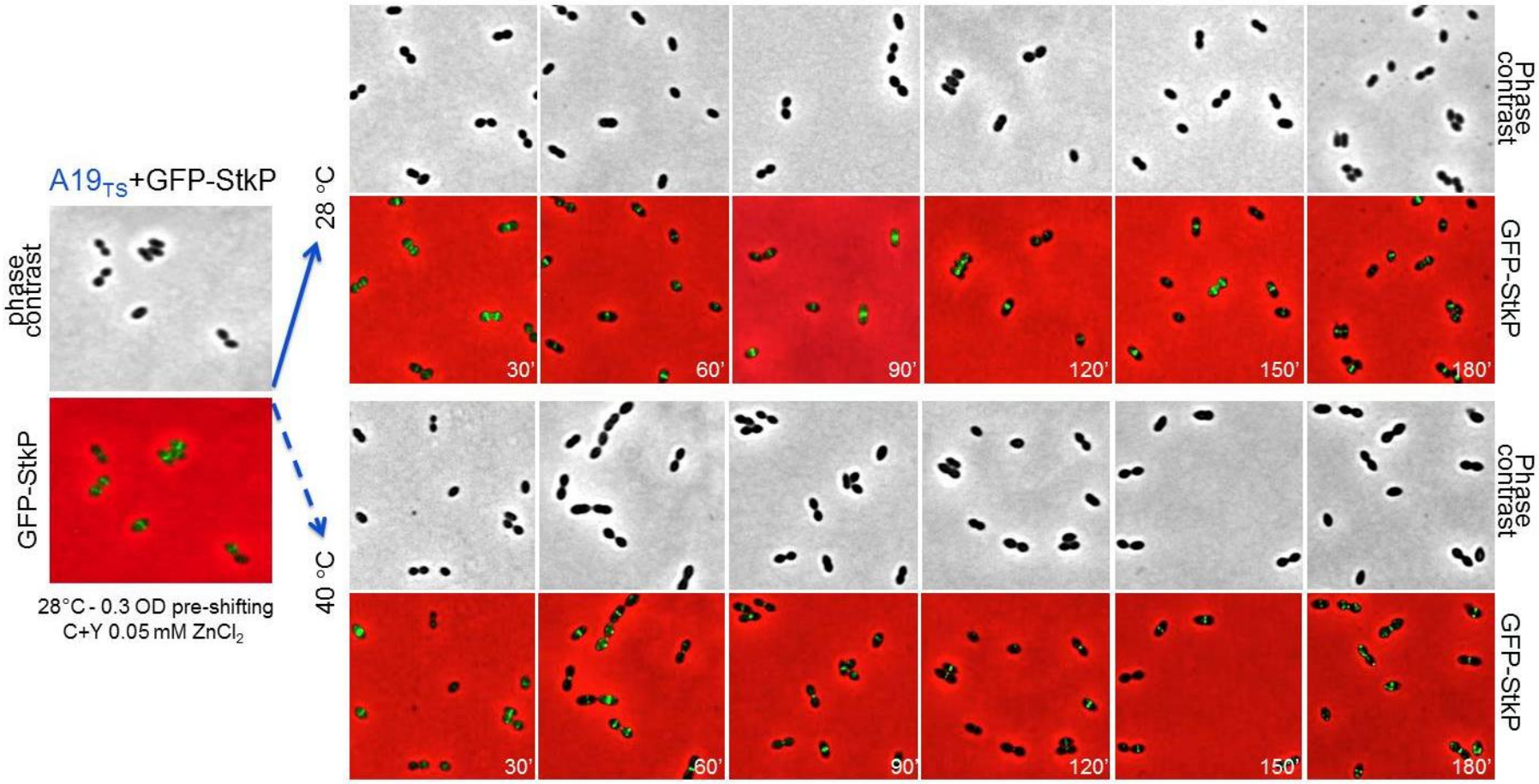

Figure 36. Expression and localization of GFP-StkP in the $A19_{TS}$ mutant in temperature-shifting experiments. As it could be anticipated by the growth curve upon shifting at 40°C, the $A19_{TS}$ phenotype seems to be complete suppressed in the presence of overexpressed StkP (native + GFP-StkP) also in uninduced conditions. Consistently, GFP-StkP is localizaed at midcell in $A19_{TS}$ at 28°C and after shifting to 40°C.

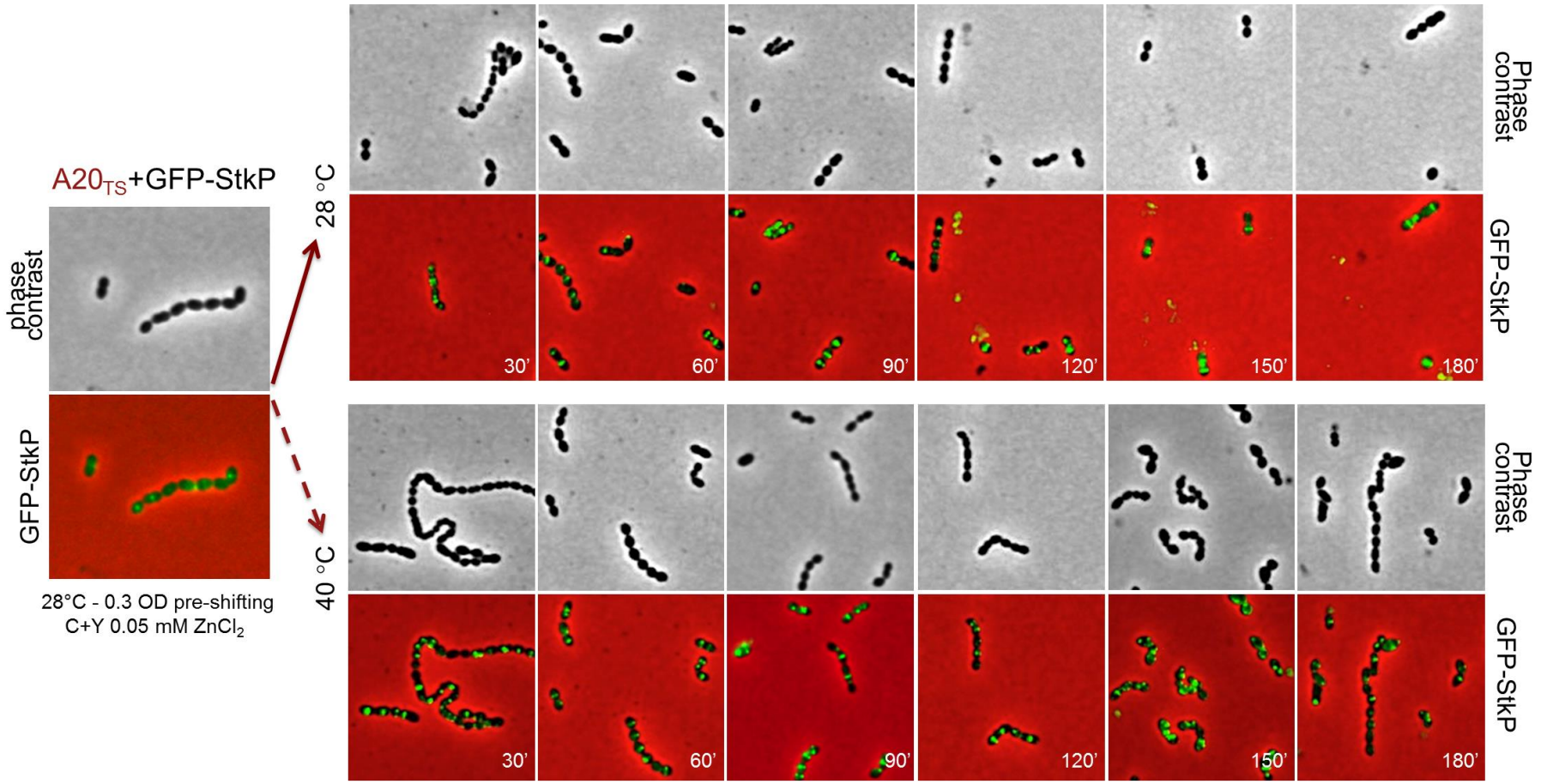

Figure 37. Expression and localization of GFP-StkP in the $A20_{TS}$ mutant in temperature-shifting experiments. Similarly to $A19_{TS}$, also in $A20_{TS}$ is Ts phenotype seems to be suppressed in the presence of overexpressed StkP (native + GFP-StkP), but this time only upon induction. Consistently, uninduced samples show a mutated morphology upon shifting to 40°C (not shown), while the induced one with 0.05 mM ZnCl2 showed normal growth and "almost normal" morphology upon shifting to 40°C. GFP-StkP is localizaed at midcell in $A20_{TS}$ at 28°C and after shifting to 40°C.

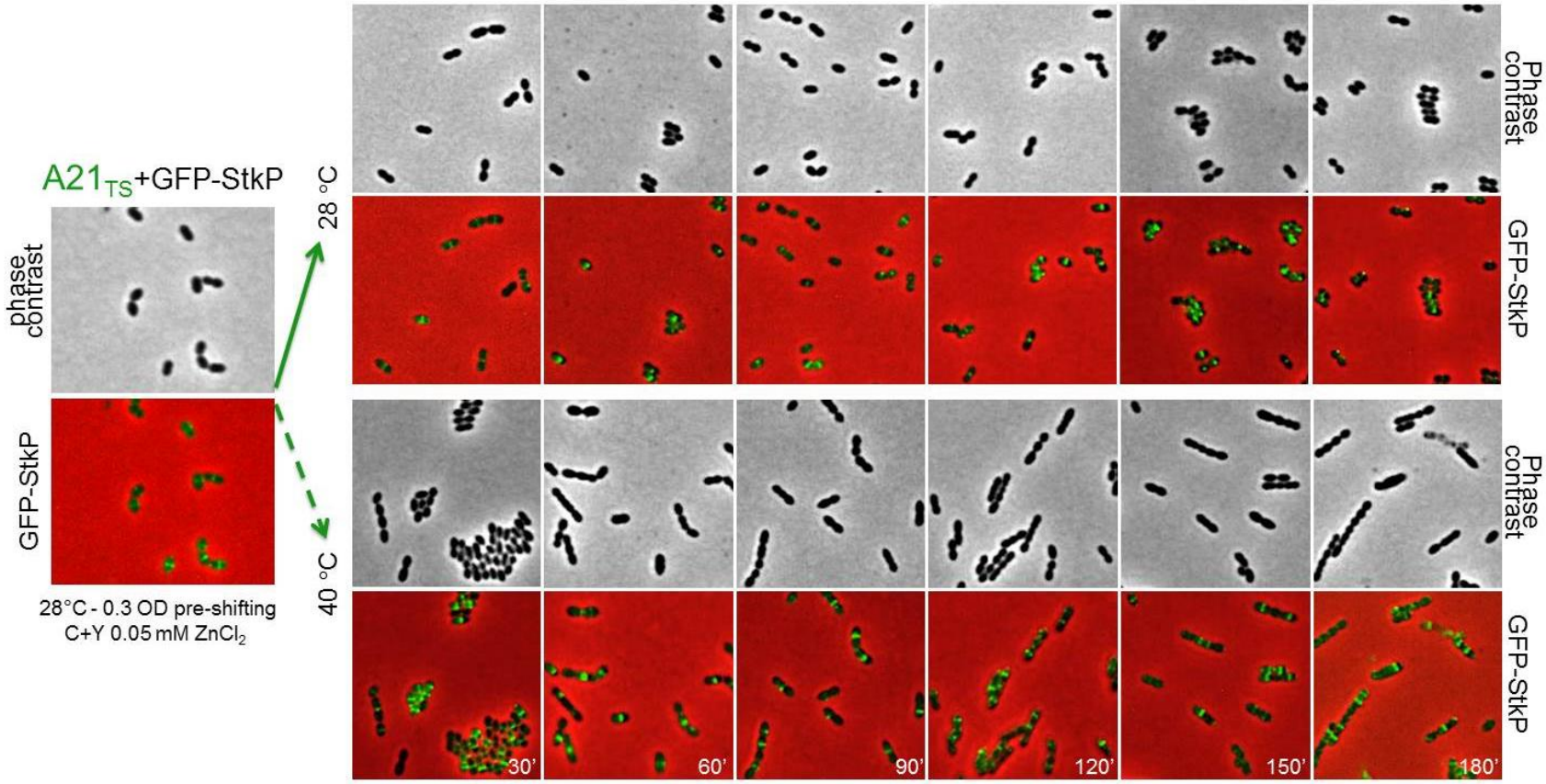

Figure 38. Expression and localization of GFP-StkP in the $A21_{TS}$ mutant in temperature-shifting experiments. Expression of GFP-StkP did not affected morphology of the $A21_{TS}$. GFP-StkP is localized in the elongated A21TS upon shifting to 40°C, suggesting that the block in cell division of $A21_{TS}$ is independent from StkP.

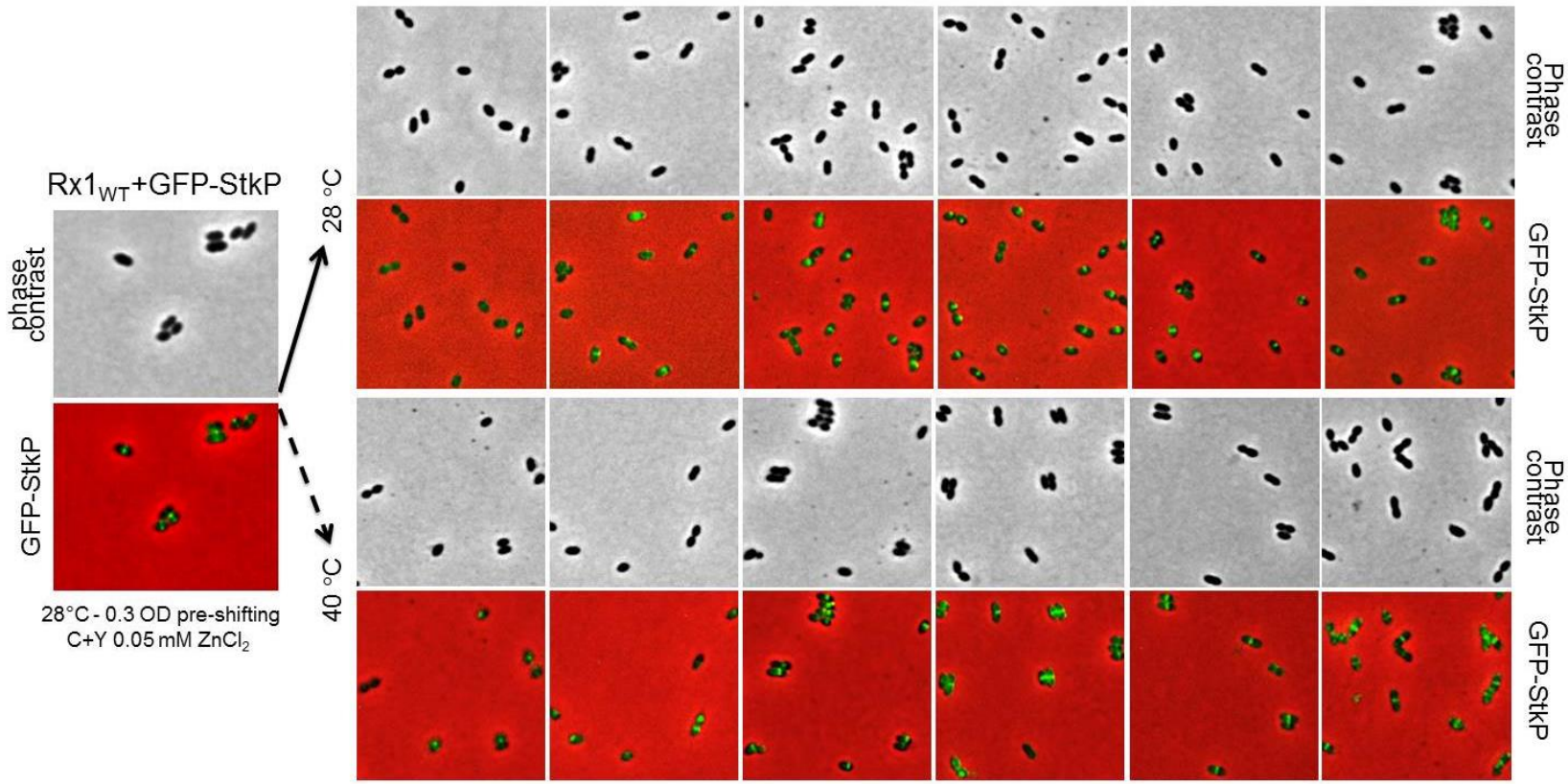

Figure 39. Expression and localization of GFP-StkP in the $Rx1_{WT}$ in temperature-shifting experiments. GFP-StkP is properly localizaed in $Rx1_{WT}$ cells at 28°C and after shifting to 40°C, confirming what already observed for the wild-type $R6_{WT}$ strain (Beilhartz et al., 2012).

Figs. 40-44 show the growth curves and the localization of GFP-PBp2x in the $Rx1_{WT}$ and in the A_{TS} mutants after shifting to 40°C and in parallel cultures at 28°C. As shown in Fig. 40, expression of GFP-PBp2x in the $Rx1_{WT}$ and in the A_{TS} mutants did not affect growth and all the GFP-PBp2x derivatives, behaved similar to their respective parent strains at 28°C and after shifting to 40°C. Moreover, both the $Rx1_{WT}$ and the A_{TS}+GFP-PBp2x derivatives grew similarly in uninduced and induced samples and no suppression of the A_{TS} phenotype was observed after shifting to 40°C.

Consistently, expression of GFP-PBp2x did not affect morphology of the $Rx1_{WT}$ and the A_{TS} mutants, and GFP-PBp2x was properly localized at the midcell and the cell poles in all the strain at 28°C whereas upon shifting to 40°C it was properly localized only in the $Rx1_{WT}$ (Figs. 41-44). In particular, in the $A19_{TS}$ mutant, PBP2x lost its septal localization after shifting to the non-permissive temperature, although slower than other markers, and then accumulated in the cells (Fig.41). In the $A20_{TS}$ mutant instead, GFP-PBP2x was localized for all time upon the shifting at 40°C (Fig. 42). Similarly to $A19_{TS,}$ PBP2x was localized in to $A21_{TS}$ cells at 28°C but lost its septal localization after shifting to the non-permissive temperature progressively accumulating in the cells (Fig. 43). As expected, GFP-PBp2x was properly localized at midcell at 28°C and 40°C in the $Rx1_{WT}$ (Fig. 44), confirming what previosly reported (Peters *et al*., 2014).

These results suggest that FtsA is not required for proper midcell localization of PBP2x, supporting the notion that PBP2x, as StkP, localize to the septum through its PASTA domain (Peters et al., 2014), neverthless interaction with FtsA may be required for for PBP2x function in proper septal PG synthesis and septal closure.

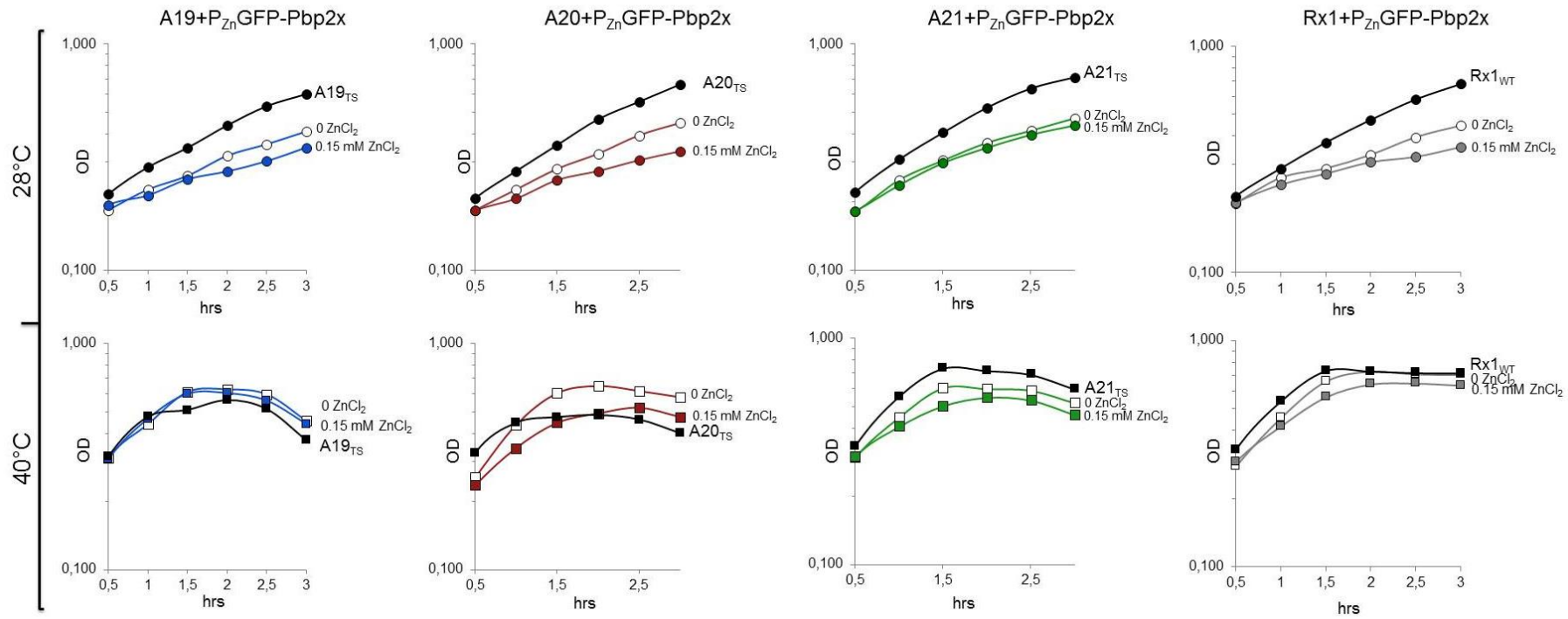

Figure 40. Growth of the Rx1$_{WT}$ and FtsA$_{TS}$+GFP-PBP2x -GFP derivatives in comparison with their respective parents in temperature-shifting experiments. Expression of GFP-Pbp2x in the Rx1$_{WT}$ and the FtsA$_{TS}$ mutants from the P$_{Zn}$ promoter did not affect growth of the Rx1$_{WT}$ and the A$_{TS}$ mutants at 28°C (upper panels) or 40°C (lower panels), although all the GFP-PBP2x derivatives grew slightly slowe at 28°C with respect to the parent strain. No suppression of the A$_{TS}$ growth phenotype.

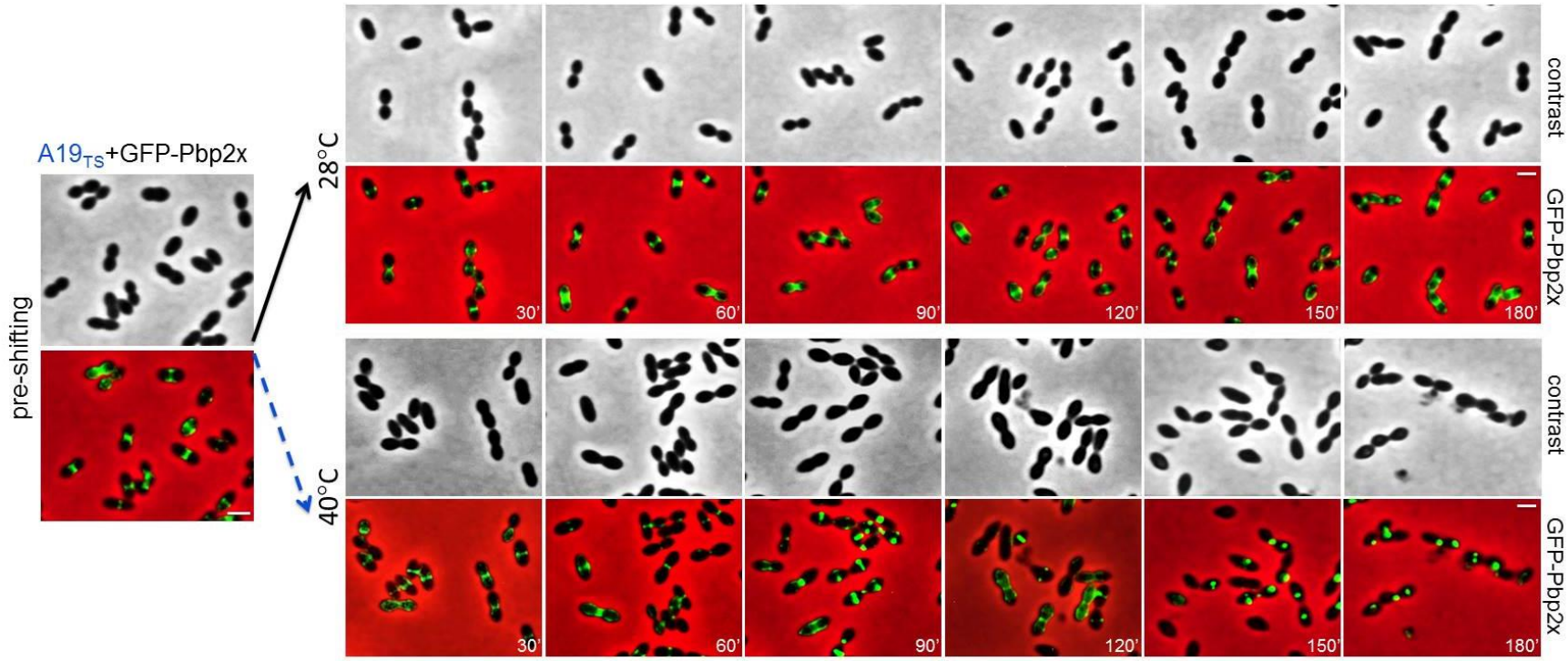

Figure 40. Expression and localization of GFP-PBB2x in the $A19_{TS}$ mutant in temperature-shifting experiments Cell morphology is similar to the parental strain, but after 60-90 min after shifting to 40°C, PBP2x idelocalized and accumulates in lysing cells.

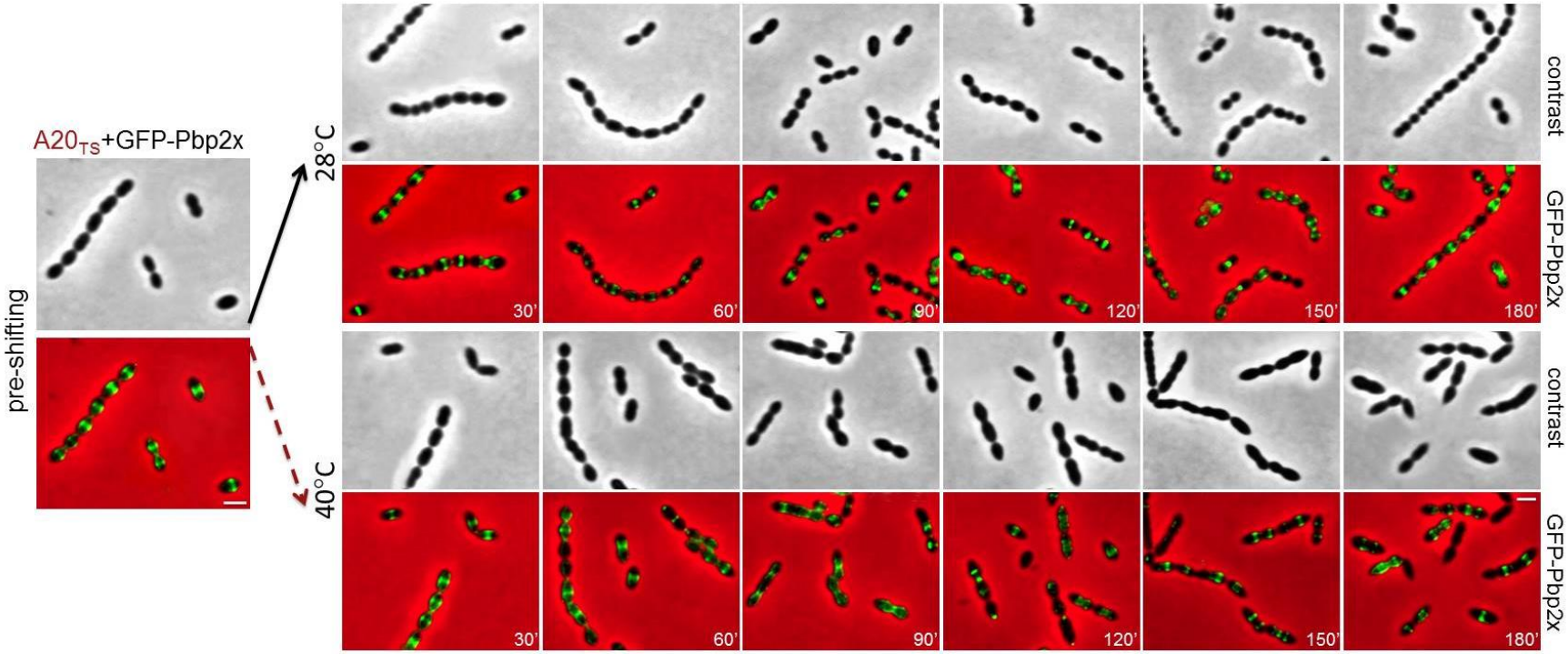

Figure 42. Expression and localization of GFP-PBP2x in the $A20_{TS}$ mutant in temperature-shifting experiments. With respect of the parental strain A20 $_{TS}$+PZnGFP-Pbp2x seems is more chainy than the parental strain. PBP2x remains localized in discrete foci of the elongated **$A20_{TS}$** after shifting to 40°C.

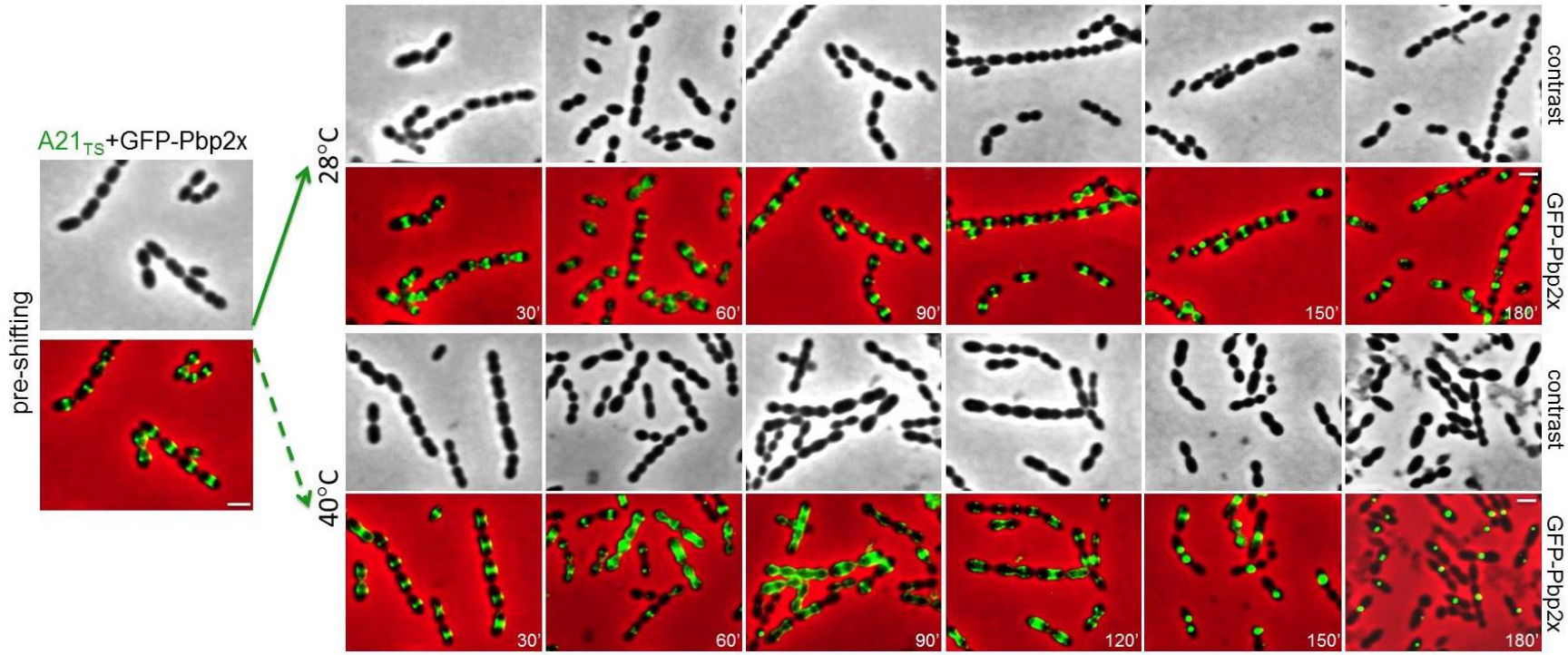

Figure 43. Expression and localization of GFP-PBP2x in the $A21_{TS}$ mutant in temperature-shifting experiments. Like $A20_{TS}$, $A21_{TS}$+P_{Zn}GFP-Pbp2x seems is more chainy than the parental strain. However in this strain , Pbp2x delocalized after 60-90 min from shifting to 40°C.

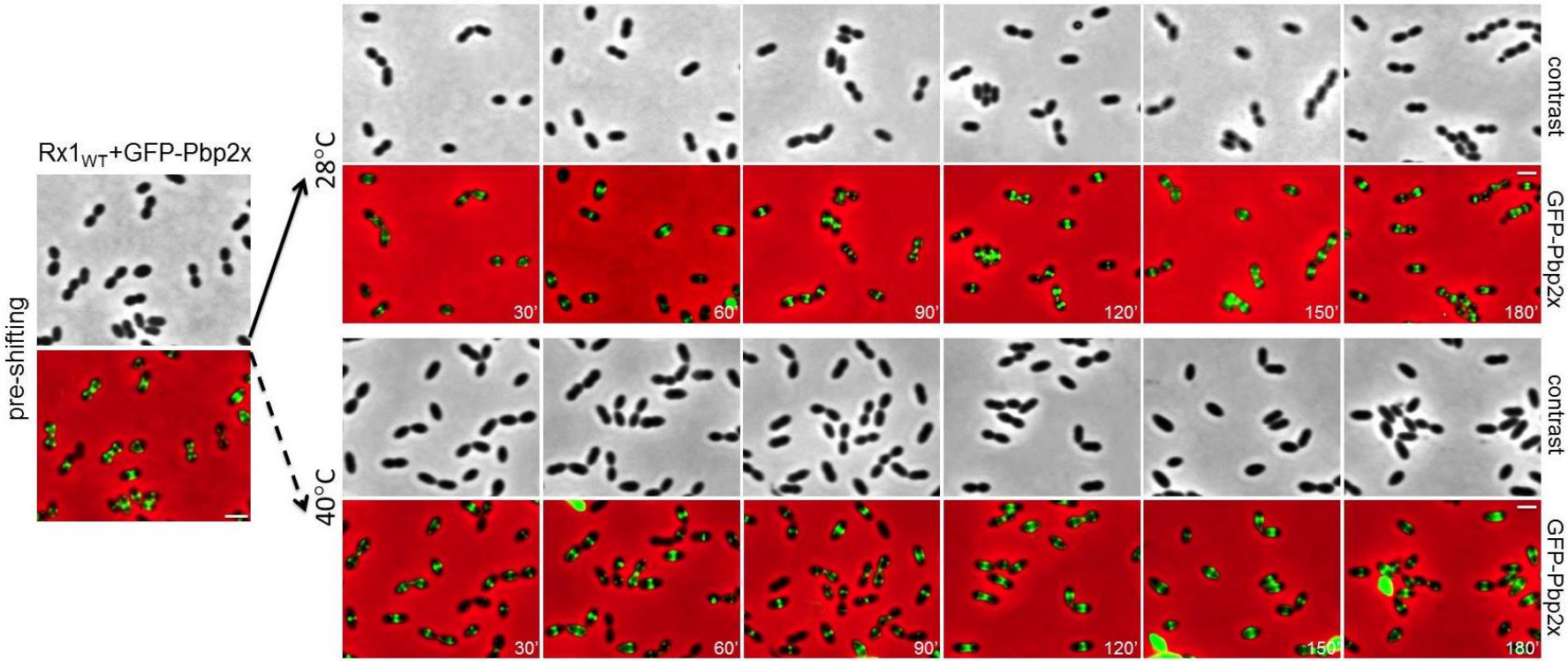

Figure 44. Expression and localization of GFP-StkP in the $Rx1_{WT}$ in temperature-shifting experiments Localization of GFP-Pbp2X in GFP-Pbp2X showed a normal septal localization profile at 28°C and after shifting to 40°C.

8. Does overexpression of GFP-StkP and GFP-GpsB suppress the $A19_{TS}$ and the $A20_{TS}$ phenotypes?

As mentioned above, the $A19_{TS}$ and the $A20_{TS}$ strains overexpressing GFP-GpsB or GFP-StkP showed partial or complete suppression of their $FtsA_{TS}$ phenotypes and correct localization of these proteins in growing and dividing mutant cells after temperature shifting to the non-permissive temperatures, suggesting that overexpression of either GFP-GpsB or GFP-StkP may compensate for the absence of functional FtsA in these mutants.

Indeed, when StkP was overexpressed (native + GFP-StkP) in the $A19_{TS}$ strain, the A19 Ts phenotype seemed completely suppressed, also in the absence $ZnCl_2$ in the medium, probably due to a leaky expression of the protein from the P_{Zn} promoter. Indeed, weak fluorescence signals at the cell division site was visible by fluorescence microscopy and the GFP-StkP band was detected by Western blotting using anti-StkP polyclonal antibodies also in uninduced samples at 28°C and 40°C (not shown). Consistently, $A19_{TS}$+GFP-StkP could grow after shifting to 40°C and $A19_{TS}$+GFP-StkP shifted to the non-permissive temperature showed a wild-type morphology, similar to that of the $Rx1_{WT}$. Therefore, to exclude the presence of intragenic suppressor mutations, the *ftsA*19 from the $A19_{TS}$+GFP-StkP derivative was amplified and sequenced and no additional mutations were detected in the *ftsA19*, suggesting that StkP overexpression could indeed suppress the A19 Ts phenotype, although the presence of extragenic suppressor mutation(s) in other parts of the chromosome cannot be ruled out. Moreover, the suppression of the $A20_{TS}$ allele by overexpressing StkP (although this time only upon induction) further supports this notion. In the case of the $A21_{TS}$ mutant, instead, StkP overexpression had no effect on the Ts phenotype, suggesting that the block in cell division of $A21_{TS}$ is independent from StkP.

Similar results were observed during GpsB overexpression of (native + GFP-GpsB). As observed with-GFP-StkP, the A19 and the A20 Ts growth defects were suppressed and GFP-GpsB was correctly localized at midcell after shifting to the non-permissive temperature. However, in this case both $A19_{TS}$ and $A20_{TS}$ cells at 40°C were morphologically altered, suggesting that, differently

from StkP, GpsB can only partially suppress the Ts defects in these two mutants. Together these results suggest a link between FtsA, StkP and GpsB, that needs to be clarify further.

Interestingly, several recent works have proposed phosphorylation through StkP as a mechanism to regulate the cell cycle in streptococci (Beilharz *et al.*, 2012; Fleurie *et al.*, 2012).

Moreover a connection between GpsB and StkP in *S. pneumoniae* has been recently proposed by Fleurie *et al.*, 2014, although many aspects remain unclear. According to their model, GpsB is required for septal localization and kinase activity of StkP and hence, for StkP-dependent phosphorylation of DivIVA and other substrates. However, in a collaboration with Prof. M. Winkler's at the University of Indiana, we established that in all the delta-*gpsB* mutants obtained using three different genetic backgrounds, StkP is still localized and their phosphoprofile is highly variable, suggesting that things are not so simple as suggested. Nevertheless, overexpression in delta-*gpsB* mutants of either GFP-StkP or GFP-FtsA can fully suppress the *delta-gpsB* phenotype, once again supporting a connection between these three important cell division proteins.

While a connection between FtsA and GpsB is reasonable, also considering that FtsA is synthenically lethal with GpsB in *B. subtilis* (Tavares *et al.*, 2008), and therefore suggesting that the proteins may have an overlapping function related to septation, the role of StkP is not. However, given the activity of StkP, it can be speculated that its function may be either linked to a particular, yet-to-be-identified substrate that needs to be phospho- or hyper-phosphorylated when FtsA or GpsB are not functional/present or to balance phosphorylation among the different substrates. Following up this suggestion, and the other issues raised in the course of this work could help to give a clearer and more comprehensive understanding of cell division in *S. pneumoniae*.

Conclusive remarks

Here, we report for the first time the isolation and characterization of three *S. pneumoniae* FtsA conditional lethal mutants. The results confirm that *S. pneumoniae ftsA* is an essential gene and validate FtsA as a cell division target.

Differently from what observed in the model rod-shaped *E. coli* and *B. subtilis*, which undergo cell filamentation if cell division is blocked at earliest stages, an early block in cell division in *S.pneumoniae* results in cell lysis, suggesting that FtsA and likely FtsZ orchestrate both growth and division in oval-shaped cocci supporting a model in which a single large machinery, located at midcell, controls both cell elongation and cell division. To work properly, such a large midcell machinery would require a regulatory mechanism to monitor the cell cycle progression and signal when it is time to stop elongating and start dividing. This regulatory mechanism is likely to be mediated by the Ser/Thr kinase StkP, which has been shown to act as a molecular switch to regulate elongation *vs* division, although the details of the mechanism, as well as all the players involved, still needs to be clarified.

Notably, in *S. pneumoniae* FtsA appears required for efficient midcell localization of FtsZ, supporting previous observations that FtsA may be necessary for anchoring FtsZ to the membrane in Gram-positives that lack a ZipA homolog. In fact, in all the $FtsA_{TS}$ strains, FtsZ was delocalized after shitfting to the non permissive temperature. As all three $FtsA_{TS}$ lost the ability to self-interact, and to polymerize and attach to the membrane, these results also support the model for FtsA function in *E. coli*, where the polymerization of the protein is crucial for FtsA function, allowing the tethering of FtsZ to the membrane, which in *S. pneumoniae* may be dispensable at the permissive temperature but becomes essential at the non-permissive one.

Beside providing new insights for cell division in *S. pneumoniae*, these mutants should offer a useful tool for determining the biological meaning of FtsA function *in vivo.*

Acknowledgments

I'd like to say a special thank you to **Orietta Massidda**, for the opportunity to make this work in her laboratory; for all the patience and support she gave me during these years, for being always available to help and teach me something new; for finding me as an old student and making me into a novel scientist.

Another special thank you goes to **Pavel Branny**, for hosting me in his lab in Prague for more than two years; for the help and for being always available to solve every problem, and giving me really useful advice: without your kindness this work could not have been done.

A big thank to **Daniela Musu**, for working with me, for the friendship, the teaching and sharing the knowledge and ideas and spending with me funny moments and hard working days.

Another thank you to all the colleagues of the Cagliari Lab: **Daniela Fadda**, **Antonella Santona, Silvia Mura** and **Federico Corona**, for being always gentle, helpful and friendly with me; and thanks to **Michael B. Whalen** for correcting the English.

Many thanks also to all the colleagues and friends of Prague: **Aleš Urlych**, **Nela Holečková**, **Linda Doubravová**, **Jana Goldová**, **Oliva Branny**, **Denisa Petráčková**, **Karolína Buriánková**, **Pepa Čáslavský**, **Honza Rasl, Tomáš Vomastek, Mila Maninová**, **Silvie Bezoušková** and **Alice Ziková**, for helping and teaching, for being always patient and gentle, and especially for being really great friends during these beautiful years. Děkuji moc kamarady!

Thanks to our collaborators in Madrid, **Miguel Vicente**, **Ana Isabel Rico** and **Marcin Krupka (**Centro National de Biotecnologia, CSIC**)**, and in Kaiserslautern, **Dalia Denapaite (**University of Kaiserslautern) , for the nice collaboration in carrying out the experiments. A thank to **Jan-Willem Veening** (University of Groningen) and to **Malcolm Winkler** (Indiana University), from the University of Indiana for kindly providing tools and methods, fundamental to carry out the work.

A very big and special thank you to my family, my **mother** and my **brother,** for the support during all this time, giving me what I needed to go ahead and believing in me all the time.

Thanks to everybody: I'll always keep you in my heart and I'll be always grateful to each one of you for making me a better scientist and person.

Andrea Mura gratefully acknowledges Sardinia Regional Government for the financial support of his PhD scholarship (P.O.R. Sardegna F.S.E. Operational Programme of the Autonomous Region of Sardinia, European Social Fund 2007-2013 - Axis IV Human Resources, Objective l.3, Line of Activity l.3.1.).

References

- Adams, D.W., and Errington, J. (2009) Bacterial cell division: assembly, maintenance and disassembly of the Z ring. *Nat Rev Microbiol* 7:642–653.

- Addinall S.G., Bi E., Lutkenhaus J. (1996) FtsZ ring formation in *fts* mutants. *J Bacteriol* 178:3877-84.

- Avery O. T., MacLeod C. M., McCarty M. (1944) Studies on the chemical nature of the substance inducing transformation of pneumococcal types: induction of transformation by a desoxyribonucleic acid fraction isolated from pneumococcus type III. *J. Exp. Med* 79:137–158.

- Battesti A., Bouveret E. (2012) The bacterial two-hybrid system based on adenylate cyclase reconstitution in *Escherichia coli*. *Methods* 58: 325–334.

- Beall B., Lutkenhaus J. (1992) Impaired cell division and sporulation of a *Bacillus subtilis* strain with the ftsA gene deleted. *J Bacteriol* 174:2398-403.

- Beilharz, K., Nováková, L., Fadda, D., Branny, P., Massidda, O., and Veening, J.W. (2012) Control of cell division in *Streptococcus pneumoniae* by the conserved Ser/Thr protein kinase StkP. *Proc Natl Acad Sci USA* 109:E905–E913.

- Bendezú, F.O., Hale, C.A., Bernhardt, T.G., and de Boer, P.A. (2009) RodZ (YfgA) is required for proper assembly of the MreB actin cytoskeleton and cell shape in *E. coli*. *EMBO J* 28:193–204.

- Berg K.H., Straume D., Håvarstein L.S. (2014) The function of the transmembrane and cytoplasmic domains of pneumococcal penicillin-binding proteins 2x and 2b extends beyond that of simple anchoring devices. *Microbiology* 160:1585-98.

- Bertsche, U., Kast, T., Wolf, B., Fraipont, C., Aarsman, M.E.G., Kannenberg, K., *et al.* (2006) Interaction between two murein (peptidoglycan) synthases, PBP3 and PBP1B, in *Escherichia coli*. *Mol Microbiol* 61:675–690.

- Bi E. & Lutkenhaus J. (1991) FtsZ ring structure associated with division in *Escherichia coli*. *Nature* 354:161–164

- den Blaauwen, T., de Pedro, M.A., Nguyen-Distèche, M., and Ayala, J.A. (2008) Morphogenesis of rod-shaped sacculi. *FEMS Microbiol Rev* 32: 321–344.

- Black S. (2010) The volatile nature of pneumococcal serotype epidemiology: potential for misinterpretation. *Pediatr Infect Dis J* 29:301-3.

- de Boer, P.A.J. (2010) Advances in understanding *E. coli* cell fission. *Curr Opin Microbiol* 13:730–737.

- Bogaert D., Groot R. De, Hermans P.W.M. (2004) *Streptococcus pneumoniae* colonisation: the key to pneumococcal disease. *Lancet Infect Dis* 4:144–148.

- Buddelmeijer, N., and Beckwith, J. (2004) A complex of the *Escherichia coli* cell division proteins FtsL, FtsB and FtsQ forms independently of its localization to the septal region. *Mol Microbiol* 52: 1315–1327.

- Busiek K.K., Eraso J.M., Wang Y., Margolin W. (2012) The early divisome protein FtsA interacts directly through its 1c subdomain with the cytoplasmic domain of the late divisome protein FtsN. *J Bacteriol* 194(8):1989-2000.

- Busiek K.K., Margolin W. (2015) Bacterial Actin and Tubulin Homologs in Cell Growth and Division. *Curr Biol* 25:R243-R254.

- Carballido-López, R., and Formstone, A. (2007) Shape determination in *Bacillus subtilis*. *Curr Opin Microbiol* 10: 611–616.

- Carettoni, D., Gómez-Puertas, P., Yim, L., Mingorance, J., Massidda, O., Vicente, M., Valencia, A., Domenici, E., and Anderluzzi, D. (2003) Phage-display and correlated mutations identify an essential region of subdomain 1C involved in homodimerization of *Escherichia coli* FtsA. *Proteins* 50: 192-206.

- Cha, J.H., and Stewart, G.C. (1997) The divIVA minicell locus of *Bacillus subtilis*. *J Bacteriol* 179:1671–1683.

- Chao Y., Marks L.R., Pettigrew M.M., Hakansson A.P. (2015) *Streptococcus pneumoniae* biofilm formation and dispersion during colonization and disease. *Front Cell Infect Microbiol* 4:194.

- Claessen, D., Emmins, R., Hamoen, L.W., Daniel, R.A., Errington, J., and Edwards, D.H. (2008) Control of the cell elongation-division cycle by shuttling of PBP1 protein in *Bacillus subtilis*. *Mol Microbiol* 68:1029–1046.

- Corbin B.D., Geissler B., Sadasivam M., Margolin W. (2004) Z-ring-independent interaction between a subdomain of FtsA and late septation proteins as revealed by a polar recruitment assay. *J Bacteriol* 186:7736-44.

- Corbin, B.D., Wang, Y., Beuria, T.K., and Margolin, W. (2007) Interaction between cell division proteins FtsE and FtsZ. *J Bacteriol* 189:3026–3035.

- Cornick J.E., Bentley S.D. (2012) *Streptococcus pneumoniae*: The evolution of antimicrobial resistance to beta-lactams, fluoroquinolones, and macrolides. *Microbes Infect* 14:573–583.

- Di Lallo G., Fagioli M., Barionovi D., Ghelardini P., Paolozzi L. (2003) Use of a two-hybrid assay to study the assembly of a complex multicomponent protein machinery: bacterial septosome differentiation. *Microbiology* 149:3353-9.

- Durand-Heredia, J., Rivkin, E., Fan, G., Morales, J., and Janakiraman, A. (2012) Identification of ZapD as a cell division factor that promotes the assembly of FtsZ in *Escherichia coli*. *J Bacteriol* 194:3189–3198.

- Eberhardt, A., Wu, L.J., Errington, J., Vollmer, W., Veening, J.W. (2009) Cellular localization of choline utilization proteins in *Streptococcus pneumoniae* using novel fluorescent reporter systems. *Mol Microbiol* 74:395–408.

- Ebersbach, G., Galli, E., Møller-Jensen, J., Löwe, J., and Gerdes, K. (2008) Novel coiled-coil cell division factor ZapB stimulates Z ring assembly and cell division. *Mol Microbiol* 68:20–735.

- Echenique J., Kadioglu A., Romao S., Andrew P.W., Trombe M.C. (2004) Protein serine/threonine kinase StkP positively controls virulence and competence in *Streptococcus pneumoniae*. *Infect Immun* 72:2434-7.

- Edwards, D.H., and Errington, J. (1997) The *Bacillus subtilis* DivIVA protein targets to the division septum and controls the site specificity of cell division. *Mol Microbiol* 24:905–915.

- Egan, A.J., and Vollmer, W. (2013) The physiology of bacterial cell division. *Ann N Y Acad Sci* 1277:8–28.

- van den Ent F., Löwe J. (2000). Crystal structure of the cell division protein FtsA from Thermotoga maritima. *EMBO J* 19:5300–5307

- van den Ent, F., Amos, L.A., and Löwe, J. (2001) Prokaryotic origin of the actin cytoskeleton. *Nature* 413:39–44.

- van den Ent, F., Johnson, C.M., Persons, L., De Boer, P., and Löwe, J. (2010) Bacterial actin MreB assembles in complex with cell shape protein RodZ. *EMBO J* 29:1081–1090.

- Erdmann J. (2010) Keeping pneumonia's vaccines effective. *Chem Biol* 17:1043–1044.

- Erickson, H.P., Anderson, D.E., and Osawa, M. (2010) FtsZ in bacterial cytokinesis:cytoskeleton and force generator all in one. *Microbiol Mol Biol Rev* 74:504–528.

- Errington, J., Daniel, R.A., and Scheffers, D.J. (2003) Cytokinesis in bacteria. *Microbiol Mol Biol* Rev 67:52–65.

- Fadda, D., Pischedda, C., Caldara, F., Whalen, M.B., Anderluzzi, D., Domenici, E., and Massidda, O. (2003) Characterization of divIVA and other genes located in the chromosomal region downstream of the dcw cluster in *Streptococcus pneumoniae*. *J Bacteriol* 185:6209–6214.

- Fadda, D., Santona, A., D'Ulisse, V., Ghelardini, P., Ennas, M.G., Whalen, M.B., and Massidda, O. (2007) *Streptococcus pneumoniae* DivIVA: localization and interactions in a MinCD-free context. *J Bacteriol* 189:1288–1298.

- Feldman, C., Anderson, R. (2014) Recent advances in our understanding of *Streptococcus pneumoniae* infection. *F1000Prime Rep* 6:82.

- Feucht, A., Lucet, I., Yudkin, M. D., Errington, J. (2001) Cytological and biochemical characterization of the FtsA cell division protein of *Bacillus subtilis*. *Mol Microbiol* 40:115–125

- Fleurie A., Lesterlin C., Manuse S., Zhao C., Cluzel C., Lavergne J.P., Franz-Wachtel M., Macek B., Combet C., Kuru E., VenNieuwenhze M.S., Brun Y.V., Sherratt D., Grangeasse C. (2014) MapZ marks the division sites and positions FtsZ rings in *Streptococcus pneumoniae*. *Nature* 516:259-62

- Garti-Levi, S., Hazan, R., Kain, J., Fujita, M., and Ben-Yehuda, S. (2008) The FtsEX ABC transporter directs cellular differentiation in *Bacillus subtilis*. *Mol Microbiol* 69:1018–1028.

- Gates F.L. (1933) The reaction of individual bacteria to irradiation with ultraviolet light. *Science* 77:350–350.

- Geissler, B., Shiomi, D. and Margolin, W. (2007) The ftsA* gain-of-function allele of *Escherichia coli* and its effects on the stability and dynamics of the Z ring. *Microbiology* 153:814 – 825.

- Gerdes, K. (2009) RodZ, a new player in bacterial cell morphogenesis. *EMBO J* 28:171–172.

- Gerding, M.A., Liu, B., Bendezú, F.O., Hale, C.A., Bernhardt, T.G., and De Boer, P.A. (2009) Self-enhanced accumulation of FtsN at division sites and roles for other proteins with a SPOR domain (DamX, DedD, and RlpA) in *Escherichia coli* cell constriction. *J Bacteriol* 191:7383–7401

- Giefing C., Meinke A.L., Hanner M., Henics T., Bui M.D., Gelbmann D., Lundberg U., Senn B.M., Schunn M., Habel A., Henriques-Normark B., Ortqvist A., Kalin M., von Gabain A., Nagy E. (2008) Discovery of a novel class of highly conserved vaccine antigens using genomic scale antigenic fingerprinting of pneumococcus with human antibodies. *J Exp Med* 205:117-31.

- Gilley R. P., Orihuela C. J. (2014). Pneumococci in biofilms are non-invasive: implications on nasopharyngeal colonization. *Front. Cell. Infect. Microbiol.* 4:163.

- Goehring, N.W., and Beckwith, J. (2005) Diverse paths to midcell: assembly of the bacterial cell division machinery. *Curr Biol* 15:R514–R526.

- Griffith F. (1928) Significance of pneumococcal types. *J. Hyg*. 27:113–159.

- Gueiros-Filho, F.J., and Losick, R. (2002) A widely conserved bacterial cell division protein that promotes assembly of the tubulin-like protein FtsZ. *Genes Dev* 16:2544–2556.

- Haeusser D.P., Margolin W. (2011) Prokaryotic cytokinesis: little rings bring big cylindrical things. *Curr Biol* 21:R221-3.

- Hale, C.A., and De Boer, P.A.J. (2002) ZipA is required for recruitment of FtsK, FtsQ, FtsL, and FtsN to the septal ring in *Escherichia coli*. *J Bacteriol* 184:2552–2556.

- Hamoen, L.W., Meile, J.-C., De Jong, W., Noirot, P., and Errington, J. (2006) SepF, a novel FtsZ-interacting protein required for a late step in cell division. *Mol Microbiol* 59:989–999.

- Hanahan D. (1983). Studies on transformation of *Escherichia coli* with plasmids. *J. Mol. Biol.* 166 557–580.

- Henriques M.X., Catalão M.J., Figueiredo J., Gomes J.P., Filipe S.R. (2013) Construction of improved tools for protein localization studies in *Streptococcus pneumoniae*. *PLoS One* 8:e55049.

- Henriques-Normark B., Normark S. (2010) Commensal pathogens, with a focus on *Streptococcus pneumoniae*, and interactions with the human host. *Exp Cell Res* 316:1408-14.

- Herricks J.R., Nguyen D., Margolin W. (2014) A thermosensitive defect in the ATP binding pocket of FtsA can be suppressed by allosteric changes in the dimer interface. *Mol Microbiol* 94:713-27.

- Higgins, M.L., and Shockman, G.D. (1970) Model for cell wall growth of *Streptococcus faecalis*. *J Bacteriol* 101:643–648.

- Higgins, M.L., and Shockman, G.D. (1976) Study of cycle of cell wall assembly in *Streptococcus faecalis* by threedimensional reconstructions of thin sections of cells. *J Bacteriol* 127:1346–1358.

- Holečková N., Doubravová L., Massidda O., Molle V., Buriánková K., Benada O., Kofroňová O., Ulrych A., Branny P. (2014) LocZ is a new cell division protein involved in proper septum placement in *Streptococcus pneumoniae*. *mBio* 6(1):e01700-14.

- Hsieh Y.C., Lee W.S., Shao P.L., Chang L.Y., Huang L.M. (2008) The transforming *Streptococcus pneumoniae* in the 21st century. *Chang Gung Med J* 31:117–124

- Huang, K.H., Durand-Heredia, J., and Janakiraman, A. (2013) FtsZ-ring stability: of bundles, tubules, crosslinks and curves. *J Bacteriol* 195:1859–1868.

- Ishikawa, S., Kawai, Y., Hiramatsu, K., Kuwano, M., and Ogasawara, N. (2006) A new FtsZ-interacting protein, YlmF, complements the activity of FtsA during progression of cell division in *Bacillus subtilis*. *Mol Microbiol* 60:1364–1380.

- Jensen S.O., Thompson L.S., Harry E.J. (2005) Cell division in *Bacillus subtilis*: FtsZ and FtsA association is Z-ring independent, and FtsA is required for efficient midcell Z-Ring assembly. *J Bacteriol* 187(18):6536-44.

- Johnston C., Campo N., Bergé M.J., Polard P., Claverys J.P. (2014) *Streptococcus pneumoniae*, le transformiste. *Trends Microbiol* 22:113–119.

- Jones, L.J., Carballido-Lopez, R., and Errington, J. (2001) Control of cell shape in bacteria: helical, actin-like filaments in *Bacillus subtilis*. *Cell* 104:913–922.

- Kadioglu, A., Weiser, J.N., Paton, J.C., Andrew, P.W. (2008) The role of *Streptococcus pneumoniae* virulence factors in host respiratory colonization and disease. *Nat.Rev.Microbiol* 6, 288–301.

- Karimova G., Pidoux J., Ullmann A., Ladant D. (1998). A bacterial two-hybrid system based on a reconstituted signal transduction pathway. *Proc. Natl. Acad. Sci. U.S.A.* 95, 5752–5756.

- Karimova G., Dautin N., Ladant D. (2005). Interaction network among *Escherichia coli* membrane proteins involved in cell division as revealed by bacterial two-hybrid analysis. *J. Bacteriol.* 187, 2233–2243.

- Kelly, A. J., Sackett, M. J., Din, N., Quardokus, E. & Brun, Y. V. (1998) Cell cycle-dependent transcriptional and proteolytic regulation of FtsZ in Caulobacter. *Genes Dev* 12:880–893.

- Klugman K.P. (2011) Contribution of vaccines to our understanding of pneumococcal disease. *Philos Trans R Soc Lond B Biol Sci* 366:2790-8.

- Krupka M., Rivas G., Rico A.I., Vicente M. (2012) Key role of two terminal domains in the bidirectional polymerization of FtsA protein. *J Biol Chem* 287:7756–7765.

- Krupka M., Cabré E.J., Jiménez M., Rivas G., Rico A.I., Vicente M. (2014) Role of he FtsA C terminus as a switch for polymerization and membrane association. *mBio* 5:e02221-14.

- Kruse, T., Bork-Jensen, J., and Gerdes, K. (2005) The morphogenetic MreBCD proteins of *Escherichia coli* form an essential membrane-bound complex. *Mol Microbiol* 55:78-89.

- Lacks S., Hotchkiss R.D. (1960) A study of the genetic material determining an enzyme in Pneumococcus. *Biochim Biophys Acta* 39:508–518.

- Land A.D., Winkler M.E. (2011) The requirement for pneumococcal MreC and MreD is relieved by inactivation of the gene encoding PBP1a. *J Bacteriol* 193:4166-79.

- Land A.D., Tsui H.C., Kocaoglu O., Vella S.A., Shaw S.L., Keen S.K., Sham L.T., Carlson E.E., Winkler M.E. (2013) Requirement of essential Pbp2x and GpsB for septal ring closure in *Streptococcus pneumoniae* D39. *Mol Microbiol* 90:939-55.

- Lara, B., Rico, A.I., Petruzzelli, S., Santona, A., Dumas, J., Biton, J., Vicente M., Mingorance J., Massidda O. (2005) Cell division in cocci: localization and properties of the *Streptococcus pneumoniae* FtsA protein. *Mol Microbiol* 55:699–711.

- Leaver, M., and Errington, J. (2005) Roles for MreC and MreD proteins in helical growth of the cylindrical cell wall in *Bacillus subtilis*. *Mol Microbiol* 57:1196–1209.

- Lenarcic, R., Halbedel, S., Visser, L., Shaw, M., Wu, L.J., Errington, J., et al. (2009) Localisation of DivIVA by targeting to negatively curved membranes. *EMBO* J 28:2272–2282.

- Liu, G., Draper, G.C., and Donachie, W.D. (1998) FtsK is a bifunctional protein involved in cell division and chromosome localization in *Escherichia coli*. *Mol Microbiol* 29:893–903.

- Lleo, M.M., Canepari, P., and Satta, G. (1990) Bacterial cell shape regulation: testing of additional predictions unique to the two-competing-sites model for peptidoglycan assembly and isolation of conditional rod-shaped mutants from some wild-type cocci. *J Bacteriol* 172:3758–3771.

- Lock, R.L., and Harry, E.J. (2008) Cell-division inhibitors: new insights for future antibiotics. *Nat Rev Drug Discov* 7:324–338.

- López R. (2006) Pneumococcus: the sugar-coated bacteria. *Int. Microbiol.* 9:179–190

- Löwe J. & Amos L. (1998) Crystal structure of the bacterial cell-division protein FtsZ. *Nature* 391:203–206.

- Lutkenhaus, J., Pichoff, S., and Du, S. (2012) Bacterial cytokinesis: from Z ring to divisome. *Cytoskeleton* 69:778–790.

- Ma X., Sun Q., Wang R., Singh G., Jonietz E.L., Margolin W. (1997) Interactions between heterologous FtsA and FtsZ proteins at the FtsZ ring. *J Bacteriol* 179:6788-97.

- Ma X. & Margolin W. (1999) Genetic and functional analyses of the conserved C-terminal core domain of *Escherichia coli* FtsZ. *J Bacteriol* 181:7531-44.

- Maggi, S., Massidda, O., Luzi, G., Fadda, D., Paolozzi, L., and Ghelardini, P. (2008) Division protein interaction web: identification of a phylogenetically conserved common interactome between *Streptococcus pneumoniae* and *Escherichia coli*. *Microbiology* 154:3042–3052.

- Massey, T.H., Mercogliano, C.P., Yates, J., Sherratt, D.J., and Löwe, J. (2006) Double-stranded DNA translocation: structure and mechanism of hexameric FtsK. *Mol Cell* 23:457–469.

- Massidda O., Kariyama R., Daneo-Moore L., Shockman G.D. (1996) Evidence that the PBP 5 synthesis repressor (psr) of *Enterococcus hirae* is also involved in the regulation of cell wall composition and other cell wall-related properties. *J Bacteriol* 178:5272-8.

- Massidda O., Anderluzzi D., Friedli L., Feger G. (1998) Unconventional organization of the division and cell wall gene cluster of *Streptococcus pneumoniae*. *Microbiology* 144:3069-78.

- Massidda, O., Nováková, L. and Vollmer, W. (2013), From models to pathogens: how much have we learned about *Streptococcus pneumoniae* cell division?. *Environmental Microbiology* 15:3133–3157.

- Mohammadi, T., Ploeger, G.E., Verheul, J., Comvalius, A.D., Martos, A., Alfonso, C., et al. (2009) The GTPase activity of *Escherichia coli* FtsZ determines the magnitude of the FtsZ polymer bundling by ZapA in vitro. *Biochemistry* 48:11056–11066.

- Mohammadi, T., Van Dam, V., Sijbrandi, R., Vernet, T., Zapun, A., Bouhss, A., et al. (2011) Identification of FtsW as a transporter of lipid-linked cell wall precursors across the membrane. *EMBO J* 30:1425–1432.

- Morlot C., Zapun A., Dideberg O., Vernet T. (2003) Growth and division of *Streptococcus pneumoniae*: localization of the high molecular weight penicillin-binding proteins during the cell cycle *Mol Microbiol* 50:845-55.

- Morlot C., Noirclerc-Savoye M., Zapun A., Dideberg O., Vernet T. (2004) The D,D-carboxypeptidase PBP3 organizes the division process of *Streptococcus pneumoniae*. *Mol Microbiol* 51:1641-8.

- Noirclerc-Savoye M., Le Gouëllec A., Morlot C., Dideberg O., Vernet T., Zapun A. (2005) In vitro reconstitution of a trimeric complex of DivIB, DivIC and FtsL, and their transient co-localization at the division site in *Streptococcus pneumoniae*. *Mol Microbiol* 55:413-24.

- Nováková L., Bezousková S., Pompach P., Spidlová P., Sasková L., Weiser J., Branny P. (2010) Identification of multiple substrates of the StkP Ser/Thr protein kinase in *Streptococcus pneumoniae*. *J Bacteriol* 192:3629-38.

- O'brien K. L., Wolfson L. J., Watt J. P., Henkle E., Deloria-Knoll M., McCall N., et al. (2009). Burden of disease caused by *Streptococcus pneumoniae* in children younger than 5 years: global estimates. *Lancet* 374:893–902.

- Oliva, M.A., Halbedel, S., Freund, S.M., Dutow, P., Leonard, T.A., Veprintsev, D.B., et al. (2010) Features critical for membrane binding revealed by DivIVA crystal structure. *EMBO J* 29:1988–2001.

- Peters K., Schweizer I., Beilharz K., Stahlmann C., Veening J.W., Hakenbeck R., Denapaite D. (2014) *Streptococcus pneumoniae* PBP2x mid-cell localization requires the C-terminal PASTA domains and is essential for cell shape maintenance. *Mol Microbiol* 92:733-55.

- Pichoff S., Lutkenhaus J. (2002) Unique and overlapping roles for ZipA and FtsA in septal ring assembly in *Escherichia coli*. *EMBO J* 21, pp. 685–693

- Pichoff S., Lutkenhaus J. (2005) Tethering the Z ring to the membrane through a conserved membrane targeting sequence in FtsA. *Mol. Microbiol*. 55:1722–1734.

- Pichoff, S. and Lutkenhaus, J. (2007) Identification of a region of FtsA required for interaction with FtsZ. *Mol. Microbiol*. 64:1129 –1138.

- Pichoff, S., Shen, B., Sullivan, B., and Lutkenhaus, J. (2012) FtsA mutants impaired for self-interaction bypass ZipA suggesting a model in which FtsA's self-interaction competes with its ability to recruit downstream division proteins. *Mol Microbiol* 83:151–167.

- Pichoff S., Du S., Lutkenhaus J. (2015) The bypass of ZipA by overexpression of FtsN requires a previously unknown conserved FtsN motif essential for FtsA-FtsN interaction supporting a model in which FtsA monomers recruit late cell division proteins to the Z ring. *Mol Microbiol* 95:971-87.

- Pinho M.G., Kjos M., Veening J.W. (2013) How to get (a)round: mechanisms controlling growth and division of coccoid bacteria. *Nat Rev Microbiol* 11:601-14.

- van der Ploeg, R., Verheul, J., Vischer, N.O., Alexeeva, S., Hoogendoorn, E., Postma, M. (2013) Colocalization and interaction between elongasome and divisome during a preparative cell division phase in *Escherichia coli*. *Mol Microbiol* 87:1074–1087.

- van der Poll T., Opal S.M. (2009) Pathogenesis, treatment, and prevention of pneumococcal pneumonia. *Lancet* 374:1543-56.

- van de Putte, P., Van D., and Roersch, A. (1964). The selection of mutants of *Escherichia coli* with impaired cell division at elevated temperature. *Mutat Res.* 106:121-8.

- Quardokus, E., Din, N. & Brun, Y. V. Cell cycle regulation and cell type-specific localization of the FtsZ division initiation protein in Caulobacter. *Proc. Natl Acad. Sci. USA* 93:6314–6319.

- Ramamurthi K.S., Losick R. (2009) Negative membrane curvature as a cue for subcellular localization of a bacterial protein. *Proc Natl Acad Sci U S A* 106:13541-5.

- Ravin A.W. (1959) Reciprocal capsular transformations of pneumococci. *J Bacteriol* 77:296-309.

- Reddy, M. (2007) Role of FtsEX in cell division of *Escherichia coli*: viability of ftsEX mutants is dependent on functional SufI or high osmotic strength. *J Bacteriol* 189:98–108.

- Rico A.I., García-Ovalle M., Mingorance J., Vicente M. (2004) Role of two essential domains of *Escherichia coli* FtsA in localization and progression of the division ring. *Mol. Microbiol.* 53:1359–1371.

- Rico, A.I., García-Ovalle, M., Palacios, P., Casanova, M., and Vicente, M. (2010) Role of *Escherichia coli* FtsN protein in the assembly and stability of the cell division ring. *Mol Microbiol* 76:760–771.

- Rico A.I., Krupka M., Vicente M. (2013) In the beginning, *Escherichia coli* assembled the proto-ring: an initial phase of division. *J Biol Chem* 288:20830-6.

- Rodrigo C., Lim W.S. (2014) The relevance of pneumococcal serotypes. *Curr Infect Dis Rep* 16:403.

- Romberg, L. & Levin, P. A. (2003) Assembly dynamics of the bacterial cell division protein FtsZ: poised at the edge of stability. *Annu. Rev. Microbiol* 57:125–154.

- Rueda, S., Vicente, M. & Mingorance, J. (2003) Concentration and assembly of the division ring proteins FtsZ, FtsA, and ZipA during the *Escherichia coli* cell cycle. *J. Bacteriol* 185:3344–3351.

- Sambrook, J., Fritsch, E. F. & Maniatis, T. (1989). Molecular Cloning: a Laboratory Manual. *Cold Spring Harbor, NY*, Cold Spring Harbor Laboratory.

- Sánchez M., Valencia A., Ferrándiz M. J., Sander C., Vicente M. (1994) Correlation between the structure and biochemical activities of FtsA, an essential cell division protein of the actin family. *EMBO J* 13:4919–4925.

- Sasková L., Nováková L., Basler M., Branny P. (2007) Eukaryotic-type serine/threonine protein kinase StkP is a global regulator of gene expression in *Streptococcus pneumoniae*. *J Bacteriol* 189:4168-79.

- Schmidt, K.L., Peterson, N.D., Kustusch, R.J., Wissel, M.C., Graham, B., Phillips, G.J., and Weiss, D.S. (2004) A predicted ABC transporter, FtsEX, is needed for cell division in *Escherichia coli. J Bacteriol* 186:785–793.

- Sham, L.T., Barendt, S.M., Kopecky, K.E., and Winkler, M.E. (2011) Essential PcsB putative peptidoglycan hydrolase interacts with the essential FtsXSpn cell division protein in *Streptococcus pneumoniae* D39. *Proc Natl Acad Sci USA* 108:E1061–E1069.

- Sham L.T., Tsui H.C., Land A.D., Barendt S.M., Winkler M.E. (2012) Recent advances in pneumococcal peptidoglycan biosynthesis suggest new vaccine and antimicrobial targets. *Curr Opin Microbiol* 15:194-203.

- Shiomi, D., Sakai, M., and Niki, H. (2008) Determination of bacterial rod shape by a novel cytoskeletal membrane protein. *EMBO J* 27:3081–3091.

- Shiomi D., Margolin W. (2008) Compensation for the loss of the conserved membrane targeting sequence of FtsA provides new insights into its function. *Mol Microbiol* 67(3):558-69.

- Straume D., Stamsås G.A., Håvarstein L.S. (2014) Natural transformation and genome evolution in *Streptococcus pneumoniae*. *Infect Genet Evol* S1567-1348.

- Szwedziak P., Wang Q., Freund S.M., Löwe J. (2012) FtsA forms actin-like protofilaments. *EMBO J* 31:2249–2260.

- Szwedziak P., Wang Q., Bharat T.A., Tsim M., Löwe J. (2014) Architecture of the ring formed by the tubulin homologue FtsZ in bacterial cell division. *Elife* 4.

- Tavares, J.R., De Souza, R.F., Meira, G.L.S., and Gueiros-Filho, F.J. (2008) Cytological characterization of YpsB, a novel component of the *Bacillus subtilis* divisome. *J Bacteriol* 190:7096–7107.

- Trueba F.J. (1982) On the precision and accuracy achieved by *Escherichia coli* cells at fission about their middle. *Arch Microbiol* 131:55-9.

- Tsui H.C., Boersma M.J., Vella S.A., Kocaoglu O., Kuru E., Peceny J.K., Carlson E.E., VanNieuwenhze M.S., Brun Y.V., Shaw S.L., Winkler M.E. (2014) Pbp2x localizes separately from Pbp2b and other peptidoglycan synthesis proteins during later stages of cell division of *Streptococcus pneumoniae* D39. *Mol Microbiol* 94:21-40.

- Typas, A., Banzhaf, M., Gross, C.A., and Vollmer, W. (2012) From the regulation of peptidoglycan synthesis to bacterial growth and morphology. *Nat Rev Microbiol* 10:123–136.

- Vicente, M., Rico, A.I., Martínez-Arteaga, R., and Mingorance, J. (2006) Septum enlightenment:assembly of bacterial division proteins. *J Bacteriol* 188:19–27.

- Walker C. L., Rudan I., Liu L., Nair H., Theodoratou E., Bhutta Z. A., et al. . (2013). Global burden of childhood pneumonia and diarrhoea. *Lancet* 381:1405–1416.

- Weart, R. B. & Levin, P. A. (2003) Growth rate-dependent regulation of medial FtsZ ring formation. *J. Bacteriol*. 185:2826–2834.

- Weiser J.N. (2010) The pneumococcus: why a commensal misbehaves. *J Mol Med* 88:97-102.

- Wheeler, R., Mesnage, S., Boneca, I.G., Hobbs, J.K., and Foster, S.J. (2011) Super-resolution microscopy reveals cell wall dynamics and peptidoglycan architecture in ovococcal bacteria. *Mol Microbiol* 82:096–1109.

- Witkin E.M. (1946) Inherited differences in sensitivity to radiation in *Escherichia coli*. *Proc Natl Acad Sci U S A* 32:59-68.

- Wu, L.J., and Errington, J. (1994) *Bacillus subtilis* SpoIIIE protein required for DNA segregation during asymmetric cell division. *Science* 264:572–575.

- Yim L., Vandenbussche G., Mingorance J., Rueda S., Casanova M., Ruysschaert J.M., Vicente M. (2000) Role of the carboxy terminus of *Escherichia coli* FtsA in self-interaction and cell division. *J Bacteriol* 182:6366-73.

- Zapun A., Vernet T., Pinho M.G. (2008) The different shapes of cocci. *FEMS Microbiol Rev* 32:345-60.